

Medical University of South Carolina

MEDICA

MUSC Theses and Dissertations

Spring 4-17-2023

Cancer-Specific Perturbations to Arginine Metabolism Blunt Replication and Performance of Oncolytic Myxoma Virus

Parker Dryja

Medical University of South Carolina

Follow this and additional works at: <https://medica-musc.researchcommons.org/theses>



Part of the [Immunotherapy Commons](#), and the [Virology Commons](#)

Recommended Citation

Dryja, Parker, "Cancer-Specific Perturbations to Arginine Metabolism Blunt Replication and Performance of Oncolytic Myxoma Virus" (2023). *MUSC Theses and Dissertations*. 791.

<https://medica-musc.researchcommons.org/theses/791>

This Dissertation is brought to you for free and open access by MEDICA. It has been accepted for inclusion in MUSC Theses and Dissertations by an authorized administrator of MEDICA. For more information, please contact medica@musc.edu.

**Cancer-Specific Perturbations to Arginine Metabolism Blunt Replication and Performance of
Oncolytic Myxoma Virus**

Parker Dryja

A dissertation submitted to the faculty of the Medical University of South Carolina in partial fulfillment of the requirements for the degree of Doctor of Philosophy in the College of Graduate studies.

Department of Molecular and Cellular Biology and Pathobiology

2023

Approved by:

Chairman, Advisory Committee

Eric Bartee

Advisory Committee

Chrystal Paulos

Jessica Thaxton

Anand Mehta

Patrick Woster

Acknowledgements

To Dr. Eric Bartee, a mentor of such quality that his graduate student would move from the breezy beaches of Charleston, South Carolina to the half-living desert of Albuquerque, New Mexico if only to remain under his tutelage. My development as a scientist would otherwise not have been possible without your investment of interest and time in working together, as well as your tolerance and patience for failure. Throughout these six years, working on all of my projects has been a collaboration, rather than me being given a list of experiments with little room for agency. Your leadership, mentorship, and friendship are as strong as your preference for wearing shorts in lieu of pants. Also, an excellent fryer of chicken wings.

To Dr. Mee Bartee, Erica Flores, Miriam Valenzuela, Heather Curtsinger, Dr. Raquela Thomas, and past members of the Bartee lab who all helped facilitate the work herein. You all contributed to my various (sometimes even successful) projects, and were a great captive audience during lab meetings to subject to discussions of arginine metabolism.

To Dr. Chrystal Paulos, Dr. Anand Mehta, Dr. Jessica Thaxton, and Dr. Patrick Woster, who have contributed no small part in shaping my work and professional development both collectively and through my experiences with them each individually.

To Dr. Thomas Benton, Dr. Catherine Mills, Katie Garrabrant, Dr. Kareem Heslop, Dr. Ravyn Duncan, Dr. Nathan Duncan, Dr. Joy Kirkpatrick, Dr. Jonathan Turner, Dr. Harmin Herrera, Dr. Alyson Black, and Marcus Strait, whose collaboration, camaraderie, and commiseration, were - and continue to be - invaluable.

To my wife Savannah, the sweetest of sweet peas. Your gentle support and patience provided the foundation for any perseverance I may have had within this program. I love you so dearly.

Table of Contents

List of Figures

Abbreviations

Abstract

Chapter 1: Oncolytic Virotherapy – Theory, Practice, and Mechanisms

1.1: Introduction	1
1.2: Cancers and Concomitant Viral Infection – OV From Bedside to Bench	2
1.3: Generic Mechanisms & Arming Strategies	4

Chapter 2: Myxoma Virus as an Oncolytic Virotherapy Platform

2.1: Introduction	16
2.2: MYXV Basic Virology	17
2.3: MYXV Development as an Oncolytic Virotherapy Agent	19

Chapter 3: Oncolytic Viruses - Strangers in a Strange Land

3.1: Introduction	21
3.2: Aberrant Arginine Metabolism in Cancer	22
3.3: Reliance of DNA Viruses on Arginine	26

Chapter 4: Central Hypothesis - The Case for Evaluating Pertinence of Arginine Metabolism to OV

4.1: Introduction	28
4.2: Specific Aims	30
4.3: Significance & Impact	31

Chapter 5: MYXV Exhibits Dependence on Arginine for Replication

5.1 Introduction	32
5.2: Methods & Materials	34
5.3: Results	37
5.4: Discussion	44

Chapter 6: Ablation of Gr-1⁺ Cells Amplifies Viral Replication in B16F10 Tumors

6.1: Introduction	49
6.2: Methods & Materials	51
6.3: Results	53
6.4: Discussion	62

Chapter 7: Loss of ASS1-mediated Arginine Biosynthesis Reduces Tumor Capacity to Support Viral Infection

7.1: Introduction	67
7.2: Methods & Materials	68
7.3: Results	72
7.4: Discussion	85

Chapter 8: Summary & Future Work

References

Appendices

List of Figures

Figure 1: Schematic illustrating the two general mechanisms of oncolytic virotherapy.

Figure 2: Urea pathway in mammals.

Figure 3: Proposed model for Arg specific barriers to achieving optimal OV.

Figure 4: MYXV specifically requires L-arginine for viral replication.

Figure 5: Treatment of B16F10 tumors alters Arg metabolism.

Figure 6: Binding of MYXV to B16F10 cells in Arg starved conditions is comparable.

Figure 7: MYXV viral gene expression and genome abundance are reduced in Arg starved conditions.

Figure 8: Amino acid starvation initiates the integrated stress response.

Figure 9: Viral burden and infection area in MyxGFP infected B16F10 tumors in α Gr-1 treated mice versus Mock.

Figure 10: Kinetics of viral replication and spread in MyxGFP infected B16F10 tumors in α Gr-1 treated mice versus Mock.

Figure 11: Depletion of MDSCs reduces the initial dose required to achieve an effective therapeutic response.

Figure 12: Activity of ARG1 reduces viral replication of MYXV in a dose-dependent manner.

Figure 13: MDSCs inhibit viral replication of MYXV ex vivo in an ARG1 and Arg dependent manner.

Figure 14: B16F10s are ASS1/ASL competent and can support cellular and viral replication with Arg biosynthesis.

Figure 15: Generation of ASS1KO cell lines.

Figure 16: Defects in Arg metabolism inhibit MYXV replication in Arg limited conditions.

Figure 17: Loss of ASS1 reduces metrics of MYXV health in B16F10 tumors.

Figure 18: Immune profiles of mock and MyxGFP treated tumors in SC and ASS1 KO cell lines.

Figure 19: Loss of ASS1 blunts therapeutic response to MYXV-mediated oncolytic virotherapy.

Figure 20: Viral reconstitution of Arg biosynthesis partially restores viral replication and therapeutic efficacy.

List of Abbreviations

ADA	Adenosine Deaminase
AdV	Adenovirus
ADP	Adenovirus Death Protein
Arg	L-Arginine
AS	Argininosuccinate
ASL	Argininosuccinate Lyase
ASS1	Argininosuccinate Synthetase 1
ARG1	Arginase-1
DAMP	Damage-Associated Molecular Pattern
FFU	Foci Forming Units
GM-CSF	Granulocyte-Macrophage Colony-Stimulating Factor
HBV	Hepatitis B Virus
HPI	Hours Post Infection
HSV	Herpes Simplex Virus
ICB	Immune Checkpoint Blockade
KO	Knockout
MDSC	Myeloid Derived Suppressor Cell
MV	Measles Virus
MYXV	Myxoma Virus
OV	Oncolytic Virotherapy
PAMP	Pathogen-Associated Molecular Pattern
PRR	Pattern Recognition Receptor
SC	CRISPR/Cas9 scramble control

SEM	Standard Error of the Mean
TIL	Tumor Infiltrating Lymphocytes
TSA	Tumor-Specific Antigen
VACV	Vaccinia Virus
VSV	Vesicular Stomatitis Virus

Abstract

PARKER DRYJA. Cancer-Specific Perturbations to Arginine Metabolism Blunt Replication and Performance of Oncolytic Myxoma Virus.
(Under the direction of ERIC BARTEE).

Oncolytic virotherapy (OV) is a class of immunotherapy for treatment of malignancy. Using viruses that exhibit natural coincidental tropisms for cancer, or others that have been engineered to the same effect, intentional infection of lesions leads to two therapeutically beneficial effects: (1) direct destruction of the infected tumor through virally-mediated cell lysis, and (2) recruitment of an otherwise blunted or absent anti-cancer immune response to affect both local and disseminated disease. A surfeit of cancer-specific changes are accumulated during progression from first genetic insult to clinical detection, presenting a dramatically altered underlying biology of cell and tissue. The viruses employed within OV have been characterized over decades, however, all largely within the context of normal and otherwise-healthy host cells bearing infections. As such, these disparities between cancerous tissues and their normal counterparts may pose barriers to viral infection not encountered or compensated for.

Dysregulations within cellular metabolism are a hallmark of cancer, and the replication of all viruses – oncolytic or not – is contingent on access to host metabolites. Despite this, no research has been conducted evaluating how metabolic changes within tumors may lead to resistance to OV infection. One such dysregulated metabolic pathway is synthesis and consumption of L-arginine (Arg), a semi-essential amino acid whose bioavailability is required for the *in vitro* replication of several oncolytic viruses. Cancer types such as hepatocellular carcinoma, sarcoma, and melanoma often clinically present as functionally auxotrophic for this amino acid due to epigenetic silencing of argininosuccinate synthetase 1 (ASS1), an enzyme responsible for the conversion of citrulline and aspartate into the Arg precursor argininosuccinate (AS).

Additionally, the recruitment of Arginase-1 (ARG1) positive myeloid derived suppressor cells (MDSCs) and tumor-associated macrophages (TAMs) further insult Arg availability within the TME.

Here, we show that the *in vitro* replication of oncolytic myxoma virus (MYXV) is dependent on the presence of bioavailable Arg, with insight towards several stages within the viral life cycle. We demonstrate that the presence of MDSCs negatively reduces viral burden within infected tumors in a B16F10 model of murine melanoma, with their depletion capable of reducing initial required MYXV dose to elicit a therapeutic response, and these effects possibly attributable to an expression of ARG1 as evidenced within cocultures *ex vivo*. Secondly, we determine the role of ASS1 in mediating tumoral capacity for viral replication *in vitro* and *in vivo* using CRISPR/Cas9 generated ASS1^{KO} cell lines. Here, we find tumors formed from functionally ASS1^{KO} B16F10 melanoma cells display multi-log reductions in MYXV replication during oncolytic virotherapy (OV) as well as significantly poorer therapeutic responses. Lastly, we demonstrate that reconstitution of Arg biosynthesis through ASS1-armed MYXV constructs at least partially rescues these effects. Collectively, these studies demonstrate an Arg-dependent replication of MYXV that may be affected by cancer-specific changes within Arg metabolism and consumption. This work is the first to characterize a metabolic barrier to achieving optimal viral replication within tumors, and indicates that consideration towards tumoral metabolism may improve replication and therapeutic efficacy of OV agents.

Chapter 1: Oncolytic Virotherapy – Theory, Practice, and Mechanism

1.1: Introduction

Oncolytic Virotherapy (OV) is a literal, biological application of the age-old adage: “the enemy of my enemy is my friend.” This class of cancer therapeutics employs viruses that are able to infect and assist in the destruction of malignancies while sparing healthy tissues from infection, with viral tropisms for cancer imparted through both virus specific factors and cellular states intrinsic to cancers. These unique viruses are used to establish genuine viral infections within tumors to destroy lesions through both direct virally-mediated cell lysis, and the subsequent induction of an anti-cancer immune response that may otherwise be absent. While OV is conceptually simple, the underlying biology has proven to be deceptively complex and nuanced. Collective consideration of cancer biology, virology, and immunology are required to elucidate mechanisms and contribute to rationally designed OV platforms, and many questions are currently unanswered as to how these viruses can best be engineered as therapeutics. Investigation into how these oncolytic viruses influence – and are influenced by – the quagmire of abnormalities within tumors bears promise to refine therapeutic strategies to maximize OV clinical response and efficacy.

1.2: Cancers and Concomitant Viral Infection – OV from Bedside to Bench

Ultimately, the field of oncolytic virotherapy owes its origins to clinical observations more than a century ago [1]. Despite the concept and rudimentary understanding of a “virus” itself was decades away from coming to fruition, clinicians had made note of curious cases where patients bearing hematological cancers exhibited regression or clinical improvement otherwise during incidence of concomitant influenza infection [2]. These observations would come to serve as the basis for developing oncolytic virotherapy as a cancer therapeutic.

After our collective understanding of viruses had improved considerably in the 1950s and ‘60s, and in combination with increased reports of cancer regression in patients bearing viral infections or vaccinations [3-6], interest renewed in attempting to exploit this phenomenon for therapeutic gain by the intentional infection of patients bearing malignancies. While the efforts of the clinical trials were successful from a theoretical perspective in demonstrating the validity of these previous observations, the clinical outcomes of these tests were – with a few notable exceptions – unimpressive at best, produced unacceptable side effects, and unsurprisingly, resulted in pathological infections within patients [1].

The advent of modern genetic engineering techniques has given way to a new wave of interest and research into oncolytic virotherapy. Genetic modifications to viruses in this context allow for the directed attenuation of viruses to reduce their pathogenicity towards healthy cells (or more succinctly: impart better cancer tropism) as well as arming viruses with transgenes to increase therapeutic efficacy. Research into modifying viruses towards these therapeutic ends progressed, and thus in 2005, the legitimacy of oncolytic virotherapy as a cancer therapeutic was solidified with the approval of Oncorine (a modified human adenovirus) by the Chinese SFDA for treatment of nasopharyngeal carcinoma in combination with chemotherapy [7].

Success in the US market was found nearly ten years later, with Imlygic (talimogene laherparepvec; a modified herpes simplex virus) approved for the treatment of metastatic melanoma in 2015 [8], which to date is currently the only FDA approved oncolytic virus for treatment of any malignancy. Currently, many phase I and phase II clinical trials are being conducted evaluating a range of OV platforms in a handful of malignancies, with an evident focus on glioblastoma and melanoma [9].

1.3 Generic Mechanisms and Arming Strategies

Mechanistically, OV causes destruction of tumors or hematological cancers through two distinct but related consequences of viral infection: cell death as a direct and indirect result of viral infection (oncolysis), and anti-cancer immune responses elicited as a result of immunogenic viral infection (oncolytic vaccination) (Fig 1) [10]. The degree of reliance on either or both of these mechanisms is collectively contingent on the specific OV agent used, directed modifications to the viral genome, and the cancer type and location being treated. With some intriguing exceptions [11], viral replication and spread throughout the tumor is critical for mediating both of these mechanisms; fulfillment of the viral life cycle and reinfection of surrounding tissues drives virally mediated destruction of the tumor and increases the potential expression of virally encoded transgenes important for mediating therapeutic responses.

Just as diverse as the swathe of viruses employed in OV are the strategies used to arm them. Though some OV agents are more amenable to genetic manipulation and insertions than others (and, as proponents of VACV and Myxoma virus (MYXV) will argue, is no small benefit), the modern approach to OV seldom uses viruses that do not bear at least some changes on a genomic level. Generally, these can be broken into four categories: changes that increase a virus's cancer-specific tropism, changes that directly increase viral toxicity to the lesion itself, changes that eliminate mechanisms of immunosuppression normally present within the wild-type virus, or changes that allow or potentiate a virally recruited anti-cancer immune response.

This chapter is bifurcated into discussing these mechanisms and arming strategies separately in favor of readability. In reality, however, these two mechanisms are very much intertwined, with some oncolysis putatively dependent on immune responses eliminating virally infected cancer cells, and oncolytic vaccination dependent on oncolysis for initiating inflammation and releasing tumor-specific antigen (TSA) [12].

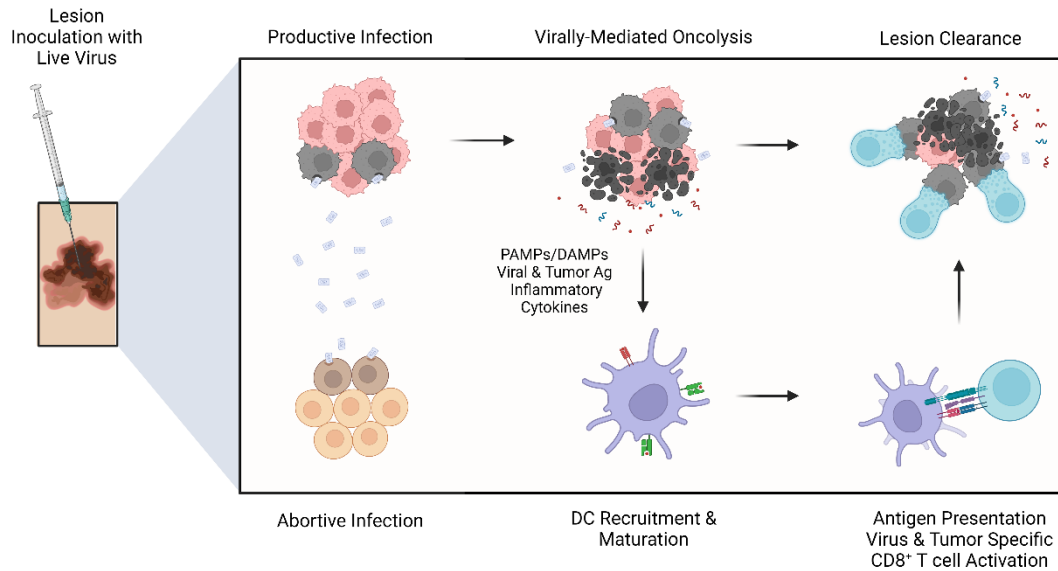


Figure 1: Schematic illustrating the two general mechanisms of oncolytic virotherapy. From left, to right: inoculation of lesions occurs by direct injection of virus, less frequently delivered systemically; viral infection is established within permissive tumor cells, but is abortive within healthy cells through various mechanisms. Viral infection generates PAMPs, DAMPs, tumor specific antigen, and inflammatory cytokines, causing DC recruitment and maturation. Priming of T cells specific to viral and tumor antigen alike leads to further tissue damage combined with sustained infection.

In normal tissues, viral pathogenesis is partly driven by virally-mediated cell death, including lysis or cell death attributed to viral processes, or programmed cell death from viral effector proteins themselves and anti-viral response pathways. For some non-enveloped viruses such as adenovirus (AdV), exit of newly synthesized and assembled virions from an infected cell largely occurs through cell lysis. Here, a late-expressed protein aptly named Adenovirus Death Protein (ADP) causes a loss of both nuclear envelope and cellular membrane integrity, forming a mechanism of virion exit from both the nucleus and cytoplasm necessary for viral dissemination [13]. Other viruses, such as human immunodeficiency virus (HIV), induce cell death by activation of several apoptotic pathways, including mitochondrial-dependent apoptosis via PUMA, BAX, and BCL2L11 [14].

Cell death as a consequence of viral infection is not exclusively pro-viral, however – the timing of this event is critical in determining successful or abortive infection [15]. Though many viruses use cell death as a means of viral release or otherwise increase their pathogenicity, antiviral host responses also result in programmed cell death to limit viral replication and drive inflammation [16]. These pathways are engaged by the detection of viral pathogen-associated molecular patterns (PAMPs) via cellular pattern recognition receptors (PRRs). Intracellular detection of viral PAMPs occurs through constitutively-expressed but interferon-upregulated TLR-3, TLR-7, and TLR-9 that recognize non-methylated CpG DNA, ssRNA, and dsRNA respectively, as well as through mitochondrial antiviral signaling (MAVS) by engagement of MDA5 and RIG-I that all induce interferon regulatory factor 3 (IRF3), interferon regulatory factor 7 (IRF7), and/or nuclear factor κ B (NF κ B) [17]. Another major contributor to viral sensing and antiviral response is the dsRNA sensor protein kinase R (PKR), one of the four known proteins responsible for activation of the integrated stress response (ISR) and a target of many viral effector proteins [18]. Induction of these pathways ultimately leads to the generation of Type I interferon (IFN I) responses that

have autocrine and paracrine functions that, in turn, activate IFN-stimulated genes (ISGs) to trigger highly antiviral cellular states [17, 19]. Beyond inducing ISGs that limit the ability of viruses to replicate within a cell, this programming sensitizes the IFN stimulated cells to apoptotic cues and pathways including the continued detection of viral PAMPs, underscoring the importance of cell death in controlling viral infection [20].

In OV, putatively some of these same mechanisms explain virally-mediated cell death when these viruses are used to treat cancer. However, this notion is challenged by the observation that there is frequently dysregulation of these same pathways in cancer that are both exploited by and used against viruses, such as inhibition of STAT1 signaling and increased expression of anti-apoptotic Bcl-2. These changes to virally-mediated cell death can actually form the basis for an OV agent's cancer tropism, where apoptosis or cell death that would normally result in abortive infection instead never occurs. Nevertheless, induction of some type of cell death is an important part of how OV works to treat malignancy. This is exemplified in some OV platforms, where tumor lysis syndrome (TLS) and associated toxicity occur in treatment of various cancers, underscoring their potentially lytic potential [21, 22].

One of the more important and earliest attempted strategies for improving OV is increasing viral tropism for cancer. With early investigative studies of OV demonstrating unacceptable secondary infection of healthy tissues with viruses such as hepatitis B virus (HBV) [23] and West Nile virus [24], directed attenuation of OV agents to reduce patient toxicity was – and remains – paramount to their development as therapeutics [1]. In reflection of this, the previously mentioned oncolytic human adenovirus 5 under the trade name of Oncorine bears modifications to increase its specificity for cancer.

Part of the AdV life cycle is pushing the host cell into S phase that AdV may access and hijack nuclear DNA replication machinery for viral genome replication, and is the function of some

AdV early gene products [25]. Here, early gene products trigger induction of p53 via their inactivation of Rb as the host cell attempts to engage cell cycle arrest and apoptosis [26]. AdV protein E1B-55k is then responsible for inhibiting p53, thus overcoming cellular arrest and/or death that would result in a loss of infection [27]. One of the modifications to Oncorine is a deletion of this *E1B55K* AdV gene, rendering this construct unable to counteract the host cell p53 response to AdV infection, thus potentially reducing its pathogenicity to human cells that have an intact p53 pathway [28]. In human cancers however, loss of function in the p53 pathway is an exceptionally common phenotype [29]. Cellular loss of p53 then obviates the need for AdV's E1B-55k, making these malignant cells permissive to infection with Oncorine, and forming the basis for its cancer specificity.

Many strategies to increase cancer specificity of OV agents follow this same core concept: deletions of virulence genes that defend against host cell responses commonly absent in cancer, or removing viral genes critical to the viral life cycle that are redundant in malignancies. Other examples of this include vaccinia virus (VACV) and herpes simplex virus (HSV) constructs bearing a loss of virally encoded thymidine kinase (TK) [30-32], measles virus (MV) dependent on cancer-specific proteases for activation rather than their wild type dependence on furin-mediated cleavage [33], and vesicular stomatitis virus (VSV) bearing critical viral genes silenced by the microRNA let-7 that is highly expressed in healthy differentiated tissue, but lowly expressed in cancers [34]. Beyond these two types, there are additionally a plethora of modifications that increase cancer tropism by engineering viral surface proteins to bind cancer-specific or cancer-upregulated surface receptors [35].

Beyond concerns of cancer specificity, OV agents have also been engineered to possess a heightened lethality to cancer cells, either directly or in combination with chemotherapeutics. One of the better examples of this strategy is the inclusion of yeast cytosine deaminase into viral

backbones [36-38]. Cytosine deaminase catalyzes the hydrolysis of free cytosine into uracil with an ammonia byproduct, and while likely evolutionarily related to cytidine deaminases such as AID and APOBEC, is absent in mammals [39]. Historically, this enzyme was targeted by the antifungal drug 5-fluoro cytosine (5-FC), which cytosine deaminase converts into toxic and highly cytostatic 5-fluoro uracil (5-FU) [40]. By itself, 5FU is also a classic antineoplastic agent, albeit one marred by tumoral resistance and unimpressive clinical responses [41]. In an elegant attempt to translate the antifungal mechanism of action into an OV context, researchers have armed OV agents with this cytidine deaminase enzyme [36-38], allowing for the systemic dosing of the comparatively better tolerated 5-FC that becomes converted to 5-FU within OV infected lesions, thus increasing tumoral cytotoxicity through viral infection and an infection specific prodrug.

An original school of thought in OV was the idea that the immune system is a burden to achieving therapeutic efficacy, rather than a boon. Partly born from the first clinical observations that infection-associated remission in cancer patients appeared to be contingent upon a state of immunosuppression [1], and studies lamenting the hindrance of existing and therapeutically-generated humoral responses against OV agents [42], the immune system was regarded as an obstacle to achieving therapeutic efficacy with OV. Now, however, it is obvious that – while antiviral immunity is certainly an obstacle – an immune response is critical to the efficacy of many OV agents, particularly in treating metastatic disease with viruses that cannot be delivered systemically. The importance of maintaining this balancing act to generate an immune response against the targeted cancer while not prematurely quenching the viral infection is a critical obstacle and point of research in OV [43-45]. Many preclinical models pertaining to OV accommodate this phenomenon by employing the use of contralateral tumor models to evaluate immune efficacy against distal lesions. Often, their experimental design consists of injecting one lesion with the OV agent in question, while leaving the secondary tumor site undisturbed. This

model is necessitated by many OV platforms not being amenable to systemic injection (unlike small molecule chemotherapeutics or antibody-based biologicals), and even with OV agents that can be delivered systemically, is an important tool to evaluate the quality of OV-recruited immune responses and their ability to affect disseminated disease.

Not unlike the establishment and spread of viral infection within a host, an important step in the development of a malignancy is winning the fight against – and even co-opting – the immune system. In order to survive and ultimately progress as a disease, it must evade and/or suppress the immune system to avoid death, going through the crucible of immune “elimination, equilibrium, and escape” [46]. “Avoiding immune destruction” is a hallmark of cancer [47], and many known oncogenes contribute to the immune evasion and suppression of developing malignancies such as EGFR driven expression of PD-L1 or HER2 driven internalization of MHC-I [48-51]. Through these mechanisms, tumors can grow unabated by the immune system and progress as a disease.

The field of cancer immunotherapy concerns itself with reversing this immunosuppression or potentiating anti-cancer immune responses to tip the scales back in favor of the immune system, leading to clearance of lesions. Modern advances within this field have led to the culmination of paradigm-shifting technologies such as immune checkpoint blockade (ICB) and adoptive cell therapies (ACT) [52]. These therapeutics have made resounding impacts in improving clinical outcomes of a staggering range of cancers, boasting impressive response rates for historically dire malignancies such as metastatic melanoma [53].

This section will discuss why OV is considered a type of cancer immunotherapy by reviewing the second general mechanism of OV: a subversion of immune escape mechanisms by their highly inflammatory infections within tumors [54]. The virally mediated lysis of tumor cells is a type of immunogenic cell death, causing the release of DAMPs and TSA from the tumor, and

viral-origin PAMPs. In most models and OV platforms, tumoral infection with an OV agent has the capacity to turn immunologically “cold” tumors “hot” (with “temperature” a common colloquialism in the field of immunotherapy regarding the level of immune infiltrates – generally specifically in reference to T cells – and relative abundance of inflammatory cytokines, where “hotter” tumors bear higher levels of each [55]) [56].

Of note, this method of oncolytic vaccination has a significant edge compared to other, more traditional types of peptide and protein based cancer vaccines that have exhibited poor therapeutic value [57]. In an OV based approach, the anti-cancer immune response generated is naturally “antigen agnostic [12]” and circumvents the need for therapeutic personalization. The immune response and T cell receptor (TCR) repertoire generated from OV infection is based off of a pool of TSAs that are specific to the infected cancer in a specific patient.

The formation of an OV-induced anti-cancer immune response begins with the engagement of the aforementioned IFN-I pathway upon tumoral infection. As a result of generating type I IFNs through viral infection and release of DAMPs/PAMPs, infiltration and maturation of innate immune cells into the tumor is triggered. Within the milieu of antigens are those of both tumoral and viral origin, and ultimately both are then presented to the T cell compartment by infection-recruited dendritic cells (DCs). This in turns generates CD4+ T cell responses and both anti-viral and anti-cancer CD8+ T cells that serve as the effector population for many OV-mediated immune responses [54, 56]. This process is critical in achieving therapeutic efficacy in many OV platforms and cancer types, especially so in the context of OV agents that can only be delivered locally, and are entirely reliant on the generated immune response to clear the secondary uninfected lesions.

Given OV’s potency in recruiting anti-cancer immunity, a wide variety of immunomodulatory transgenes have been tested in various OV platforms, as well as their outright

combination with immunotherapies as separately delivered agents. Largely, this consists of virally-encoded ICB, interleukins, or various other cytokines [35]. A significant advantage in using OV agents armed with these transgenes is their directed and explicit expression within tumors – transgenes are only expressed where there is viral infection. Historically, treatment of cancer patients with systemically delivered cytokines such as IFN- α , IFN- γ , IL-1, and IL-2 have demonstrated varying degrees of clinical efficacy, but tend to suffer from potent toxicities [58]. In OV, arming cancer-specific OV agents with these transgenes circumvents the toxic potential inherent to systemic delivery, and is undoubtedly a significant advantage to this technology. By the same token, however, the dosing control imparted by systemic infusion is lost in an OV arming strategy without intricate inducible promoter systems, as well as information regarding its abundance [59]. Furthermore, expression of these transgenes only occurs so long as ongoing viral infection is maintained, which may be even more difficult to control without sustained and repeated doses of OV into a lesion.

Combination of OV with ICB is a now commonly explored method for improving OV-mediated immune responses. ICB consists of blocking the binding of immune receptors responsible for attenuating inflammation and promoting self-tolerance with their ligands. Some of these pathways, such as PD-L1/PD-1, are frequently co-opted by cancers with respective ligands overexpressed to aid in immunosuppression [60, 61]. Given its prolific rise and clinical fulfillment of promises made in preclinical trials, combination of ICB with many modalities of cancer therapy have been investigated, certainly including OV [62]. Combination of OV with ICB consists of combination of the therapies separately (i.e., tumoral infection with an OV agent while ICB is provided systemically [63]), or in a combined single-platform, where the viruses encode secreted proteins or polypeptides (usually full antibodies (mAbs), fragment antigen-binding (Fab), or single-chain variable fragments (scFv)) capable of blocking engagement of checkpoint receptors [35].

In one of the original studies pioneering this strategy, Engeland et al. demonstrated that arming MV with α PD-L1 antibodies was more efficacious in tumor control compared to the IgG-Fc MV strain in a B16 model of murine melanoma recombinant with MV receptor CD20 [64]. The MV- α PD-L1 treated cohorts were characterized (compared to MV-IgG-Fc) with clear shifts in the composition of their tumor infiltrating lymphocytes (TIL), notably with an increase from a 1:1 ratio of CD8⁺ T cell:Treg to 2:1. Importantly, researchers in this study also compared the relative performance of systemic α PD-L1 combined with MV-IgG-Fc against the MV- α PD-L1 monotherapy and found no difference between the two cohorts. While still maturing, arming OV with ICB agents has been studied across many other platforms, and continues to be a promising strategy for improving OV-mediated immune responses [65].

OV platforms armed with one or two of several interleukins have also been tested, and capitalize on the localized nature of OV. One of the more infamous interleukins evaluated as a cancer therapeutic is IL-12. IL-12 is a highly pleiotropic inflammatory cytokine, structurally made up of heterodimer consisting of two subunits encoded by separate genes (IL-12p35, IL-12p40; *IL12a*, *IL12b*, respectively) covalently bound by a disulfide bond [66]. Production of IL-12 is typically limited to cells of monocytic lineage – DCs, macrophages, and monocytes themselves – and is an important mediator between innate and adaptive immunity [67]. IL-12 driven immune responses are characterized by the differentiation of CD4⁺ T cells into a Th1 phenotype, in turn prioritizing cellular immunity and production of IFN- γ that can be a potent effector of anticancer activity [68-70]. In the mid 1990's, several clinical trials were conducted using systemically dosed IL-12 for the treatment of cancer. These trials yielded unimpressive results putatively from a combination of factors, including an exceptionally poor therapeutic index and lack of an ability to preferentially affect tumoral immune populations over circulating immune cells [58]. At the time, prospects for using IL-12 as an immunotherapy were largely diminished by one phase-II study

treating patients with renal carcinoma, where systemic delivery of IL-12 at high doses resulted in the death of two of the 17 patients enrolled, leading to an FDA-imposed temporary moratorium on IL-12 trials [71].

Recognizing the potential of IL-12 therapy and the unique position of OV in solving these previous issues, in 1996 Bramson et al. constructed an Adv5-based OV platform with *IL12a* and *IL12b* inserted into the E1 and E3 region, respectively (AdmIL-12.1). Performance of this construct was evaluated using spontaneous tumors from MMTV-PyMT transgenic mice that were subcutaneously transplanted into syngeneic FVBs. Here, performance of the AdmIL-12.1 construct was markedly improved over the unarmed control virus, with a doubling of median survival time from 28 ± 3 days to 52 ± 4 days, an increase of CR from 0% to 31%, and higher IFN- γ in both the tumor draining lymph node and tumor bed itself [72]. Importantly, determination of expression kinetics revealed large amounts of IL-12 (peaking at 4 days post infection with $\sim 7 \mu\text{g/g}$ tumor) accumulating in the tumor over time, but demonstrated minimal amounts of IL-12 circulating within the bloodstream. This kinetic portion of the study highlights two highly advantageous factors of OV platforms delivering therapeutic cytokines: the cytokines are produced gradually and continually rather than the spikes and furrows seen in single-bolus systemic delivery, and the produced cytokine is largely contained within infected tumor tissue. Several groups have expanded on this use of IL-12 in OV platforms with similar successes in pre-clinical models [73].

Other cytokines have successfully been used in OV backbones; Imlytic itself capitalizes on the important function of DCs mentioned above by virtue of having two copies of human granulocyte-macrophage colony stimulating factor (hGM-CSF) inserted into its genome [74]. GM-CSF is a cytokine with several functions, and strongly induces myelopoiesis and differentiation of monocytic progenitors into DCs. While excessive production of GM-CSF can be pro-tumorigenic as a cytokine involved in maintaining immune compartments such as M2 macrophages and

myeloid-derived suppressor cells (MDSCs), in GM-CSF independent cancers, GM-CSF leads to increased differentiation and infiltration of DCs, as well as their antigen presentation, which are important to OV-mediated immune responses [56, 75]. Imlygic's incorporation of *GM-CSF* into its backbone thus causes GM-CSF production and secretion within virally infected cells. In the original studies, tumor control of contralateral A20 lymphoma bearing mice was comparable between GM-CSF armed (JS1/GM-CSF) and unarmed strains (JS1) within the infected lesion. However, in imparting control over the uninfected lesion, JS1/GM-CSF exhibited superior efficacy [74]. In the same study, it was shown that splenocytes from tumor bearing mice treated with JS1/GM-CSF secreted more IFN- γ in both monocultures and when co-cultured with A20 cells *ex vivo*, collectively suggesting an ability of JS1/GM-CSF to generate a more robust anti-cancer immune response.

All of these studies illustrate the benefits of incorporating therapeutic transgenes into an OV agent's backbone, particularly when there are concerns or limitations with systemic delivery of the immunomodulator itself. These arming strategies that block immunosuppression or drive inflammation capitalize on the natural ability of OV to engage the immune system and recruit an anti-cancer immune response, and are an exciting topic of continued research in the field of OV [76-79].

Chapter 2: Myxoma Virus as an Oncolytic Virotherapy Platform

2.1: Introduction

The variety of viruses used as OV agents is extensive, and each with drawbacks and benefits that are a reflection of their underlying biology. The prototypic rhabdovirus vesicular stomatitis virus (VSV) is able to infect a range of cancers with defects in IFN response pathways, can efficiently induce apoptosis through both mitochondrial and death receptor pathways, benefits from a lack of pre-existing humoral immunity in humans, and can infect metastatic disease when delivered systemically under the right conditions [80, 81]. However, its small genomic size (11kb; five genes) yields few amenable insertion sites and only accommodates small transgenes, and its poor-fidelity RNA polymerase may lead to transgene instability [82]. Human adenoviruses, such as human adenovirus 5, require specific cell-surface receptors for binding and entry, and suffer from pre-existing antiviral immunity that limits their capacity for system delivery, but are amenable to insertion of multiple transgenes [83]. Given their diverse biology, the choice of OV agent significantly impacts which arming strategies are viable, possible routes of delivery, and the range of cancers targetable.

The work described herein employs myxoma virus (MYXV) as an OV agent, a virus that has only recently been developed as an OV platform and has several important benefits for use as an OV. The majority of research both characterizing the virology of MYXV as well as evaluating its potential as an OV platform were performed in the lab of Dr. Grant McFadden, who has done extensive work characterizing MYXV in both its normal and OV context [84-91]. This chapter will summarize some of this work into the history and basic virology of MYXV, the brief history of its development as an oncolytic virus and its basis for cancer tropism, and lastly the arming strategies and cancer types in which it has been tested.

2.2: MYXV Basic Virology

MYXV is a leporipoxvirus that was originally endemic to American rabbits prior to human intervention in the 1950s. In the South American rabbit *Sylvilagus brasiliensis*, infection with MYXV causes mild disease with the formation of fibromas at infection sites, utilizing biting insects as a natural vector [92]. First described as a mysterious disease affecting a cohort of European rabbits at a lab in Uruguay, MYXV was observed to cause a dramatically more severe form of the disease compared to their South American relatives. In these rabbits, infection with MYXV rapidly causes systemic disease with the development of non-cancerous tumors on the head and anogenital regions, with the original South American strain of MYXV virtually 100% lethal to European rabbits [92-94]. After the deliberate populating of Australia with European rabbits in 1879 to provide animals for sport hunting, the invasive lagomorphs quickly became a disruptive nuisance to both the natural ecosystem and farmers growing crops alike [94, 95]. As a pest control measure, the intentional introduction of MYXV was tested in Australia in 1950. MYXV rapidly spread through the population of this invasive species, and resulted in a massive 95% reduction in their numbers over a decade [88, 96]. Simultaneously, MYXV was illegally spread to Europe in 1952 by a French researcher and farmer who sought to also co-opt this virus as a pest control measure, obtaining the virus from a lab in Switzerland [93]. Despite the unfortunate circumstances – particularly in Europe where the disease now affected native rabbit populations – the introduction of MYXV into these populations posed an exceptionally rare and impactful insight into the epidemiology of emergent diseases and co-evolution of virus and host that remain ongoing to this day [92].

As a poxvirus, MYXV is a brick shaped virus, has a large double-stranded DNA (dsDNA) genome, and exclusively replicates within the cellular cytoplasm. The Lausanne strain (isolated in 1949 in Brazil [97]; the same strain used to develop MYXV as an OV agent) genome consists of

159 unique viral genes, with 12 of these genes present in duplicate in the terminal inverted repeat (TIR) regions of the viral genome [84].

Binding and entry in MYXV is mediated not through binding to specific cellular receptors, but is putatively mediated through electrostatic binding to negatively charged glycosaminoglycans – such as the ubiquitously expressed heparan sulfate – giving it the ability to bind and enter a broad range of cell types [87, 98]. The basis for MYXV's cellular and species tropism, rather, is its ability to manipulate intracellular pathways of antiviral response and cell growth. The pathway responsible for determining MYXV's species tropism is STAT1 antiviral signaling through the IFN-I response pathway mediated by IRF3 induction via Erk1/2, ultimately exerting an anti-MYXV effect through PKR-independent phosphorylation of eIF2 α . This pathway was rigorously interrogated and culminated in the demonstration that loss of STAT1 in *STAT1*^{-/-} mice was capable of breaking this species barrier to MYXV infection [89]. Logically, MYXV contains viral effector proteins capable of inhibiting this STAT1 signaling in rabbits, but some of these critical proteins are not cross reactive with non-rabbit targets, such as M-T7 (a secreted neutralizing binding protein of IFN- γ and a range of chemokines [86]) [88].

Beyond IFN-I/STAT1 signaling as a basis for tropism, tropism of MYXV has also been shown to be dependent on the activation of the pro-survival and growth signaling pathway of Akt. Encoded within MYXV is a viral effector protein, M-T5, that is responsible for the binding and activation of Akt via Akt phosphorylation. MYXV constructs lacking this M-T5 protein were shown to result in abortive infection in cells lacking basal activation of Akt pathways, but were still capable of productive infection in Akt active cells, indicating the importance of this pathway for determining MYXV's cellular tropism [90, 91].

2.3 MYXV Development as an Oncolytic Virotherapy Agent

Interest in using MYXV for OV stemmed largely from the same studies that defined its basic virology. With a cellular and species tropism that was reliant on functional IFN-I responses, STAT-1 pathway, and Akt activity, MYXV's basis for tropism strongly overlaps with dysfunctional and aberrant signaling through these respective pathways that is widely associated with many cancer types [99, 100]. In large part, this natural potential tropism for cancer indicated its possible use as an OV platform.

The first study evaluating MYXV as an OV agent was conducted in an orthotopic model of human glioma using cell lines and patient-derived xenografts in CD-1 nude mice. The construct used here was a minimally modified MYXV (Lausanne strain) bearing no genetic modifications beyond insertion of GFP between the M135R and M136R ORFs [85]. *In vitro*, this vMyxGFP construct was demonstrated to cause efficient virally-mediated cell death, with 7/8 glioma lines tested exhibiting a susceptibility to MYXV infection that was positively correlated with levels MYXV gene expression and production of infectious particles. *In vivo*, inoculation of mice bearing singular glioma lesions with a modest dose of 5×10^6 FFU/mouse vMyxGFP yielded an 80% CR in the U-87 model, and significant reduction of tumor burden in the U-251 model, possibly correlated to their susceptibility to MYXV observed *in vitro*. This tumor clearance was restricted to only injected lesions, as mice bearing contralateral tumors in each hemisphere of the brain saw no therapeutic benefit in the secondary, uninfected tumor. In this study, susceptibility to MYXV *in vitro* was predictive of therapeutic response *in vivo*, with the more infection-resistant U-251 cell line exhibiting stronger resistance to MYXV OV than the U-87 cell line that was highly permissive to infection.

Notably, this therapeutic response was eliminated with the use of UV inactivated virus, demonstrating live virus and viral replication mediated therapy, rather than some adjuvant-based

effect on the immune system by simply providing viral material. This specific result is consistent throughout studies pertaining to MYXV-mediated OV, which have further demonstrated that therapeutic response through both virally-mediated cell death and recruitment of an anti-cancer immune response are entirely contingent on occurrence of MYXV replication [101-103].

Since the original 2005 study in glioma, MYXV has been confirmed as an OV agent capable of affecting a range of malignancies in preclinical models with varying degrees of efficacy, with a portion of studies focused on small cell lung cancer melanoma [104]. Contrary to results observed in glioma and multiple myeloma (MM), MYXV-mediated disease control of these tumor models is largely immune dependent [105, 106]. As MYXVs anti-cancer effects in these models are immune mediated/immune dependent, many arming strategies have focused on transgenes to drive inflammation as ways to improve therapy [104]. These studies capitalize on several advantages of MYXV as an OV agent: a large capacity for bearing transgenes, receptor-independent binding and entry, a natural tropism against malignant cells, and a lack of pre-existing humoral immunity in humans. Though non-lytic *in vivo* for a portion of tested tumor models, the qualities above position MYXV as an excellent OV agent for mediating oncolytic vaccination and modifying anti-cancer immune responses through inserted transgenes.

Chapter 3: Oncolytic Viruses - Strangers in a Strange Land

3.1: Introduction

Viruses are obligate intracellular parasites. Every amino acid, every molecule of ATP, every nucleotide for RNA and DNA synthesis will have to be entirely sourced from the host cell in order to make more of themselves, propagate infection to additional cells, tissues, and ultimately, new hosts. The importance of nutrient accessibility to viral replication is well described in literature pertaining to the basic biology of viruses, and underscored by observations that many viruses encode manipulators of host metabolism.

As viruses, all OV agents, too, must rely entirely on host metabolism in order to replicate and express transgenes that are important to eliciting a therapeutic response. Critically, oncolytic viruses evaluated thus far are all non-oncogenic and co-opted as therapeutics – these viruses did not evolve to replicate and exist within cancerous tissues, rather the unique circumstances of their virology and that of malignancy allows for coincidental infection. The tissues these viruses normally infect are in many ways disparate from the tumors they are used to treat, including marked changes to facets of cellular metabolism and nutrient availability. Metabolic dysfunctions found in advanced cancers could potential pose as barriers to viral replication. The bodies of literature defining the ways viruses demand cellular resources for replication, and the other which defines hyper-consumptive and competitive behaviors in cancers, both suggest metabolic considerations for OV are worth considering. However, the interplay of tumoral metabolism and how it affects the efficacy of OV remains unstudied.

Having defined the basis of OV, the viruses used therein, and the multitude of strategies used to arm them, this chapter defines the importance of L-arginine (Arg) to cancers and viruses separately, and culminates in the question central to this work: how do cancer-specific changes in Arg metabolism affect the ability of MYXV to replicate and generate a therapeutic response?

3.2: Aberrant Arginine Metabolism in Cancer

L-arginine is an amino acid considered conditionally essential, as the biological capacity for Arg synthesis can be insufficient to meet cellular demand in several circumstances where consumption is high (such as bacterial infection and wound repair [107, 108]). An important member of the urea cycle, a large portion of Arg biosynthesis and immediate turnover occurs during hepatic generation of urea from toxic biogenic ammonia; meanwhile, using the same enzymatic pathway, generation and release of Arg occurs in the kidneys [108]. While the complete host of enzymes involved in the urea cycle are exclusive to the liver, a portion of this pathway is expressed within a larger collection of tissue types. Characterized by argininosuccinate synthetase 1 (ASS1) and argininosuccinate lyase (ASL), a subset of the urea cycle allows for limited biosynthesis of Arg provided cellular access to L-citrulline (Cit) and L-asparagine (Asp) (Fig 2).

Import of Arg is known to be specifically mediated through several redundant Na⁺-independent cationic amino acid transporters (CATs) of the solute-carrier transporter 7 (SLC7) family that also control import of L-lysine (Lys), L-histidine (His), and L-ornithine (Orn) [109]; less specific import of Arg can also occur through more universal amino acid transporter complexes, such as Na⁺-dependent transport through ATB⁰⁺ [110, 111]. While redundant in function, CATs exhibit varying affinities for their substrates, and their expression has been suggested to be regulated by stress responses [112]. Expression of specific CATs is variable between tissue types, such as the lower Arg affinity CAT2a expressed in liver and skeletal muscle cells, and the higher Arg affinity CAT2b expressed in macrophages upon activation (a reflection of heightened Arg reliance after induction of the iNOS or Arginase-1 pathways that both require Arg as a substrate) [109, 113]. General CAT expression is ubiquitous in mammalian cells, and have even been exploited as surface receptors for viruses [114].

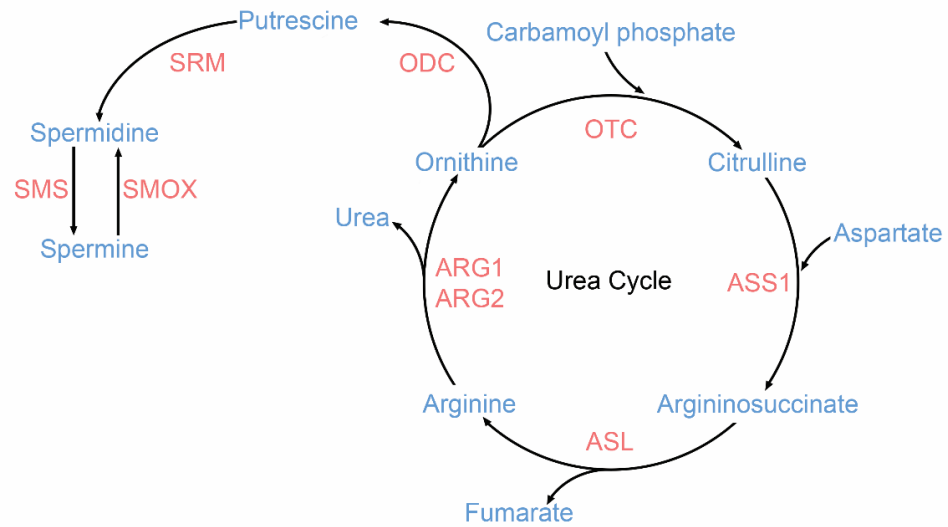


Figure 2: Urea pathway in mammals. OTC is exclusive to liver and kidney cells; ARG1/ARG2 is found in liver, kidney, and some myeloid cells. The rest of the urea cycle enzymes are ubiquitously expressed at various levels and are important enzymes in supporting Arg and polyamine biosynthesis. Red denotes enzymes, blue denotes metabolites. OTC = ornithine transcarbamoylase, ASS1 = argininosuccinate synthetase, ASL = argininosuccinate lyase, ARG = arginase, ODC = ornithine decarboxylase, SRM = spermidine synthase, SMS = spermine synthase, SMOX = spermine oxidase.

In cancer, dysregulation of Arg metabolism is observed across several types of malignancies [115, 116]. In some, such as melanoma [117, 118], various sarcomas [119-121], hepatocellular carcinoma [117, 122, 123], and prostate carcinoma [124], ASS1 frequently becomes epigenetically silenced, turning these cancers into Arg auxotrophs and thus entirely reliant on exogenous Arg pools. Though the pressure and ultimate benefit to losing capacity for Arg biosynthesis is under investigation and appears to be cancer-specific, studies demonstrated loss of ASS1 can cause an increase in nucleotide biosynthesis by decreased Asp turnover [125], increased angiogenesis [126], increased redox potential and intracellular pH maintenance in low-pH conditions [127], immune evasion by depriving T cell responses of vital Arg [128, 129], and exhibits a possible correlation with tumor metastasis [127].

It goes to follow, then, that loss of Arg biosynthesis may render affected cancers susceptible to Arg starvation. The merit of this concept has been investigated, with biologics such as pegylated arginine deiminase (ADI-PEG, ADI an enzyme responsible for the hydrolysis of Arg into Cit and NH_3^+ byproduct) exhibiting modest activity against ASS1- cancers [116, 119, 124, 130]. Though characterized by underwhelming responses thus far, the modest tumor control offered by ADI-PEG supports the notion that loss of Arg biosynthesis is a clinically relevant phenomenon.

Excess consumption of Arg within tumors also occurs through factors extrinsic to the cancer cells themselves. Myeloid-derived suppressor cells (MDSCs) are a collection of myeloid-lineage cells named as such due to their potent capabilities of immunosuppression [131]. MDSCs are recruited by a handful of CC and CXC chemokines, with the MDSC-recruitment chemokine repertoire and MDSC subtype cancer specific [132, 133]. Within tumors, MDSCs contribute to a myriad of factors that aid in the survival, maintenance, and ultimately progression of the disease. This includes induction of angiogenesis, suppression of T cell activation and function, metastasis,

differentiation into tumor-associated macrophages (TAMs), secondary recruitment of M2 macrophages and Tregs, and additional metabolic remodeling of the TME [131, 133-136].

One of the ways in which MDSCs and M2 macrophages alter the metabolic landscape of the TME is through expression of Arginase 1 (ARG1) [137, 138]. ARG1 is a cytosolic enzyme responsible for the hydrolysis of Arg into L-ornithine and a urea byproduct, the former of which is a vital precursor within L-proline and polyamine metabolism. Infiltration of ARG1⁺ cells within ASS1 silenced cancers poses a paradox, wherein the MDSC/TAM mediated turnover of Arg via ARG1 should starve tumors of this necessary amino acid, as seen in studies evaluating the therapeutic potential of ADI-PEG. Together, these observations suggest ASS1⁻ tumors and ARG1⁺ cells maintain a regulated state of Arg homeostasis, where Arg consumption and turnover are kept high enough to benefit tumors by starving anti-cancer T cell responses of Arg and increasing ornithine content for proline/polyamine metabolism, but not so high as to entirely starve the cancers themselves as seen with therapeutic doses of ADI-PEG.

3.3: Reliance of DNA Viruses on Arginine

Entirely outside of the context of malignancy, work has been conducted on evaluating the specific importance of Arg access to diverse sets of DNA viruses – including those employed in OV – such as VACV, AdV, and HSV. Consistent in all of these viruses, a lack of Arg halts or stunts viral replication [139-141].

Arg dependency in VACV was originally suggested by the observation that reductions in VACV titers in cells contaminated with mycoplasma were attributed to a mycoplasma-mediated depletion of Arg in culture media [142]. Interrogation of VACV replication kinetics in Arg variant media determined an Arg concentration of 15-30 μM necessary for detectable viral replication, with viral yield dose-dependent up until a plateau at an Arg concentration of 90-120 μM [139]. Using radiolabeled thymidine, uridine, and leucine, it was determined that DNA, RNA, and protein synthesis were markedly reduced as a result of Arg starvation, and notably affected both viral and cellular replication. More biologically significant, however, was the experiment demonstrating that in radiolabeled Arg pulse-chase experiments, uptake and incorporation of Arg was dramatically higher in VACV infected cultures compared to uninfected controls [139]. Beyond driving cellular import of Arg, VACV infection also appears to increase Arg biosynthesis. In a study evaluating ASS1/ASL activity in VACV infected cells that had access to Arg, it was determined that ASS1/ASL activity increased 2-10 fold in HeLa and Mouse L cells depending on the Arg and Cit content of the culture media [143]. Collectively, these studies demonstrate that VACV requires access to Arg for viral replication, and can increase cellular import and synthesis through either active (virally-mediated) or passive (increasing Arg consumption resulting in cellular compensation) mechanisms.

In studies pertaining to AdV, elimination of Arg in cultures halted viral replication entirely. Though production of viral protein did occur albeit at a reduced rate, Arg starvation appeared to

halt some late-stage process critical to virion assembly. Additional experiments determined that – even at 50 μ M Arg and rescue of cellular phenotype – AdV replication was still reduced by 1,000-fold [144]. Around the same time, separate studies identified several Ad core proteins as being particularly rich in Arg content [145, 146], and were later defined as AdV proteins pV, pVII, and pMu [147]. These proteins have been characterized as having DNA binding activity critical to the AdV life cycle, including modulation of host response, transcriptional regulation of newly synthesized viral genomes, and packaging of stable virions, where the cationic nature of these Arg residues is critical for binding and packaging negatively charged DNA [147].

In HSV, loss of Arg in cultures of infected cells significantly ablated viral replication [140, 141]. This observation was later given additional biological relevance by experiments noting that proteose-peptone elicited intraperitoneal macrophages were capable of inhibiting HSV replication in an ARG1 dependent manner *ex vivo*, a process that was reversible by excess Arg [148]. Though the experimental conditions are likely too artificial to identify ARG1 as an explicitly antiviral response that functions through Arg deprivation, it does demonstrate that ARG1 activity can function in an antiviral capacity (at least, for HSV) under certain conditions.

Chapter 4: Central Hypothesis - The Case for Evaluating Pertinence of Arginine Metabolism to OV

4.1: Introduction

The two mechanisms driving therapeutic efficacy within oncolytic virotherapy, virally-mediated oncolysis and oncolytic vaccination, are contingent on the replication and tumoral spread of the OV agent employed with few exceptions [11, 35, 79]. However, the biological barriers that attenuate the capacity of tumors to support viral infection remain poorly understood. Studies identifying and addressing these barriers inform arming practices and OV platform design to ultimately benefit clinical performance of oncolytic virotherapies.

Viral access to Arg within a tumor may pose one such barrier. Clearly, though mechanistic insight is lacking in some models, Arg may be of particular importance for viral replication in DNA viruses. Beyond the context of Arg, these studies demonstrate the reliance of viruses on host cells for nutrients, and exemplify how poor nutrient availability can negatively impact viral replication.

The collective factors affecting tumoral Arg metabolism indicate an environment that is highly competitive for Arg pools. Attempts to treat tumors via OV with changes along the ASS1/ARG axis may result in the viral agent having to compete for Arg beyond the “typical” conditions in which they have evolved to compete. Given these two phenomena, we hypothesize that the cancer-specific depressions of arginine content within tumors may starve oncolytic myxoma virus of a nutrient necessary for its replication. The visual summarization of this hypothesis is as seen in Model 1.

In this work, we test this hypothesis by determining the reliance of MYXV on Arg for viral replication, and explore how these two cancer-specific perturbations to Arg metabolism – the presence of ARG1⁺ myeloid cells and loss of tumoral ASS1 – may contribute to resistance of MYXV infection in melanoma.

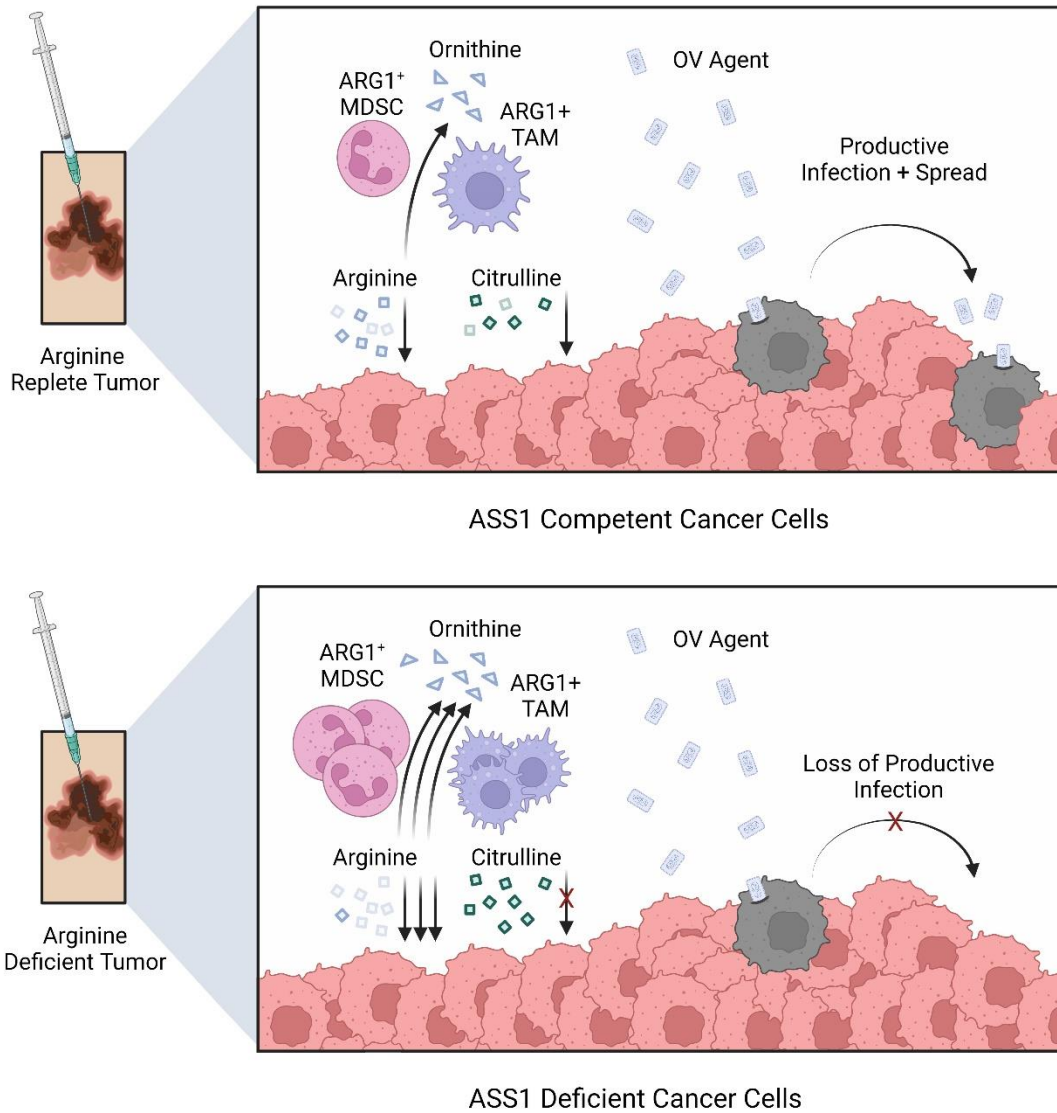


Figure 3: Proposed model for Arg specific barriers to achieving optimal OV. In Arg replete tumors (top; characterized by a low infiltration of ARG1⁺ MDSCs and TAMs, and Arg autotrophy via ASS1 expression), tumoral tissues support viral infection with cellular pools of Arg. In Arg deficient tumors (bottom; characterized by high infiltration of ARG1⁺ MDSCs and TAMs, and Arg auxotrophy due to loss of ASS1 expression), tumoral tissues lose capacity to support infection by having less virally accessible Arg.

4.2: Specific Aims

Specific Aim 1: Given existing studies describing the dependency of several DNA viruses, including the poxvirus VACV, MYXV is likely dependent on access to cellular Arg for viral replication [139-142, 144, 149]. This specific aim will extend this line of study into the context of MYXV to determine its reliance on Arg content for viral replication. Here, the relevant Arg concentrations to achieving optimal MYXV replication will be determined by evaluating full viral replication (defined as the production of infectious progeny) in the context of host cells grown in Arg variant growth medias. From here, the block imposed upon viral replication will be investigated by determining viral binding and entry, expression of viral proteins and transition from early/late protein synthesis, and viral genome replication.

Specific Aim 2: The infiltration of MDSCs within tumors is a negative prognostic indicator for immunotherapy response and disease progression in general [133, 150]. One of the effects exerted by this pathological immune compartment is depression of tumoral Arg through the expression of ARG1. In this specific aim, we will determine how the presence of these cells *in vivo* contributes to MYXV replication and ultimately therapeutic response. The possible contribution of Arg/ARG1 in modulating viral replication will be explored specifically in an *ex vivo* context. The ability of MDSCs to suppress viral replication *ex vivo* in an Arg/ARG1 dependent manner will be evaluated in co-cultures with ARG1⁺ MDSCs in Arg variant medias with or without ARG1 inhibitors.

Specific Aim 3: Loss of the Arg biosynthetic enzyme ASS1 is highly prevalent in several cancer types, including melanoma, non-small-cell lung cancer, and ovarian cancer. In this specific aim, we will identify how loss of Arg biosynthesis through loss of ASS1 impacts capacity of host cells to support viral infection in Arg limited conditions. Lastly, we will determine if inclusion of Arg biosynthetic enzymes into the backbone of MYXV can self-rescue any limitations imposed upon viral replication by cellular loss of ASS1.

4.3: Significance & Impact

The goal of this research is to further identify barriers to achieving optimal viral replication of oncolytic viruses within tumors, and its completion poses a significant contribution to the field of oncolytic virotherapy. Though the necessity of viruses to co-opt host resources and their need to modulate host metabolism to this end has been well-defined throughout virology, and a separate body of work defines similar effects in the incidence of cancer, currently only one published work has been performed thus far even tangentially addressing this possible important overlap [151]. While proposed in review articles in the context of glucose metabolism, no studies have been conducted or proposed evaluating how metabolic changes beyond energetics within the TME may reduce tumoral capacity to support infection, and as such, the work proposed herein is completely novel. Determining if these cancer-specific modulations to Arg metabolism coincidentally pose an antiviral factor within the TME carry implications for informing clinical employment of oncolytic virotherapy. Just as importantly, this work may reveal a completely novel strategy for improving therapeutic response through recombinant viruses: the modulation of metabolism within the TME by inclusion of metabolic enzymes into the viral backbone.

Chapter 5: MYXV Exhibits Dependence on Arginine for Replication

This chapter has been modified from the following publication, under major revision:

Dryja PC, Curtsinger H, Bartee E. Defects in Intratumoral Arginine Metabolism Attenuate the Replication and Therapeutic Efficacy of Oncolytic Myxoma Virus. *Journal for the Immunotherapy of Cancer*. 2022.

5.1: Introduction

The field of Oncolytic Virotherapy (OV) employs viruses as therapeutic agents in the treatment of a wide range of malignancies, where tumors are inoculated with viruses that exclusively – or at least, preferentially – replicate in cancerous tissues to cause their destruction. The conception of this unique class of cancer treatments was born from clinical observations as far back as the late 1800s, with clinicians noting that, in rare instances, patients with ovarian cancer and leukemia would exhibit significant regression after concomitant viral infection (the exact etiological nature of these illnesses and concept of “viruses” were of course unknown, at the time) [1]. Efforts to exploit this phenomenon for therapeutic benefit waxed and waned over proceeding decades, with progress of the field stalling in the late 1900s from a combination of poor therapeutic efficacy and safety concerns. Now, however, the advent of modern genetic manipulation techniques has opened doors for entirely novel and promising OV platforms that boast genetic modifications improving both cancer specificity and therapeutic potential.

OV causes destruction of cancers through two related mechanisms: cell death from viral infection (oncolysis), and anti-cancer immune responses recruited to the tumor as a result of immunogenic viral infection (oncolytic vaccination) [152]. Naturally, given these mechanisms, it is unsurprising that viral replication and spread within the tumor is important to mediate any therapeutic benefit, where non-replicative controls exhibit reduced or loss of efficacy. Barring some very interesting exceptions [11], one of the few threads uniting a wide variety of viruses employed in OV is the observation that some degree of viral replication, or partial continuance of

the viral life cycle, is critical to achieving a therapeutic response. As a result, identifying and overcoming the biological barriers hindering viral replication within tumors is a worthwhile endeavor.

In contrast to the normal tissues these viruses have evolved over eons to exist in and exploit, the malignant tissues they're now used to treat exhibit a staggering range of changes in metabolism and nutrient availability. A commonly dysregulated metabolic pathway in cancer is L-arginine (Arg) biosynthesis, resulting in Arg auxotrophy and competition within tumors [115-117, 119, 124]. Coincidentally, a common metabolic dependency of DNA viruses appears to be having access to Arg [139-141, 143, 145, 148, 149]. Identifying and investigating how this loss of Arg biosynthesis in cancer may stress viral replication could inform and refine approaches to OV. In this chapter, the degree of reliance of MYXV on Arg content is evaluated, as well as partial exploration into the obstacle Arg starvation thus imposes.

5.2: Methods & Materials

Cell Lines and Culture Reagents: Both the BSC40 and B16F10 cells lines were purchased from the American Type Culture Collection (Manassas, VA). ASS1^{KO} B16F10 cell lines were generated using a CRISPR/Cas9 system targeting murine ASS1 (gRNA sequence: TCAGGCCAACATTGGCCAGA; plasmid: PX459) as previously described [153, 154]. B16F10 cells treated with a scrambled gRNA (referred to in this paper as ASS1^{wt} cells) have been previously described [153]. Cell lines were maintained in standard Dulbecco's Modified Eagle Medium (DMEM) (Corning, Corning, NY). For screens with media lacking each amino acid, media was created by starting with DMEM lacking all essential amino acids (United States Biological, Salem, MA) and reconstituting it with all the amino acids typically found in DMEM (Sigma-Aldrich, St. Louis, MO) barring the amino acid of interest. For non-screen experiments, media specifically lacking Arg was created by starting with DMEM lacking Arg (United States Biological, Salem, MA) and supplementing with 3.7g/L sodium bicarbonate and the specified concentrations of filter-sterilized L-Arg-HCl (VWR, Radnor, PA). Arg free media reconstituted with 400μM L-Arg-HCl was used for all control conditions. For citrulline rescue conditions, Arg free media was supplemented with 400μM L-Citrulline (Sigma-Aldrich, St. Louis, MO). All growth medias were supplemented with 10% fetal bovine serum (VWR, Radnor, PA) and 1× penicillin/streptomycin/glutamine (Corning, Corning, NY). Cultures were checked quarterly for mycoplasma contamination using PCR.

Flow Cytometry: Post infection with MYXV at an MOI of 5, cells were washed 2x with aliquots of PBS, lifted from plates via trypsinization, and pipetted into FACS tubes containing media. Original washing aliquots were included into FACS tube to include suspended cells lifted from the plate as a result of viral infection. Cell suspensions were then centrifuged at 200xg for 5 minutes, resuspended in PBS. Centrifugation/wash steps were repeated 2x. Biotium Live-or-Dye™

594/614 Fixable Viability Dye was added to samples and stained for 5 minutes, followed by 2x washes with PBS and 200xg centrifugation steps. Cells were fixed in 2% PFA, and ran through a BD Fortessa for acquisition. Data was analyzed using FlowJo™ (V10.4).

Viral Constructs and Infection: Both viral constructs used in the current manuscript, including recombinant MYXV expressing green fluorescent protein (MyxGFP) and recombinant MYXV expressing both the soluble ectodomain of programmed cell death protein 1 as well as interleukin 12 (MyxPD1/IL12) are based on the Lausanne strain of MYXV [155, 156] and have been previously described [154, 157]. Virus was amplified in BSC40 cells and purified using gradient centrifugation as previously described [158]. Infections were carried out by incubating cells in media containing the desired amount of virus for 30 minutes and subsequently removing viral inoculum and replacing it with fresh media. To quantitate infectious virus, cell pellets from either cell culture or infected tumor samples were freeze-thawed over three cycles in liquid nitrogen and a 37°C water bath. Pellets were frozen a fourth time in liquid nitrogen and then thawed/sonicated for 3 minutes. Resulting homogenates were finally serially diluted and plated onto confluent BSC40s. The number of GFP⁺ foci was then quantified 48 hours post-infection and used to determine the titer of original samples.

Metabolomics: B16F10 tumors were isolated from C57Bl/6J mice four days post-treatment with 1×10^7 foci forming units (FFU) of MyxGFP. Tumors were immediately snap-frozen in liquid nitrogen at point of harvest. Frozen tumors were weighed, and then broken into coarse homogenates using mechanical percussion in liquid nitrogen cooled vessels. 30-50mg of frozen coarse homogenates were then suspended in 80% methanol at 20 μ L/mg tissue. Suspensions were sonicated, centrifuged at 12,000xg, and the resulting supernatants analyzed via LC-MS by the Metabolomics Core Facility at Robert H. Lurie Comprehensive Cancer Center of Northwestern University (Chicago, IL) as previously described [159]. Samples were normalized against total ion

count (TIC) and comparisons drawn between groups across peak area. Analysis of metabolomics data was performed using metaboanalyst [160] on TIC normalized data sets, with data re-plotted via ggbiplot R package.

PCR: DNA was extracted from 1×10^6 cells via Zymo Quick-DNA Miniprep kit (Zymo Research, Irvine, CA). DNA content and quality was quantified on a Nanodrop system prior to cDNA synthesis. PCR was conducted using the PowerUp SYBR Green system (Thermo Fisher, Waltham, Massachusetts) on a 7500 Fast Real-Time PCR System (Thermo Fisher, Waltham, Massachusetts) using a primer set for amplification through M152-M154 MYXV ORFs (152F: TTATTATAAAAACGACGGG, 154R: GGTCAGTTACGATCTTTG).

5.3 Results

MYXV replication is dependent on bioavailable Arg

Several studies have indicated that Arg deprivation is sufficient to block replication of the prototypic poxvirus vaccinia and other DNA viruses [140, 142-144, 148, 149, 161, 162]. However, the specific impact of this deprivation on MYXV replication has never been studied. We therefore examined the ability of MYXV to replicate in B16F10 cells cultured in the presence or absence of 13 essential or semi-essential amino acids (Fig 4A). The results indicated that the absence of numerous amino acids reduced the abundance of infectious MYXV progeny 24 hours post infection. Interestingly, of the amino acids tested, removal of Arg had the most potent inhibitory effect on viral yields.. Consistent with these results, we also observed that removal of exogenous Arg from cell culture media resulted in a dramatic reduction in the abundance of virally derived GFP (Fig 4B), and little-to-no production of new infectious viral particles at any time post infection (Fig 4C) in B16F10s and two additional cell lines tested (A9F1, BSC40). These changes could not be explained by a general loss of cellular viability since Arg deprivation resulted in cytoostasis but did not appear to acutely kill cells over the duration of these experiments (Appendix A). Titrations of exogenous Arg into cultures of both B16F10 and BSC40 cells revealed a strong dose dependency between the production of new infectious MYXV progeny and the bioavailability of exogenous Arg with maximal replication occurring at concentrations $\geq 100\mu\text{M}$ and an EC_{50} of $\sim 50\mu\text{M}$ (Fig 4D). Critically, this EC_{50} is well within the physiological range of Arg, which has been reported to be between 50-150 μM in the serum of healthy mice and 45-110 μM in healthy humans [163-166].

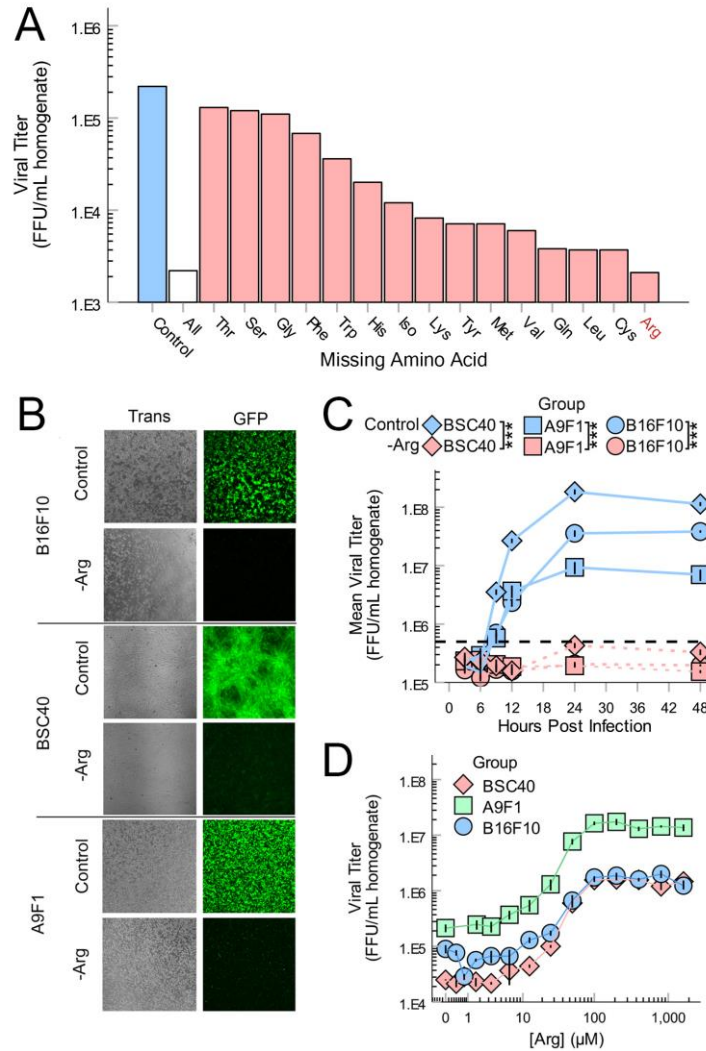


Figure 4: MYXV specifically requires L-arginine for viral replication. (A) Viral yield of MyxGFP in B16F10 cells 24 hours post infection after being incubated in DMEM missing the indicated amino acids 24 hours prior to infection (HPI) (48 hours total). Control = DMEM reconstituted with all missing amino acids. All = DMEM missing all amino acids. **(B)** Transmitted light and GFP fluorescence images of BSC40s infected with MyxGFP 24 HPI after being incubated in DMEM missing Arg (-Arg DMEM). **(C)** Single-step growth curves of MyxGFP in B16F10s after incubation in -Arg DMEM for 24 hours prior to infection (48 hours total). Dashed horizontal black line indicates concentration of input virus (1E+5 FFU/mL). **(D)** Foci forming assay from 24-72 HPI of MyxGFP in BSC40 cells after incubation in -Arg DMEM for 24 hours prior to infection. **(E)** Dose dependency of MyxGFP on Arg content for replication in B16F10s and BSC40s. **Statistics: (C-D)** Unpaired Student's t-test. n = 3. *** p < 0.005.

Since our previous results suggested that MYXV replication was dependent on bioavailable Arg, we next sought to determine if Arg pathways were biologically relevant to MYXV infection in the context of OV. To test this, B16F10 tumors were established on syngeneic mice and then either mock treated or treated with MYXV. Four days post-treatment, tumors were harvested and the abundance of various metabolites analyzed using whole tissue metabolomics. Interestingly, metabolite set enrichment analysis (MSEA) of the resulting dataset revealed that Arg metabolism was the most highly altered metabolic pathway following MYXV treatment (Fig 5A) including significant changes in the urea cycle metabolites fumarate and citrulline (Fig 5B). Taken together, these data demonstrate that MYXV requires bioavailable Arg to complete its replication cycle and that infection alters Arg metabolism *in vivo* during OV.

After observing a complete ablation of MYXV replication in Arg starved cells with a dose response curve in physiological ranges, and metabolomics suggesting Arg biosynthesis pathways were relevant to MYXV infection, we next sought to determine the specific impact of Arg loss on the viral life cycle. To observe a potential impact on viral binding and entry, Arg starved cells were inoculated with a MYXV construct bearing a fusion-tagged M093 core protein with Venus fluorescent protein (MyxVenus) on ice to prevent entry [167](Fig 6A) and imaged immediately after. Cultures were taken off ice to permit entry and imaged 2.5 hours thereafter. For a quantitative readout, this experiment was repeated with Cy5 labeled MYXV [168], and cells harvested for flow cytometry and quantification of bound virus (Fig 6B). Initial results demonstrated that binding and entry were largely unaffected, with a slight signal increase in Arg starved cells (likely artificial from a change in stoichiometry of virus:cell, with fewer cells in Arg starved groups as a result of cytostasis), but nothing that would account for loss of replication observed in previous experiments.

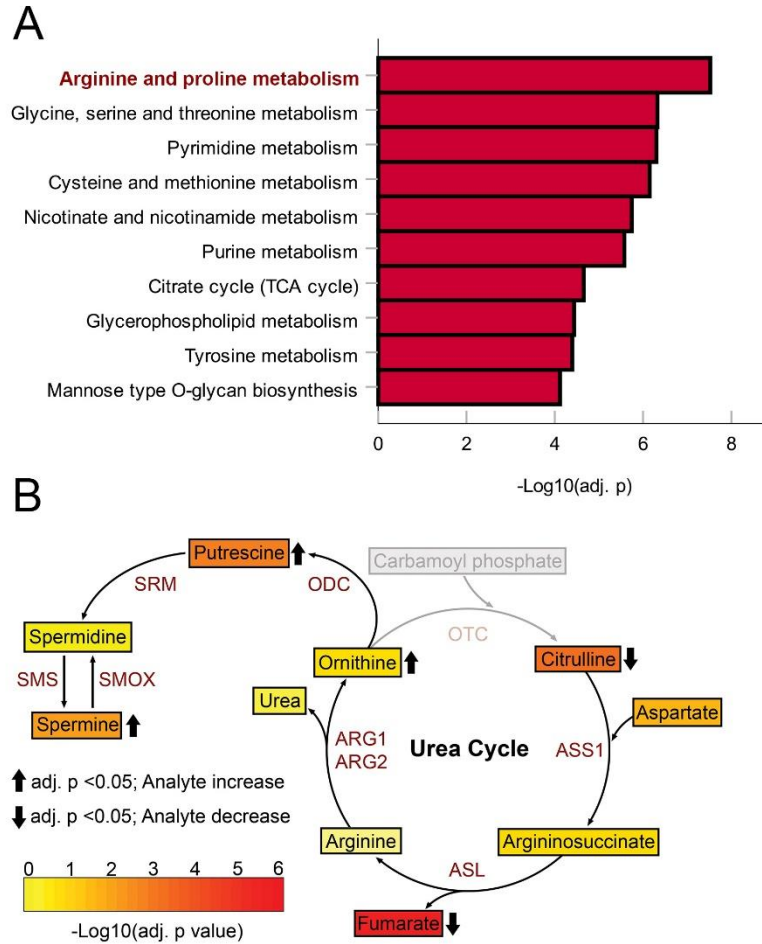


Figure 5: Treatment of B16F10 tumors alters Arg metabolism. B16F10 tumors established in C57Bl/6J mice were treated with either PBS (Mock) or MyxGFP. Four days post treatment, tumors were harvested and immediately snap frozen in liquid nitrogen. Whole tumor homogenates were then used to quantify a set of 189-metabolite species via LC-MS. **(A)** Metabolite Set Enrichment Analysis (MSEA) of LC-MS results. **(B)** Heatmap indicating significance of change in metabolite concentrations measured in LC-MS panel involved in the urea cycle and polyamine biosynthesis. Color indicates $-\text{Log}_{10}(\text{adj. } p \text{ value})$. Arrows indicate significant (adj. $p \text{ value} < 0.05$) increases or decreases in MyxGFP treated cohort relative to Mock cohort. Gray indicates species not evaluated in this panel.

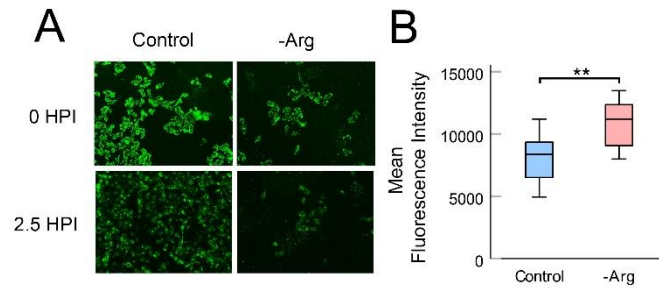


Figure 6: Binding of MYXV to B16F10 cells in Arg starved conditions is comparable. (A) Fluorescence images of MyxVenus 0 hours after binding (top) and 2.5 hours after binding/entry (bottom) in Control and -Arg conditions. **(B)** Boxplot of mean fluorescence intensities (MFI) of B16F10 samples bound with Cy5 labeled MYXV 0 hours after binding, quantified via flow cytometry. **Statistics: (B)** Unpaired Student's t-test. n = 6. ** p < 0.01.

Next, a time course across 24 hours was conducted comparing GFP expression within mock and Arg starved cells infected with MYXV (Fig 7A), quantified via flow cytometry. Early expression of GFP was comparable between cells until 5 hours post infection, after which the comparative difference grew in magnitude. Importantly, the shift from early production of GFP to late production of GFP can be observed in the Arg starved cells (Fig 7B), though with about a 10-fold reduction in GFP intensity compared to controls, implying that some shift from early to late gene expression does occur in Arg starved cells. Next, genome synthesis of MYXV was quantified by measuring viral genomes over a similar time course (Fig 7C). Not unlike the GFP expression, genome abundance became significantly reduced by 6 hours post infection, with an average ΔCt of 3.30 comparing Arg starved cells to mock at 24 hours. Again, geometrically, the kinetics of genome production were quite comparable, simply with a significant reduction in magnitude in Arg starved cells.

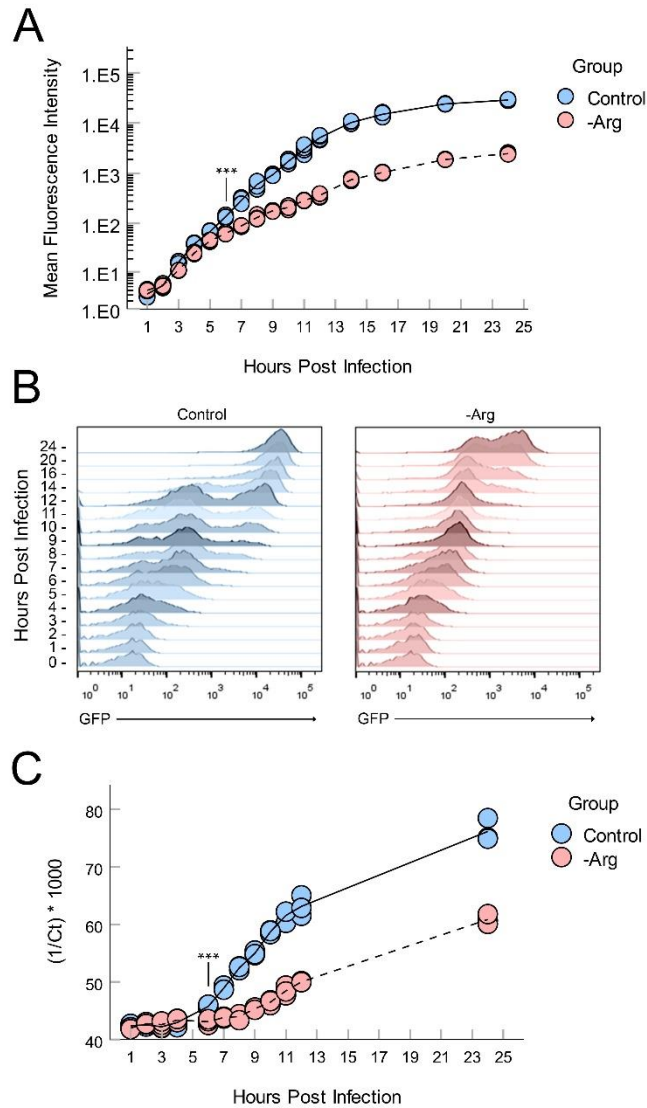


Figure 7: MYXV viral gene expression and genome abundance are reduced in Arg starved conditions. (A) Dot plot of MFI of GFP within individual samples of MYXV infected B16F10s grown in Control and -Arg media through 24 HPI (48 hours of Arg starvation total) via flow cytometry. Significance is maintained at the point indicated and every point thereafter. **(B)** Representative histogram distributions of GFP fluorescence intensity from samples in (A). **(C)** Dot plot of MYXV genomes in cells conditioned as in (A-B) quantified via qPCR. Y-axis represents inverse Ct values per sample multiplied by 1000. Significance is maintained at the point indicated and every point thereafter. **Statistics: (A),(C)** Unpaired Student's t-test comparing Control and -Arg per time point. *** $p < 0.05$. $n = 3$ for both experiments.

4.4: Discussion

The results in this section critically demonstrate that – like in other DNA viruses – access to Arg may be of particular importance to MYXV replication. MYXV exhibited a strong dependency on Arg for viral replication, with a 3-log reduction in production of new infectious particles barely above the background input of virus remaining from the initial inoculum.

The obstacle(s) for this loss of viral replication is likely multifactorial. Initial experiments quantifying viral binding demonstrated no meaningful differences in the ability of MYXV to bind Arg starved cells compared to controls. This is a somewhat expected result, as binding and entry of MYXV to cells is putatively both independent of specific cellular receptors and redundant in nature [98, 169], and is likely to be unaffected so long as the amount of negatively charged moieties on the cellular surface – such as heparan sulfate – remain unchanged. It is possible Arg starvation may change endocytic trafficking within cells by stalling synthesis of proteins, including those required for endocytosis. While not directly quantifiable by the approaches here (fluorescent signal is internal during entry, and disseminated within cells upon uncoating, but theoretically the same total cellular intensity whether bound, entering, or uncoated when quantified via flow cytometry), imaging of infected cultures under these conditions did not glaringly suggest entry and/or uncoating were majorly affected. GFP production and genome synthesis were both more markedly reduced in Arg starved cultures, but still not to a degree representing a 3-log decrease in production of infectious progeny. Importantly, both metrics followed the same geometric patterns but with reduced maximums, implying the virus was able to commit to completion steps in the viral life cycle up to and through late gene expression.

It is possible that a certain stoichiometry of viral components is required for production of infectious progeny and is simply not met; this notion is challenged, however, by the observation that new infectious particles are first detectable between hours 6-9 in control conditions, but

despite viral protein (by GFP expression) and genomes in Arg starved cells being even higher at 12/24 hours compared to the 6-9 range in controls, there is still markedly more infectious particles produced at hour 9 in controls compared to 12/24 in Arg starved groups. It is also unlikely that all viral translation will be affected the same by lack of Arg, as some genes encode more Arg residues than others do. It is certainly possible that the block in MYXV replication is a result of a specific Arg-rich protein being translated at particularly low/non-existent rates. In its primary structure, eGFP is underrepresented in Arg content as it contains only 6 Arg residues of the 239 sized protein (2.5%), and may be a poor surrogate in this regard to evaluate global MYXV protein production. This under-representation is compared to the 4.2% frequency of Arg within proteins of vertebrates, and is an interesting outlier where the coding frequency of Arg is significantly less than expected given a coding redundancy of 6 codons [170].

This concept is particularly worth considering as Arg residues are very commonly found in proteins as mediators of protein:protein and protein:nucleic acid interactions due to its cationic guanidinium group [171]. Protein and nucleic acid binding are functions that are profoundly common in viral proteins associated with packaging/assembly, necessitated both by mandatory inclusion of core proteins and concentrating negatively charged RNA/DNA into a virion, and could be the source of this phenomenon. This is exemplified in AdV, with several assembly related proteins disproportionately rich in Arg residues [144]. This may be the case in MYXV as well, as evidenced by evaluating the Arg content of MYXV ORFs with known or predicted protein products (Appendix B). Here, several outliers are observed to be particularly enriched in Arg content, including M000.5L, M3.1L/R, M156R, M005L/R, and M093 (uncharacterized, uncharacterized, predicted eIF2 α mimetic/RNA binder, M-T5 – Akt phosphorylator, core protein, respectively). Interestingly, as previously mentioned, M-T5 is an important host range factor in MYXV [91] mediating Akt phosphorylation, but also responsible for protection host cells against cell cycle

arrest by competitive binding to Cullin-1 (a subunit of the skp, cullin, F-box (SCF) E3 ubiquitin ligase complex) [172]. M093, a major viral core protein of MYXV, exhibits similarly increased Arg content compared to that described in Adv; *Adenoviridae* and *Poxviridae* are quite evolutionarily distinct [173], but as DNA viruses, both require charge stabilization of their DNA genomes during viral packaging, and the heightened Arg content of M093 may indicate a similar function of Arg in Adv core proteins. Experiments evaluating assembly would be required to verify these explanations, such as electron microscopy, to determine what degree of particle assembly is occurring. It would additionally be worthwhile to determine the content of M093 and MT5 being produced in an Arg starved context, but lack of specific antibodies may make this approach more difficult without designing a MYXV construct bearing a non-disruptive tag. MyxVenus, used in this study, could be used in this capacity, but the presence of the Venus fluorescent protein fused to M093 itself induces a major replication defect, and may not be an appropriate tool to use in this sense.

These experiments aimed to coarsely characterize the phenotype of MYXV replication under Arg starved conditions and to confirm the possibly biological relevance of this dependency, but offer no insight as to the cellular/viral mechanisms leading to arrest of a specific step in the viral life cycle. One potential model is that lack of Arg simply prevents effective translation of these aforementioned Arg rich proteins by eliminating a critical building block. While this model is conceptually attractive, the observation that cells starved of Arg do not die somewhat argues that factors beyond a prolonged lack of protein synthesis may be playing a role. An alternative model is that the lack of Arg activates the integrated cellular stress response. The integrated cellular stress response is mediated by the activity of four proteins: GCN2, PKR, HRI, and PERK responding to amino acid deprivation, viral infection, heme deprivation, and ER stressors respectively [174], visualized in Fig 9. GCN2's activation as a result of amino acid starvation is triggered by its binding to uncharged tRNAs. This activation subsequently blocks overall protein

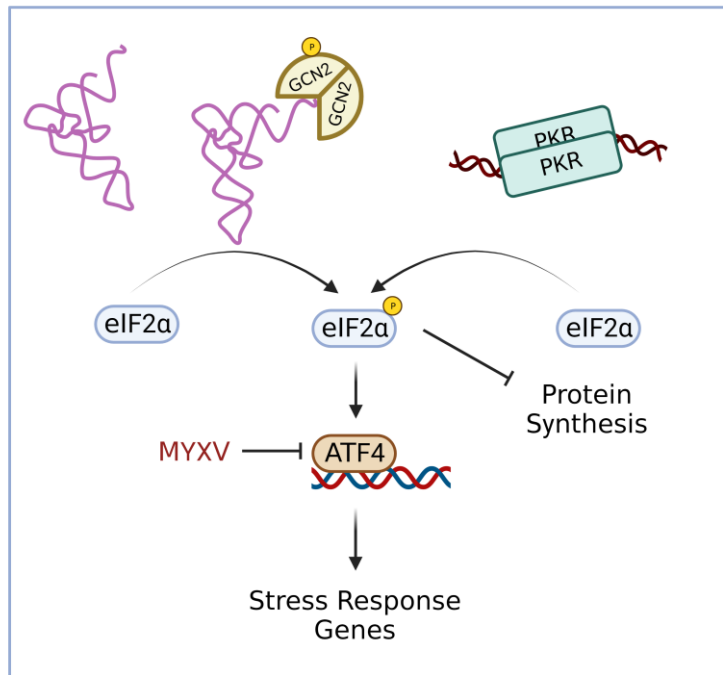


Figure 8: Amino acid starvation initiates the integrated stress response. Starvation of amino acids results in the buildup of uncharged tRNAs. The homodimer of General Control Nonderepressible 2 (GCN2) binds to and is activated by binding to either uncharged tRNAs or the exposed P-stalk of stalled ribosomes (not shown). GCN2 then phosphorylates eIF2 α , thus inhibiting initiation of mRNA translation to halt protein synthesis. Phosphorylation of eIF2 α additionally causes mRNA transcripts of ATF4 to become translated. Here, the normally inhibitory uORF2 of ATF4 mRNA (that causes dissociation of ribosomal machinery after its translation) is skipped, in turn allowing for translation of ATF4. ATF4, a transcription factor normally blocked by MYXV infection, then promotes transcription of genes related to stress response, such as amino acid import and biosynthesis, redox maintenance, and autophagy. Beyond amino acid starvation, the integrated stress response is triggered by HRI and PERK (not shown), as well as PKR, a detector of dsRNA that is an important mediator of antiviral and interferon responses.

translation by phosphorylating eIF2 α [154, 175], as well as repressing mTORC1 via Sestrin2 (this latter effect is contingent on simultaneous starvation of leucine, however, as L-leucine binding to Sestrin2 prevents its ability to inhibit GATOR2-GATOR1-RagB pathway ultimately repressing mTORC1) [176]. Phosphorylation of eIF2 α is a well-established antiviral measure that functions by globally stalling translation to affect cell and virus alike [177]. Arginine itself has a separately dedicated pathway functioning through mTORC1 through CASTOR1, though this pathway may be suppressed within certain cancers [178, 179]. Interestingly, activation of this integrated stress response leads to translation and/or recruitment of proteins also sometimes associated with an antiviral response, such as ATF4, and this has been previously shown to be translationally inhibited by MYXV indicating it is a pathway relevant to antiviral host response in MYXV [180]. Similarities between the overall responses to amino acid starvation and viral infection may therefore cause a scenario where lack of Arg induces a cellular state sufficiently overlapping with an anti-viral response to cause severe inhibition of viral replication. This notion is reinforced by evidence that GCN2 has been demonstrated to be directly activated in virally infected cells implying a role for this pathway within a genuine anti-viral response [181-184].

Regardless of the mechanism at hand, MYXV appears to particularly depend on Arg access for viral replication compared to others, quite like the historical studies describing Arg dependency in other DNA viruses. As the metabolic state of a cell and virus are inextricably connected, the degree of reliance on Arg in relation to other amino acids could very well be cell type specific that reflects the synthesis, accumulation, and consumption of different amino acids. Nevertheless, this brief study confirms the notion that Arg is an important amino acid in MYXV infection, and loss of Arg access may act as a barrier to optimal MYXV replication.

Chapter 6: Ablation of Gr-1⁺ Cells Amplifies Viral Replication in B16F10 Tumors

This chapter has been modified from the following publication, under major revision:

Dryja PC, Flores EB, Bartee E, Myeloid-Derived Suppressor Cell-Mediated Alterations of Arginine Metabolism within the Tumor Microenvironment Inhibit Oncolytic Myxoma Virus Infection. *Molecular Therapy – Oncolytics*. 2022.

6.1: Introduction

Oncolytic virotherapy (OV) represents a class of immunotherapeutics that employs a spectrum of viruses to treat numerous types of cancer. These oncolytic viruses exploit various defects intrinsic to malignant cells to establish tumor-specific infections while sparing surrounding healthy tissues. The clinical impact of OV occurs through two main mechanisms. For some viruses, efficacy is largely mediated through the lytic potential of the virus with tumor regression being caused by the rapid destruction of directly infected malignant cells. For other viruses, including myxoma virus (MYXV), efficacy is driven primarily by the virally initiated recruitment of anti-tumor immune cells [152]. Fundamentally, however, both of these mechanisms rely on the replication and spread of the oncolytic agent within treated tumors and the factors that influence this replication are not completely understood.

Outside of OV, it is well established that all viral replication relies on host metabolism, and the ways in which viruses both actively and passively influence metabolism during 'normal' infections are well-studied [185-187]. Unlike the healthy tissues these viruses evolved to infect, however, metabolism within the tumor tissues they are used to treat is markedly different [188-190]. Indeed, this metabolic dysregulation is considered one of the fundamental hallmarks of cancer [47]. One such type of metabolic dysregulation is increased turnover of L-arginine (Arg) through the function of Arginase-1 (ARG1), an enzyme responsible for the hydrolysis of Arg into L-ornithine and urea, that is commonly expressed in tumoral myeloid derived suppressor cells (MDSCs) and tumor associated macrophages (TAMs) [128, 138, 191]. Strikingly, despite relatively

robust bodies of work separately defining the metabolic dependencies of viruses and the metabolic changes within the tumor microenvironment (TME), studies into the impact of intratumoral metabolism on OV performance remain lacking. Given our previous results implicated Arg and Arg metabolism as pertinent to MYXV, we next sought to determine if the function of ARG1 through MDSCs could contribute to low levels of Arg that could blunt MYXV replication. Here, we test this hypothesis by evaluating possible correlation of tumoral MDSC burden and tumoral viral burden, if the removal of MDSCs potentiates MYXV replication, and if MDSCs can suppress viral replication in an ARG1 dependent manner.

6.2: Methods & Materials

Mouse Models: Female C57Bl/6J or NOD/*scid*/*IL2Rγ*^{null} (NSG) mice aged 6–10 weeks were subcutaneously (SQ) seeded with 1×10^6 tumor cells in 50 μ L of cold PBS on top of the lower abdomen. In experiments measuring therapeutic response, only mice bearing palpable 25mm² tumors at time of treatment were considered for use. For immune depletion studies, mice were treated with the following antibodies via intraperitoneal injections: α Gr1 (NIMP-R14 200 μ g), α NK1.1 (RK136, 300 μ g), α CD8 (53–6.7, 100 μ g), α CD4 (GK1.5, 100 μ g). All depletions were delivered 24 hours prior to intratumoral infection with either MyxGFP or MyxPD1/IL-12.

Cell Lines and Culture Reagents: The B16F10 cell line used for murine models was a CRISPR scramble control from the original ATCC cell bank. hARG1 was purchased from VWR (10797-002 VWR, Radnor, PA) and reconstituted in PBS prior to use. Arginine variant medias were created using Dulbecco's MEM High Glucose without arginine (D9812-07A; United States Biological, Salem, MA) reconstituted with 3.7g/L sodium bicarbonate, with filter-sterilized 40mM L-Arginine-HCl (97062-466, VWR, Radnor, PA) in PBS added into the media at specified concentrations. Arginine free media reconstituted with 400 μ M L-Arginine-HCl was used for all control conditions. Cell lines were maintained in standard DMEM (Corning, Corning, NY). All growth medias were supplemented with 10% FBS (VWR, Radnor, PA) and 1 \times penicillin/streptomycin/glutamine (Corning, Corning, NY). Cultures were checked quarterly for mycoplasma contamination by qRT-PCR. For inhibition of ARG1, Nor-NOHA (N-o-Hydroxy-L-norarginine; f-3865 1000, Bachem, Bubendorf, Switzerland) acetate salt was used at a concentration of 5 μ M dissolved in PBS.

Histology: B16F10 tumors harvested from mice at the specified times were embedded in OCT and frozen at -80°C. Sagittal sections of tumors were cut in a cryostat at 8 μ m section thickness. Images were generated using a Leica TCS SP8 confocal microscope on non-fixed tumor

sections with excitation at 488nm. Resulting image stacks were mosaic merged on LASX acquisition software. Final images were used to quantify infection area, foci count, and foci characteristics in Fiji [192].

Flow Cytometry: Tumor portions were recorded for weight, crushed over a 40 μm mesh strainer, and rinsed with 2 mL of PBS. Cell suspensions were then centrifuged at 750 RCF for 5 minutes, and subsequent cell pellets used for flow cytometry or viral titering (later described). Cells were stained using standard flow cytometry methods with vital dye and the following antibodies: αCD45 (30-F11), αCD11b (M1/70), αLy6C (AL-21), αLy6G (1 A8), αCD3 (145-2C11), αCD4 (RM4-5), αCD8 (53-6.7), $\alpha\text{NK1.1}$ (PK136), $\alpha\text{IL-7R}$ (SB-199), αCD49B (DX5). All antibodies used for flow cytometry were obtained from BD Biosciences (San Jose, CA).

Viral Constructs: Both viral constructs used (MyxGFP, MyxPD1/IL-12) are based on the Lausanne strain of MYXV [155, 156] and have been previously described [154, 157]. Virus was clonally isolated through 4⁺ rounds of sequential plaque purification for GFP⁺/TdTR⁺ foci, amplified in BSC40 cells, and purified using gradient centrifugation as previously described [158].

Viral Titering: To liberate virus from infected cells, cell pellets from either cell culture or infected tumor samples were freeze-thawed over three cycles in liquid nitrogen and a 37°C water bath. Pellets were frozen a fourth time in liquid nitrogen and sonicated for 3 minutes. Resulting homogenates containing virus were serially diluted in a logarithmic series and plated onto confluent BSC40s. GFP⁺ foci were quantified 48 hours post-infection to determine viral titer of original samples.

Statistical Methods: All statistical analyses were performed in SPSS, with each specific test notated within figure legends. All error bars indicate SEM unless noted otherwise in figure legends.

6.3: Results

Depletion of MDSCs improves MYXV replication in vivo

Within the TME, ARG1 is predominantly expressed by immune suppressive white blood cells, most notably myeloid-derived suppressor cells (MDSCs) [150, 193, 194]. Since our previous results indicated that the presence of ARG1 can negatively influence MYXV replication, we next evaluated whether the abundance of these cells might correlate with viral yields *in vivo*. Consistent with our overall hypothesis, linear regression analysis revealed that, in the absence of additional interventions, a strong negative correlation existed between the amount of infectious virus produced in a virally treated tumor and the presence of granulocytic-MDSCs (G-MDSCs) within the tumor (Fig 9A). Based on this data, we next asked whether removal of these cells from tumors might improve subsequent viral replication. The results indicated that specific depletion of G-MDSCs (CD45⁺/CD11b⁺/Ly6C^{lo}/Ly6G⁺) and monocytic-MDSCs (M-MDSCs) (CD45⁺/CD11b⁺/Ly6C^{hi}/Ly6G⁻) from tumors through injection of α Gr-1 depleting antibody resulted in significant increase in both viral titers (Fig 9B) and area of infection within tumors (Fig 9C-D). These effects were not observed following similar depletion of other immunological subsets tested (Appendix C) suggesting that MDSCs might represent a major immune cell impacting MYXV replication within tumors. To better understand how depletion of MDSCs was enhancing MYXV replication, we next asked whether the elimination of these cells altered the initial establishment or subsequent persistence of MYXV infections. We observed that, up to four days post-infection, the total viral burden in tumors was comparable between control and α Gr-1 treated cohorts. At six days post viral treatment, however, overall viral titers in control cohorts began to decay while titers in α Gr-1 treated animals were maintained (Fig 10A). Histological analyses of tumors revealed a similar phenotype, with the total number of viral foci being statistically similar until 4

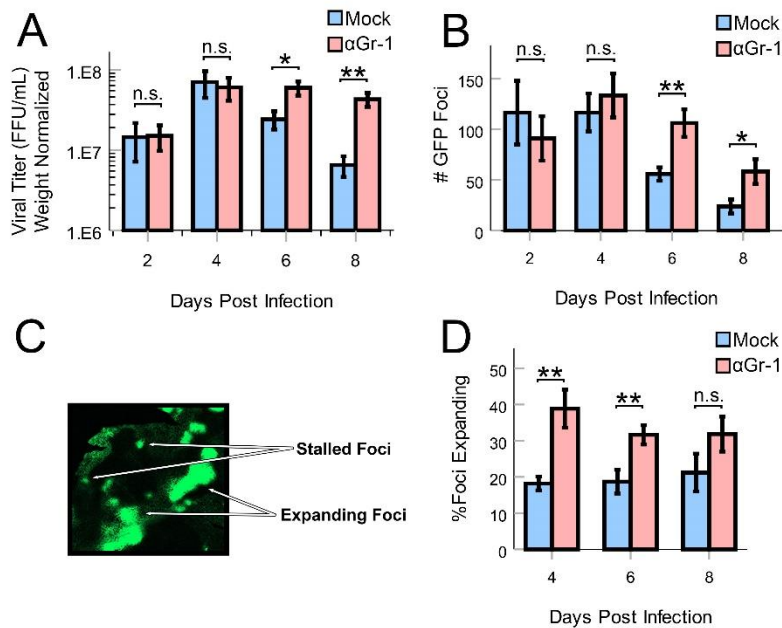


Figure 9: Viral burden and infection area in MyxGFP infected B16F10 tumors in α Gr-1 treated mice versus Mock. (A) Linear regression analysis evaluating the correlation of tumoral viral burden and their proportion of tumoral Gr-1+ cells within living CD45+ subpopulation 8 days post infection. **(B)** Dot plot (dots) and averages (dotted line) of MyxGFP titer from Mock and α Gr-1 treated tumors 24 hours prior to infection with MyxGFP 8 days post infection. **(C)** Representative fluorescence images of tumor sections under the same treatment conditions seen in (B). **(D)** Dot plot (dots) and averages (dotted line) of MyxGFP infection area in tumors from (C). **Statistics:** (B) Unpaired Student's t-test, *** $p < 0.001$, $n = 8-10$ mice. (D) Unpaired Student's t-test, ** $p < 0.01$, $n = 21-27$ mice.

days post-infection, but subsequently decreasing in control animals while being better maintained in α Gr-1 treated cohorts (Fig 10B). Visual analysis of viral foci throughout this time course revealed two distinct phenotypes: expanding foci that presented as large infections made up of numerous cells and stalled foci made up of relatively few cells. Interestingly, while the total number of foci was similar at 4 days post viral treatment, a higher percentage of these foci displayed an expanding phenotype in α Gr-1 treated animals compared to controls (Fig 10D). Collectively, these results suggest that depletion of MDSCs increases viral burden in tumors by promoting sustained replication and spread.

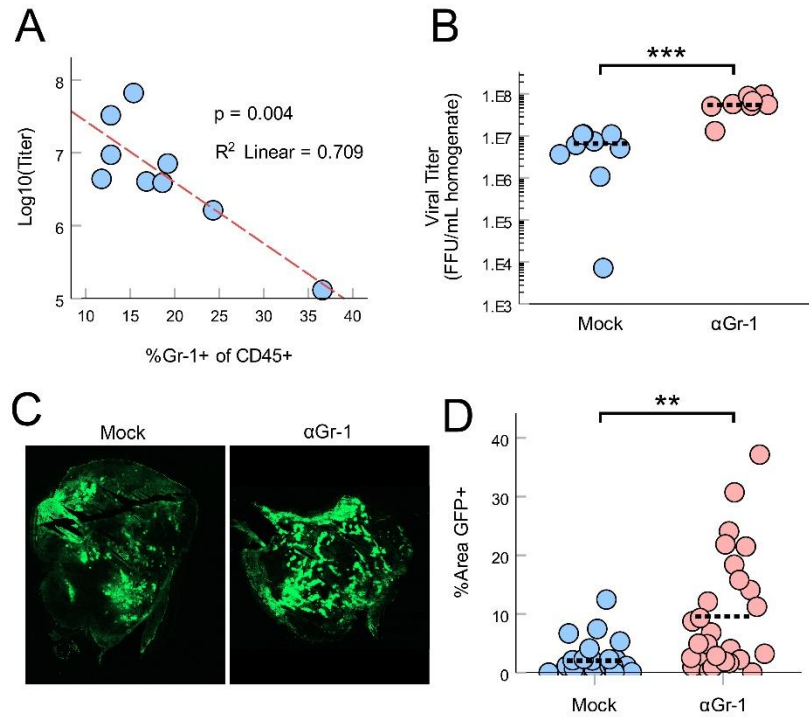


Figure 10: Kinetics of viral replication and spread in MyxGFP infected B16F10 tumors in α Gr-1 treated mice versus Mock. B16F10 tumors of C57Bl/6J mice were depleted of MDSCs and infected with 1×10^7 FFU of MyxGFP 24 hours after depletion. Tumors were harvested 2-8 days post infection for viral quantification and histological analyses. **(A)** Detonator plot of tumoral MyxGFP titer. **(B)** Detonator plot of viral foci number in tumor tissue sections. **(C)** Representative fluorescence image of MyxGFP infected tumor displaying “expanding” and “stalled” foci quantified in (D). **(D)** Detonator plot of % of total foci considered “expanding” in tumor tissue sections from mice in (B). **Statistics:** (A-B,D) Unpaired Student’s t-test. n.s. = no significance, * $p < 0.05$, ** $p < 0.01$. Error bars indicate SEM. $n = 8-9$ mice per group, per day.

MDSC depletion reduces the initial dose of MYXV required to achieve a therapeutic response

Since elimination of MDSCs appeared to improve the viral health of oncolytic MYXV during therapy, we hypothesized that this depletion might enhance the overall therapeutic response to MYXV-based OV. To test this, mice bearing contralateral B16F10 tumors were depleted of MDSCs via injection of α Gr-1 and then treated with a single suboptimal initial dose of a recombinant MYXV construct expressing soluble PD1 and IL12 (Fig 11A)[157]. Under these low-dose conditions, treatment with α Gr-1 allowed for significantly improved tumor control, particularly in the directly injected lesion, resulting in enhanced overall survival (Fig 11B-C). These data suggest that preconditioning of tumors through depletion of MDSCs might allow for effective OV to be achieved using lower initial doses of virus.

ARG1 can block MYXV replication in vitro, and ARG1+ MDSCs block MYXV replication in an ARG1 dependent manner

Our previous results in Chapter 5 demonstrated that MYXV requires a significant pool of extracellular Arg for viral replication. Critically, it has been previously shown that extracellular Arg can be altered *in vivo* by ARG1 – an enzyme commonly expressed in several myeloid lineage cells associated with cancer [128, 138]. We therefore asked whether the presence of ARG1 would also inhibit MYXV replication under otherwise Arg replete conditions. B16F10 cells grown in standard DMEM were dosed with a log₂ dilution series of ARG1 for 24 hours and subsequently infected with MyxGFP at an MOI=5. Cells were then harvested 24 hours post infection and total viral yields determined (Fig 12A-B). The results indicated that incubation of cells with concentrations of ARG1 beyond 1 μ g/mL resulted in a reduction in virally derived GFP (Fig 12A) as well as a ~2log reduction in total viral titer (Fig 12B) with an IC₅₀ of ~0.8 μ g/mL, suggesting that the presence of exogenous ARG1 can negatively impact MYXV replication.

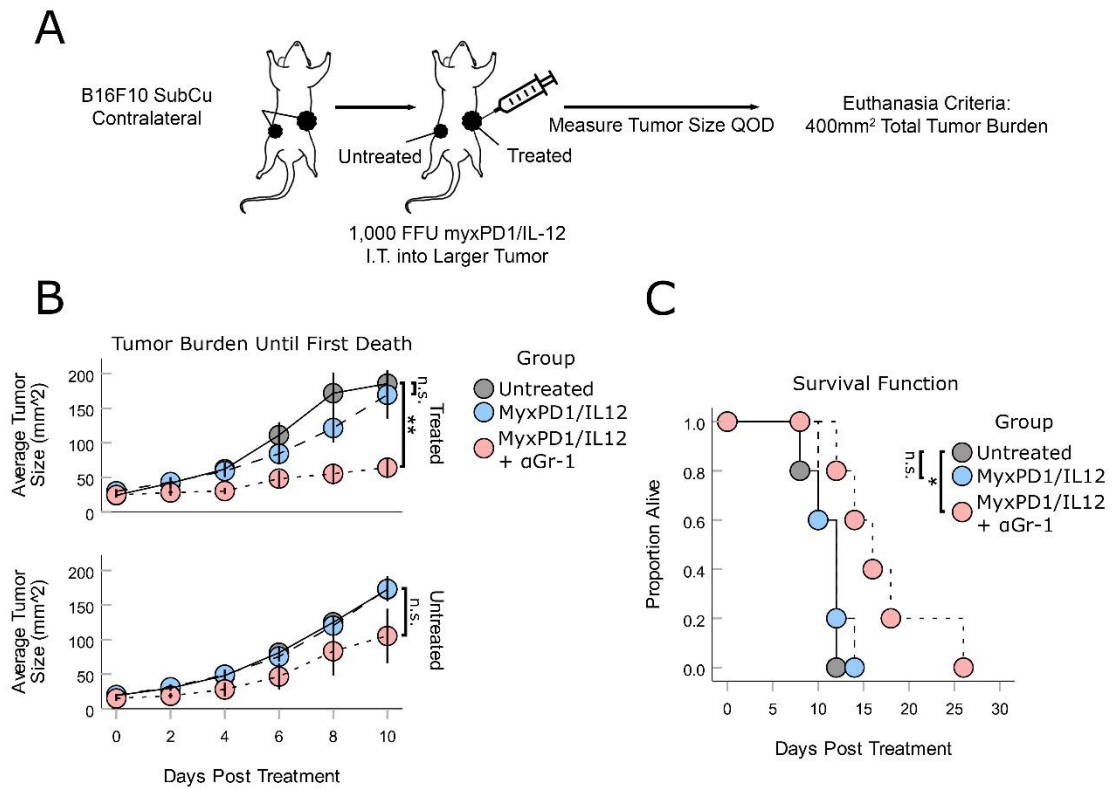


Figure 11: Depletion of MDSCs reduces the initial dose required to achieve an effective therapeutic response. (A) Schematic depicting experimental design of experiments in (B) and (C). C57Bl/6J mice bearing contralateral B16F10 tumors were treated with α Gr-1 24 hours prior to infection with MyxGFP at a dose of 1000 FFU/injection in the larger tumor. Tumor area was measured every other day until reaching a total tumor burden (sum of tumor A and tumor B) of 400mm². n = 5 mice per group. **(B)** Growth curves of both treated and untreated tumors until the day of first death in any cohort. **(C)** Survival curves by group. **Statistics:** (B) ANOVA with Tukey's HSD post hoc. ** p < 0.01. Error bars indicate SEM. n = 5 mice per group. (C) Breslow tests comparing respective groups.

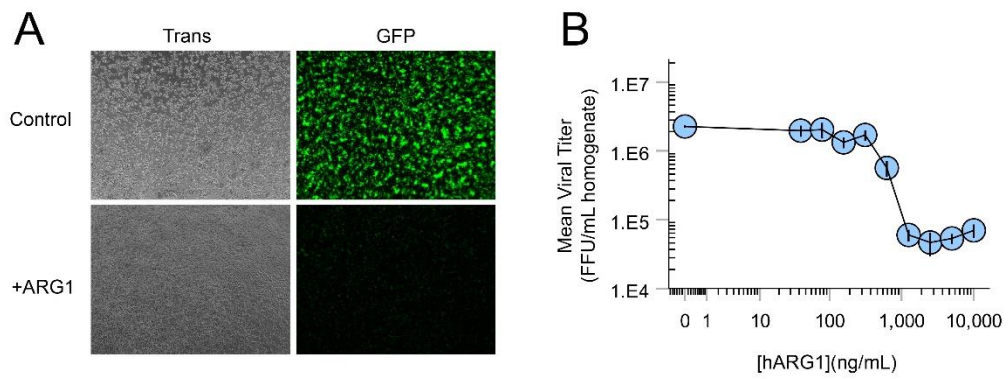


Figure 12: Activity of ARG1 reduces viral replication of MYXV in a dose-dependent manner. (A) Transmitted light and GFP fluorescence images taken 24 HPI in MyxGFP infected B16F10 cultures treated with 5 μ g/mL hARG1 or vehicle control 24 hours prior to infection. **(B)** Dot plot of mean viral titer 24 HPI in MyxGFP infected B16F10 cultures treated with a dose escalation of hARG1 or vehicle control 24 hours prior to infection. Error bars indicate SEM. n = 3.

In tumors, ARG1 is primarily expressed in immune suppressive MDSCs. Therefore, we next evaluated whether the presence of these cells might influence viral yields in a co-culture model (Fig 13A-C). Splenocytes were harvested from C57Bl/6J mice bearing large (~200mm²) B16F10 tumors, and granulocytic MDSCs (G-MDSCs; CD45⁺/CD11b⁺/Ly6C^{lo}/Ly6G⁺) were isolated using FACS. Splenic T cells (CD45⁺/CD3⁺) were also sorted as a control. Both sorted populations were then added to cultures of B16F10s at a 1:5 ratio. Cells were co-cultured for 24 hours in DMEM containing 80μM Arg – a concentration that marked the beginning of the plateau range for viral replication in previous experiments (Fig 4D) – in order to render any possible changes in Arg content apparent in viral yields (Schematic in Fig 13A). Cultures were then infected with MyxGFP at an MOI=5. Viral replication within each co-culture was then assessed after 24 hours by visually assessing expression of virally derived GFP (Fig 13A) as well as quantifying the production of infectious progeny (Fig 13B). The results indicated that GFP signal was markedly reduced in wells co-cultured with G-MDSCs and overall viral yield was reduced by 69%. Neither of these effects were observed in co-cultures containing splenic T cells. To determine if the observed reduction in viral health was mediated through altered Arg availability, a similar experiment was conducted in which G-MDSCs were co-cultured with B16F10 cells in either the presence of excess Arg (400μM) or the ARG1 inhibitor Nor-NOHA (5μM) (Fig 13C). The results indicated that both addition of excess Arg or direct inhibition of ARG1 eliminated the inhibition of viral replication seen following co-culture with G-MDSCs. Taken together, these results demonstrate that ARG1⁺ G-MDSCs can directly inhibit MYXV replication *in vitro* by depressing pools of Arg.

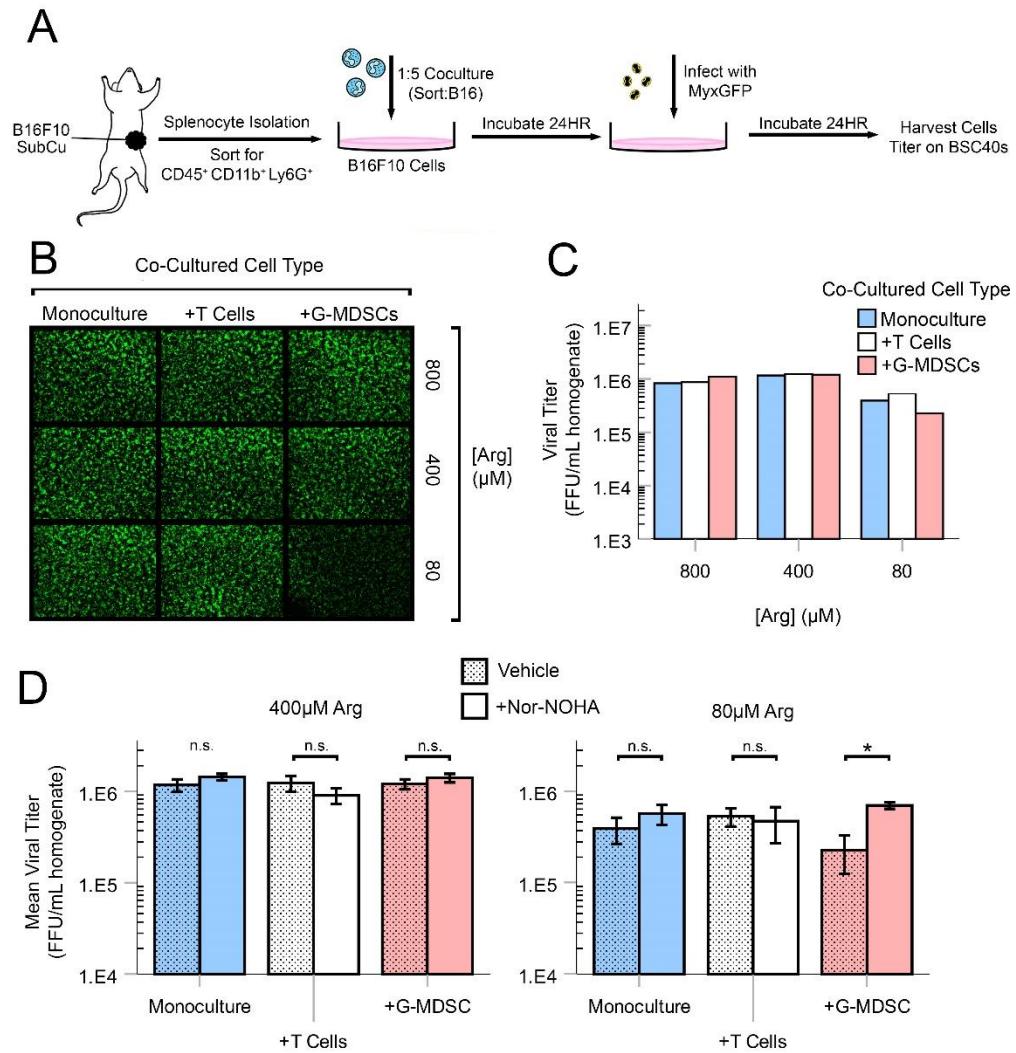


Figure 13: MDSCs inhibit viral replication of MYXV *ex vivo* in an ARG1 and Arg dependent manner. (A) Schematic depicting co-culture experiments seen in (B-D). **(B)** Transmitted light and GFP fluorescence images 24 HPI in MyxGFP infected B16F10 cultures co-cultured with the designated cell type 24 hours prior to infection in Arg variant media. **(C)** Bar graph of viral titers from samples seen in (B), n = 1 per group. **(D)** Detonator plots of replication of experiment in (B-C) using the ARG1 inhibitor Nor-NOHA (5μM). **Statistics:** (D) Unpaired Student's t-tests comparing vehicle control and Nor-NOHA within co-culture groups at different Arg concentrations. n = 3. * p < 0.05. Error bars indicate SEM.

6.4 Discussion

Although the efficacy of OV is dependent on replication of the viral agent within the TME, the barriers to replication and spread remain poorly understood. Previous work has clearly established that an intact antiviral host response represents one major obstacle to achieving effective infection within treated tumors [195, 196]. However, even within the context of severe immunodeficiency, such as totally immune deficient NSG mice, many oncolytic infections – including MYXV - still fail to achieve complete tumor control [106]. These data suggest that barriers to viral infection exist beyond the context of antiviral immune responses. Determining the identity of these barriers therefore represents an opportunity to improve our basic understanding of OV as well as enhance its therapeutic potential. In this context, our results suggest that metabolic deficiencies resulting from the presence of ARG1⁺ MDSCs within the TME may represent one such novel barrier.

Consistent with the bioavailability of arginine playing a key role in MYXV infection, our results demonstrated that depletion of ARG1⁺ MDSCs improved overall viral health *in vivo*. Interestingly, these results are largely counter to the canonical role of MDSCs in chronic viral infection. Indeed, previous work has suggested that the presence of these cells is often positively correlated with viral burden in patients with HCV and HIV, a phenomenon largely attributed to their ability to suppress anti-viral immune response allowing for robust infection [197, 198]. These chronic infection studies, however, occur in the context of viral infection of normal host tissue. Therefore, we feel that the apparent contradiction in the role of MDSCs might be due to the inherently stressed metabolic nature of the TME [47, 190]; additionally, previous studies have demonstrated the potential capacity of ARG1 in activated macrophages to act in an antiviral fashion [148].

The histological analyses of infected tumors demonstrate that removal of MDSCs does not influence the total number of infection events initiated after treatment, but rather influences the percentage of these events that successfully propagate over time. As observed *in vitro*, removal of arginine during viral infection results in non-productive single-cell infections much like the non-expanding foci observed *in vivo* – the presence of MDSCs may therefore be decreasing the areas within the TME that are amenable to viral infection by virtue of decreasing local arginine content. It is critical to point out, however, that our study cannot rule out MDSCs impacting MYXV replication through mechanisms other than arginine metabolism *in vivo*. Even within the realm of amino-acid metabolism, MDSCs have also been shown to cause reductions in available cysteine and tryptophan [199, 200] - both of which were also required for MYXV replication *in vitro* (Fig 4A). Without more specific interrogations into the role of ARG1 depressing viral titers *in vivo*, some of the observed data could therefore be due to the culmination of several metabolic factors being reversed rather than a specific liberation of arginine, a notion that is further supported by the widespread changes to metabolic compartments observed during intratumoral infection with MYXV. Beyond these considerations, it is also of note that use of α Gr-1 as a tool to specifically interrogate MDSC function is particularly poor and has many inconsistencies within the literature, but has no better commercially available alternative [201].

The specific impact of MDSCs within this study is complicated further by lack of professional agreement in what cell markers and attributes constitute an MDSC, and furthermore which cell types are included in this heterogeneous collection. In mice, the two subtypes of MDSCs - monocytic (M-MDSC), and granulocytic/polymorphonuclear (G/PMN-MDSC) - are defined as CD11b⁺/Ly6C^{hi}/Ly6G⁻ and CD11b⁺/Ly6C^{lo}/Ly6G⁺ respectively. Using only these molecular descriptors as the basis for classifying MDSCs leaves real overlap with canonical monocytes, and particularly neutrophils in the case of G-MDSCs [202]. Indeed, utilizing only cell surface markers

as the basis for identification does not allow for the distinguishing of MDSCs and their non-MDSC counterparts. As such, our verification that α Gr-1 treatment depleted MDSCs via flow cytometry of treated tumors (unpublished observation) in these experiments may well have been observing the depletion of these other immune subsets beyond MDSCs. Lacking the ability to distinguish these cell populations, and not being able to cause the selective depletion of MDSCs *in vivo* while sparing monocytes and neutrophils, reduces the certainty that the phenomenon of “MDSCs” reducing viral burden is one that is truly attributable to MDSCs. Given the context of this study, it is particularly worth considering that the observations herein may be a product not from the removal of MDSCs within tumors, but from the elimination of monocytes and neutrophils that can act in an antiviral capacity; their respective contributions to antiviral immunity may be responsible for our observations here. However, this discrepancy is a common thread uniting many studies involving MDSCs. While it is certainly worth considering as a contextual piece of information, solving this issue of MDSC nomenclature and characterization is beyond the scope of this study.

Interestingly, while depletion of MDSCs improved OV efficacy during treatment with suboptimal viral doses, it had no effect on the efficacy of high-dose therapies (Fig 11). This effect is reminiscent of previous work which indicated that – at least for MYXV-mediated OV – therapeutic response is a thresholded event, where efficacy requires a baseline dose of MYXV that is not improved with further dose increases [203]. Assuming our higher therapeutic dose was already above this threshold, this might explain why no improved tumor control was observed. In contrast, depletion of MDSCs increasing the proportion of tumor tissue that is infection-permissive in theory would allow for the threshold to be reached by using much smaller initial doses of MYXV, which is precisely the phenotype observed in our histological analyses. Even if no therapeutic advantage to blocking the effects of ARG1 exists at sufficiently high doses, the

potential to reduce the amount of necessary dose to elicit maximal response is still of logistic and commercial worth.

Additionally, the effects of ARG1 expression via MDSCs within the TME impacting OV performance may be reduced in mice compared to what may be seen in a human context as a result of the underlying biology of human MDSCs. In mice, ARG1 protein is retained within the cytoplasm of MDSCs where the expression of CAT2b increases Arg import for ARG1 mediated lysis of Arg into ornithine and urea. In humans, however, ARG1 is actively released into the TME from intracellular granules of PMN-MDSCs [204]. This active secretion of ARG1 into the TME by human MDSCs obviates the need for MDSCs to first import Arg in order to cause its degradation; secreted ARG1 may then be better dispersed throughout the tumor, and perhaps more importantly, may be more effective at reducing Arg content by virtue of eliminating the requirement of MDSCs to first compete for Arg import. Furthermore, the circulating content of Arg in humans is somewhat lower compared to mice (41 μ M-114 μ M in healthy humans [164], but 100-120 μ M in mice [166]), reducing the amount of Arg that ARG1 needs to eliminate before it becomes restrictive on viral replication within the TME.

Furthermore, this difference in the biology of ARG1 in mice and humans provides an opportunity to more easily block its activity *in vivo*. Protected within a cell, methods to inhibit ARG1 activity by encoding an ARG1-inhibitory protein or peptide within a therapeutic OV construct would be exceptionally limited. However, as a result of MDSC ARG1 being secreted within the TME, it becomes more targetable. The potential for ARG1 to be inhibited by antibodies has been explored and confirmed in by previous groups [205], and the development of a MYXV construct encoding an scFv against ARG1 would be poised to take advantage of this biological difference.

Ultimately, our results demonstrate that MDSCs may be effectively antiviral coincident with their function within the TME, and therefore negatively impact OV performance. Though further study is required to verify a mechanism *in vivo*, these cell populations *ex vivo* demonstrably depress MYXV titers through an Arg and ARG1 dependent mechanism, indicating a potential role within the tumor.

Chapter 7: Loss of ASS1-mediated Arginine Biosynthesis Reduces Tumor Capacity to Support Viral Infection

This chapter has been modified from the following publication, under major revision:

Dryja PC, Bartee M, Curtsinger H, Bartee E. Defects in Intratumoral Arginine Metabolism Attenuate the Replication and Therapeutic Efficacy of Oncolytic Myxoma Virus. *JITC*. 2022.

7.1: Introduction

Oncolytic Virotherapy (OV) is a type of cancer immunotherapy used to treat cancers by delivering naturally or engineered cancer-specific viruses directly into lesions. This intentional infection of tumors causes destruction of malignancies through two mechanisms: by virally-mediated cell death (oncolysis), and by recruitment of an anti-cancer immune response generated as a result of infection (oncolytic vaccination). In both cases, viral replication is largely required to mediate these mechanisms, particularly when employing OV agents recombinant with therapeutic transgenes.

Viruses replicate by hijacking cellular host processes for their own gain. This includes access to metabolism, as all viruses are metabolically inert, and completely rely on co-opting host metabolites to replicate [206, 207]. In cancer, metabolism is commonly dysregulated – the chaotic and poorly vascularized nature of tumors, combined with a tendency of rapid proliferation in some cancer types, leads to a nutritive competition within the TME [208-211]. In the context of OV, this increased competition for nutrients may be excessive to result in reduced replication, and is likely different from what these viruses have evolved to accommodate. As such, perturbations to tumoral metabolism may pose a barrier to optimal OV performance.

Our previous work demonstrated that MYXV exhibits a strong dependency on Arg for viral replication. In this chapter, we evaluate the impact of tumoral dysregulations within L-arginine (Arg) biosynthesis via loss of argininosuccinate synthetase 1 (ASS1) as a potential factor restricting replication of MYXV within tumors.

7.2 Methods & Materials

Cell Lines and Culture Reagents: Both the BSC40 and B16F10 cells lines were purchased from the American Type Culture Collection (Manassas, VA). ASS1^{KO} B16F10 cell lines were generated using a CRISPR/Cas9 system targeting murine ASS1 (gRNA sequence: TCAGGCCAACATTGGCCAGA; plasmid: PX459) as previously described [153, 154]. B16F10 cells treated with a scrambled gRNA (referred to in this paper as ASS1^{wt} cells) have been previously described [153]. Cell lines were maintained in standard Dulbecco's Modified Eagle Medium (DMEM) (Corning, Corning, NY). Media lacking Arg was created by starting with powdered –Arg DMEM (United States Biological, Salem, MA) and supplementing with 3.7g/L sodium bicarbonate, 110mg/L sodium pyruvate, and 16mg/L phenol red, and subsequently filter-sterilized. Arg free media reconstituted with 400 μ M L-Arg-HCl was used for all control conditions. For citrulline rescue conditions, Arg free media was supplemented with 400 μ M L-Citrulline (Sigma-Aldrich, St. Louis, MO). For argininosuccinate rescue conditions, Arg free media was supplemented with 400 μ M argininosuccinic acid disodium salt hydrate (Sigma-Aldrich, St. Louis, MO). All growth medias were supplemented with 10% fetal bovine serum (VWR, Radnor, PA) and 1 \times penicillin/streptomycin/glutamine (Corning, Corning, NY). Cultures were checked quarterly for mycoplasma contamination using PCR.

Mouse Models: Female C57Bl/6J mice aged 6–10 weeks were seeded with 1 \times 10⁶ tumor cells (B16F10 ASS1^{WT}/ASS1^{KO}) in 50 μ L of cold phosphate buffer saline (PBS) subcutaneously (SQ). Tumors were allowed to establish until they reached \sim 25mm² prior to use. Mice that did not establish consistent tumors were removed prior to the initiation of the experiment. In experiments measuring therapeutic response, mice were euthanized when their tumors reached 15mm in any direction. All experiments were approved by the University of New Mexico Health Science Center institutional animal care and use committee under protocol #20-201002-HSC.

Histology: B16F10 tumors harvested from mice at the specified times were embedded in optimal cutting temperature compound and frozen in liquid nitrogen-chilled isopentane for cryosectioning. Sagittal sections of tumors were cut in a cryostat at 8µm section thickness. Images were collected on an Evos M5000 microscope using the GFP filter cube. Final images were used to quantify infection area, foci count, and foci characteristics in Fiji [192].

Flow Cytometry: Tumor portions were recorded for weight, crushed over a 40 µm mesh strainer, and rinsed with 2 mL of PBS. Cell suspensions were then centrifuged at 750xg for 5 minutes, and subsequently stained using standard flow cytometry methods. Data was analyzed using FlowJo™ (V10.4). The following antibodies were used in this study: Biotium Live-or-Dye™ 594/614 Fixable Viability Dye, CD8-PerCP (clone 53-6.7), CD25-PE/Cy5.5 (clone PC61), CD3-PacBlue (clone 500A2), CD45-BV510 (clone 30-F11), CD69-PE/Cy7 (clone H1.2F3), CD4-PE Fire 700 (clone GK1.5), F4/80-APC (clone T45-2342), Ly6c-BV421 (clone HK1.4), Ly6g-Spark blue 550 (clone 1A8), CD11b-BV570 (clone M1/70), I-Ab-Alexa 532 (clone M5/114.15.2), CD11c-BV786 (clone HL3), B220-APC/Cy5.5 (clone RA3-6B2), NK1.1-BV750 (clone PK136), CD49b-Alexa 647 (clone HMα2), NKp46-BV650 (clone (29A1.4), TIM3-PE/CF594 (clone 5D12), PDL1-BV480 (clone J43), CD49a-BV711 (clone Ha31/8). Antibodies were obtained from BD Biosciences (San Jose, CA, USA), Biolegend (San Diego, CA), and Invitrogen (Waltham, MA, USA).

PCR: mRNA was extracted from 1×10^6 cells using an RNEasy Plus kit (Qiagen, Hilden, Germany) after lysis through a QIAshredder homogenization column (Qiagen, Hilden, Germany). RNA content and quality was quantified on a Nanodrop system prior to cDNA synthesis via Superscript IV VILO RT system (Thermo Fisher, Waltham, Massachusetts). PCR was conducted using the PowerUp SYBR Green system (Thermo Fisher, Waltham, Massachusetts) on a 7500 Fast Real-Time PCR System (Thermo Fisher, Waltham, Massachusetts) using the indicated primers

(Table 1). PCR products were visualized via agarose gel electrophoresis on a 2% w/v agarose gel with ladder stained by ethidium bromide.

Table 1: List of PCR primers used within this chapter of the study.

Target	Direction	Sequence
ASL	Forward	ATAAAGTGGAGCCCTGAAGAAA
	Reverse	GGGTCTGGGATTTAAGGTGTAG
ASS1	Forward	CTTGAGGAAGCCAGGAAGAA
	Reverse	AGAGGTGCCCAGGAGATAG
OTC	Forward	CATGGGACAAGAGGATGAGAAG
	Reverse	GAACACTAATGACCGTGGAGAA

Viral Constructs and Infection: Both viral constructs used in the current manuscript, including recombinant MYXV expressing green fluorescent protein (MyxGFP) and recombinant MYXV expressing both the soluble ectodomain of programmed cell death protein 1 as well as interleukin 12 (MyxPD1/IL12) are based on the Lausanne strain of MYXV [155, 156] and have been previously described [154, 157]. Virus was amplified in BSC40 cells and purified using gradient centrifugation as previously described [158]. Infections were carried out by incubating cells in media containing the desired amount of virus for 30 minutes and subsequently removing viral inoculum and replacing it with fresh media. To quantitate infectious virus, cell pellets from either cell culture or infected tumor samples were freeze-thawed over three cycles in liquid nitrogen and a 37°C water bath. Pellets were frozen a fourth time in liquid nitrogen and then thawed/sonicated for 3 minutes. Resulting homogenates were finally serially diluted and plated onto confluent BSC40s. The number of GFP⁺ foci was then quantified 48 hours post-infection and used to determine the titer of original samples.

Metabolomics: CRISPR/Cas9 Scramble control or ASS1^{KO} B16F10 tumors were isolated from C57Bl/6J mice four days post-treatment with 1×10^7 foci forming units (FFU) of MyxGFP. Tumors were immediately snap-frozen in liquid nitrogen at point of harvest. Frozen tumors were weighed, and then broken into coarse homogenates using mechanical percussion in liquid nitrogen cooled vessels. 30-50mg of frozen coarse homogenates were then suspended in 80% methanol at 20 μ L/mg tissue. Suspensions were sonicated, centrifuged at 12,000xg, and the resulting supernatants analyzed via LC-MS by the Metabolomics Core Facility at Robert H. Lurie Comprehensive Cancer Center of Northwestern University (Chicago, IL) as previously described [159]. Samples were normalized against total ion count (TIC) and comparisons drawn between groups across peak area. Analysis of metabolomics data was performed using metaboanalyst [160] on TIC normalized data sets, with data re-plotted via ggbiplot R package.

7.3: Results

Intrinsic Arg biosynthesis can support MYXV replication in ASS1-competent cells

In the absence of exogenous Arg, many cells can directly biosynthesize this amino acid through the urea cycle. This biosynthesis requires the primary metabolic precursors citrulline and aspartate as well as expression of the urea cycle enzymes ASS1 and Argininosuccinate lyase (ASL), but are frequently silenced within some cancer types, including melanoma [115]. Since our previous studies had demonstrated that MYXV replication required bioavailable Arg, we next asked whether intrinsic Arg biosynthesis could rescue viral replication in the absence of this amino acid. To test this, we first evaluated expression of the urea cycle components in B16F10 cells using PCR and western blotting. The results demonstrated that, despite previous reports suggesting that ASS1 is frequently silenced in human melanomas, the murine-lineage B16F10s evaluated here expressed both ASS1 and ASL mRNA and protein (Figs 12A-B). Additionally, while removal of Arg induced cytostasis in B16F10 cells, this effect could be partially rescued by supplementation with exogenous citrulline (Fig 14C) suggesting that these cells were functionally Arg-autotrophic. Critically, citrulline supplementation also largely rescued MYXV replication in B16F10 cells (Fig 14D). Taken together, these data suggest that intrinsic Arg biosynthesis is sufficient to support MYXV replication when Arg pools are limited.

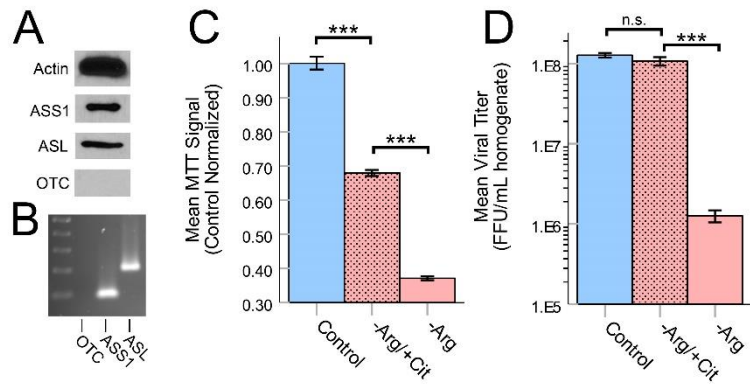


Figure 14: B16F10s are ASS1/ASL competent and can support cellular and viral replication with Arg biosynthesis. (A) Western blot for Actin, ASS1, ASL, and Ornithine Transcarbamoylase (OTC) using B16F10 cells grown in standard DMEM. **(B)** PCR products of ASS1 and ASL from B16F10 RNA isolate. **(C)** Detonator plot of MTT assay of B16F10 cells cultured for 24 hours in control DMEM (Control), Arg deficient DMEM supplemented with 400µM citrulline (-Arg/+Cit), or Arg deficient DMEM (-Arg). **(D)** Detonator plot of mean MyxGFP titers 24 HPI in B16F10 cells cultured in Control, -Arg/+Cit, and -Arg media 24 hours prior to infection. **Statistics: (C-D)** One-way ANOVA with Tukey's HSD post hoc. *** $p < 0.005$. $n = 3$ per condition.

Loss of ASS1 decreases MYXV replication both in vitro and in vivo

Since our previous results suggested that Arg biosynthesis plays a major role in determining the outcomes of MYXV replication under Arg limiting conditions, we next determined whether a tumor's ASS1-status might influence its responsiveness to MYXV-based OV. To facilitate this study, we first generated a series of functionally ASS1-deficient B16F10 cell lines (ASS1^{KO}: KO1, KO4) using CRISPR/Cas9 genome editing. These cell lines exhibited normal growth and morphology when cultured in standard DMEM (Fig 15A) but now produced a truncated version of the ASS1 protein (Fig 15B). Critically, while the cytostasis induced by removal of Arg could not be rescued by addition of citrulline in these cell lines it could be rescued by the addition of the downstream metabolite AS demonstrating that these cells were now functionally ASS1^{-/-} (Fig 15C). Consistent with our previous results, both the ASS1^{WT} and ASS1^{KO} cells produced similar amounts of infectious MYXV progeny in the presence of exogenous Arg (Fig 16A). However, the addition of citrulline was now unable to rescue viral replication in the ASS1-deficient cells while the addition of AS could rescue viral replication in both the ASS1^{WT} and ASS1^{KO} cells (Fig 16B).

After confirming the expected phenotypes *in vitro*, we next determined if loss of Arg synthesis by ASS1^{KO} was visible within the metabolome. ASS1^{WT} and ASS1^{KO} tumors were harvested from mice 18 days post seeding yielding tumors approximately 50-80mm² in size, snap frozen at point of harvest, and processed for LC-MS analysis. As expected, the "Arginine Biosynthesis" KEGG pathway was the most significantly altered (Appendix D) largely driven by increased citrulline content within the ASS1^{KO} tumors.

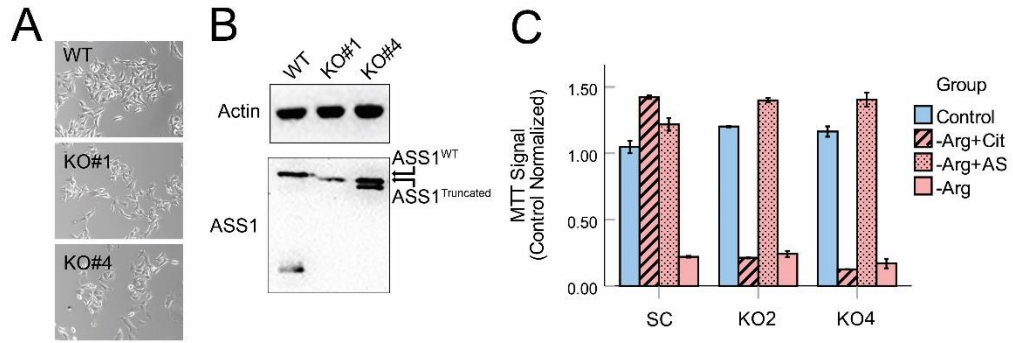


Figure 15: Generation of ASS1^{KO} cell lines. (A) Morphology of SC, KO1, and KO4 cell lines. **(B)** Western blot for Actin and ASS1 of B16F10 CRISPR/Cas9 gRNA Scramble (SC) and B16F10 ASS1^{KO} KO1/KO4. **(C)** Detonator plot of MTT signal of SC and KO1/KO4 cell lines 24 hours in Control, -Arg/+Cit, -Arg/+AS (argininosuccinate; 400 μ M), and -Arg media, relative to Control samples within each group. Error bars indicate SEM.

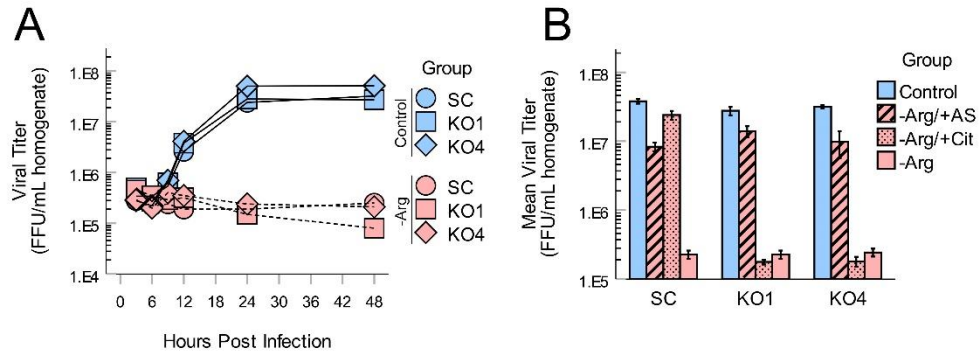


Figure 16: Defects in Arg metabolism inhibit MYXV replication in Arg limited conditions. (A) Single-step growth curves of MyxGFP in SC, AC1, and AC4 cell lines preconditioned for 24 hours in Control and -Arg media. **(B)** MyxGFP titer 24 hours post infection in SC, KO1, and KO4 cell lines preconditioned for 24 hours in Control, -Arg/+Argininosuccinate, -Arg/+Citrulline, and -Arg.

To determine whether loss of ASS1 might influence MYXV replication *in vivo*, syngeneic mice were implanted subcutaneously with either ASS1^{WT} or ASS1^{KO} B16F10 cells. Seven days post implantation, tumors were treated with either PBS or a single bolus of 1×10^6 FFU of MYXV. Six days after viral treatment, tumors were harvested and viral infection determined by visually assessing expression of virally derived GFP in tumor sections as well as by quantifying the abundance of infectious virions. Consistent with previous reports [212, 213], six days post treatment ASS1^{WT} B16F10 tumors displayed numerous distinct foci of infection (Figs 15A-B) and contained high numbers of infectious MYXV particles (Fig 17C). In contrast, tumors formed from all four ASS1^{KO} cell lines displayed significantly reduced visual signs of infection (Figs 15A-B) as well as a ~ 2 log reduction in infectious virus (Fig 17C). Taken together, these results suggest that loss of ASS1 prevents intrinsic Arg biosynthesis and that this can negatively impact MYXV-replication *in vivo*.

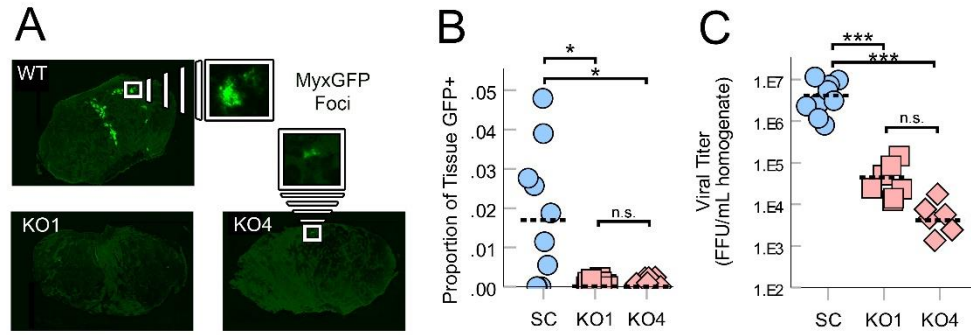


Figure 17: Loss of ASS1 reduces metrics of MYXV health in B16F10 tumors. SC, KO1, and KO4 B16F10 tumors of C57Bl/6J mice were treated with 1E+6 FFU of MyxGFP. Six days post infection, tumors were harvested, bisected, and processed for frozen sectioning and quantification of viral titer. **(A)** Images of tumor sections that displayed the median (or upper-median in the case of even sample number) amount of infection area within each cohort; GFP signal indicates area of infection. **(B)** Dot plot of infection area in infected tissues seen in (A) as percent of total tissue displaying GFP signal. Dotted bars indicate mean value for each group. **(C)** Dot plot of viral burden within tumors from (A-B). Dotted bars indicate mean value for each group. **Statistics:** (B) One-way ANOVA with Games-Howell post-hoc. * $p < 0.05$. n.s. = no significance. $n = 8-10$ mice per group. (C) One-way ANOVA with Tukey's HSD post-hoc. *** $p < 0.001$. n.s. = no significance. $n = 6-9$ mice per group.

Loss of ASS1 increases therapeutic resistance to MYXV oncolytic virotherapy

While some OV platforms are reliant on direct oncolysis for tumor debulking, the efficacy of MYXV is largely driven through the virally-recruited immune response [105]. Additionally, the ASS1 substrate citrulline has been implicated in regulating various immune functions [214-216]. We therefore asked whether the induction of this immune response might be impacted by a tumor's ASS1-status. Interestingly, despite the published role of citrulline in immune activation, the immune profiles of ASS1^{WT} and ASS1^{KO} tumors were extremely similar to each other in the absence of viral treatment (Fig 18A). Additionally, consistent with previous reports [213], MYXV-based treatment of tumors induced substantial changes to tumors overall immune profile (Fig 18) highlighted by increased numbers of CD8⁺ T cells and changes to the overall myeloid compartment (Fig 18B). Interestingly, despite the significant reduction in the numbers of infectious virions produced, these changes were largely conserved between ASS1^{WT} and ASS1^{KO} tumors with PCA analysis being unable to distinguish tumors based on ASS1 status. (Fig 18C). Despite the phenotypic similarities between the immune responses in ASS1^{WT} and KO tumors, treatment of KO tumors induced significantly lower levels of IFN- γ suggesting that either the loss of ASS1 or the reduced levels of viral replication resulted in reduced immune functionality (Fig 18D).

Since our previous analysis had suggested that the immune response induced by viral treatment might be less robust in ASS1^{KO} tumors than that induced in WT tumors, we finally wished to determine whether these tumors might displayed reduced responsiveness to MYXV-based OV. Since the therapeutic response of B16F10 tumors to WT MYXV is typically negligible, in order to address this question we established B16F10 tumors in syngeneic mice and then treated them with a recently described doubly recombinant MYXV construct which expressed both a PD1 inhibitor and IL12 (vPD1/IL12 [105]) (Fig 19A). Consistent with both the reduced viral replication and the lessened immune functionality, we observed that ASS1^{KO} tumors treated with

vPD1/IL12 displayed a less pronounced response to viral therapy including earlier tumor relapse and poorer overall survival (Figs 17B and 17C). Taken together, these data suggest that ASS1 status might significantly impact the responsiveness of tumors to MYXV-based OV.

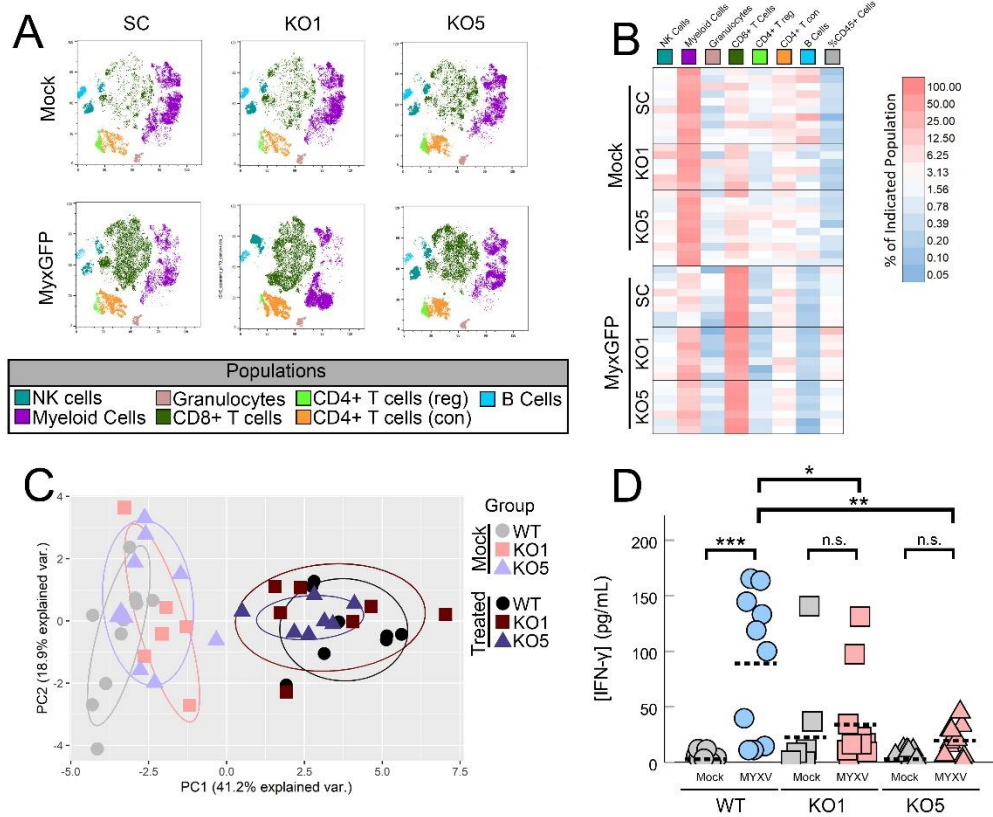


Figure 18: Immune profiles of mock and MyxGFP treated tumors in SC and ASS1 KO cell lines. (A) t-SNEs of flow cytometry performed on SC, KO1, and KO5 tumors in Mock and MyxGFP Tx groups. t-SNEs performed on samples pre-gated for doublet discrimination, vital dye, and CD45 positivity. $n = 6-10$ mice per group. **(B)** Heatmap of various immune subsets quantified from groups seen in (A) expressed as population percentages of parent CD45+ gate (Columns 1-7) or population percentage of parent living cells gate (Column 8). **(C)** PCA of quantitation results seen in (B). **(D)** Dot plot of IFN- γ content in tumor supernatants via ELISA from mice in (A). Concentrations normalized against total protein content determined via separate Bradford assay (not shown). **Statistics:** (D) One-way ANOVA with Tukey's HSD post hoc. * $p < 0.05$, ** $p < 0.01$, *** $p < 0.005$.

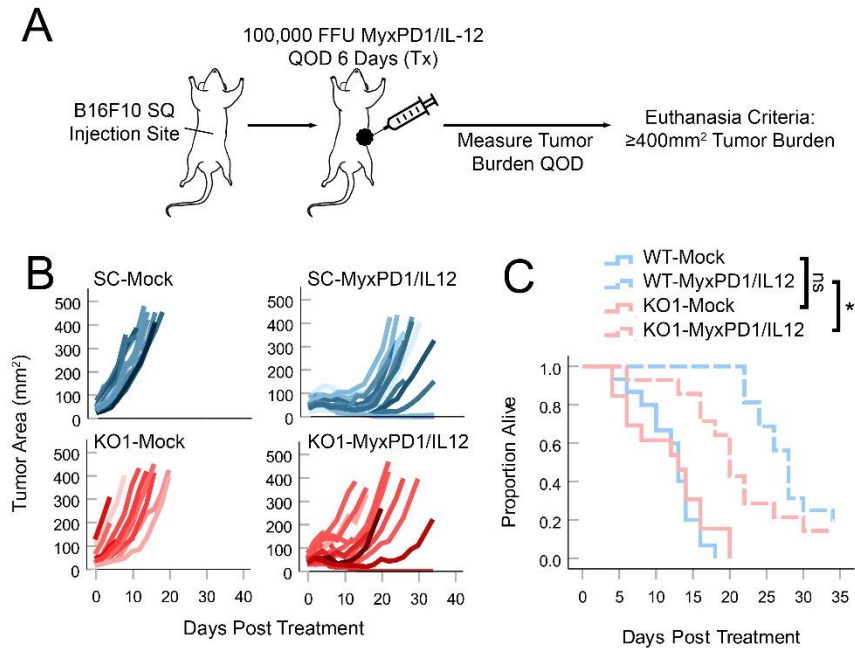


Figure 19: Loss of ASS1 blunts therapeutic response to MYXV-mediated oncolytic virotherapy. B16F10 SC or B16F10 KO1 tumors were established in C57Bl/6J mice, and mice were sorted and binned upon tumor sizes reaching $\sim 25\text{mm}^2$ into Mock and Treated cohorts. Treated cohorts received $1\text{E}+5$ FFU injections of MyxPD1/IL-12 intratumorally every other day for 6 days (3 treatments total), and tumor burden monitored every other day in all cohorts. $n = 13-16$ mice per treatment group. **(A)** Schematic of treatment regimen. **(B)** Spaghetti plots tracking individual tumor sizes over time. **(C)** Survival plots of mice. **Statistics:** Significance determined by Breslow test for survival. * = $p < 0.05$; ns = no significance.

Viral reconstitution of Arg biosynthesis partially rescues phenotypes associated with loss of cellular ASS1

Given the partial loss of efficacy and reduction of viral burden observed in ASS1^{KO} tumors, we next determined if reconstituting the Arg biosynthesis pathway through arming MYXV with ASS1 would improve performance within ASS1^{KO} tumors. To address this, three MYXV constructs were generated bearing ASS1 as seen in Fig 20A. *In vitro* testing confirmed that viral replication was Cit rescuable in Arg starved conditions with MyxASS1 infection regardless of cellular ASS1 status (Fig 20B). A similar effect but impartial rescue was observed *in vivo*, where viral burden of ASS1^{KO} tumors were comparatively increased in the MyxASS1 treated tumors, but this increase was not to the baseline observed in ASS1^{WT} controls (Fig 20C). After observing a partial rescue of viral burden *in vivo*, we compared the therapeutic efficacy of MyxPD1/IL-12 and Myx/ASS1/PD1/IL-12 in ASS1^{WT} and ASS1^{KO} tumors (Fig 20D-E). Contrary to viral replication within tumors seen in previous experiments, tumor control of ASS1^{KO} tumors with Myx/ASS1/PD1/IL-12 was entirely comparable to performance in ASS1^{WT} tumors, unlike the Myx/PD1/IL-12 control. Interestingly, the Myx/ASS1/PD1/IL-12 construct performed better than Myx/PD1/IL-12 control even within the ASS1^{WT} tumors.

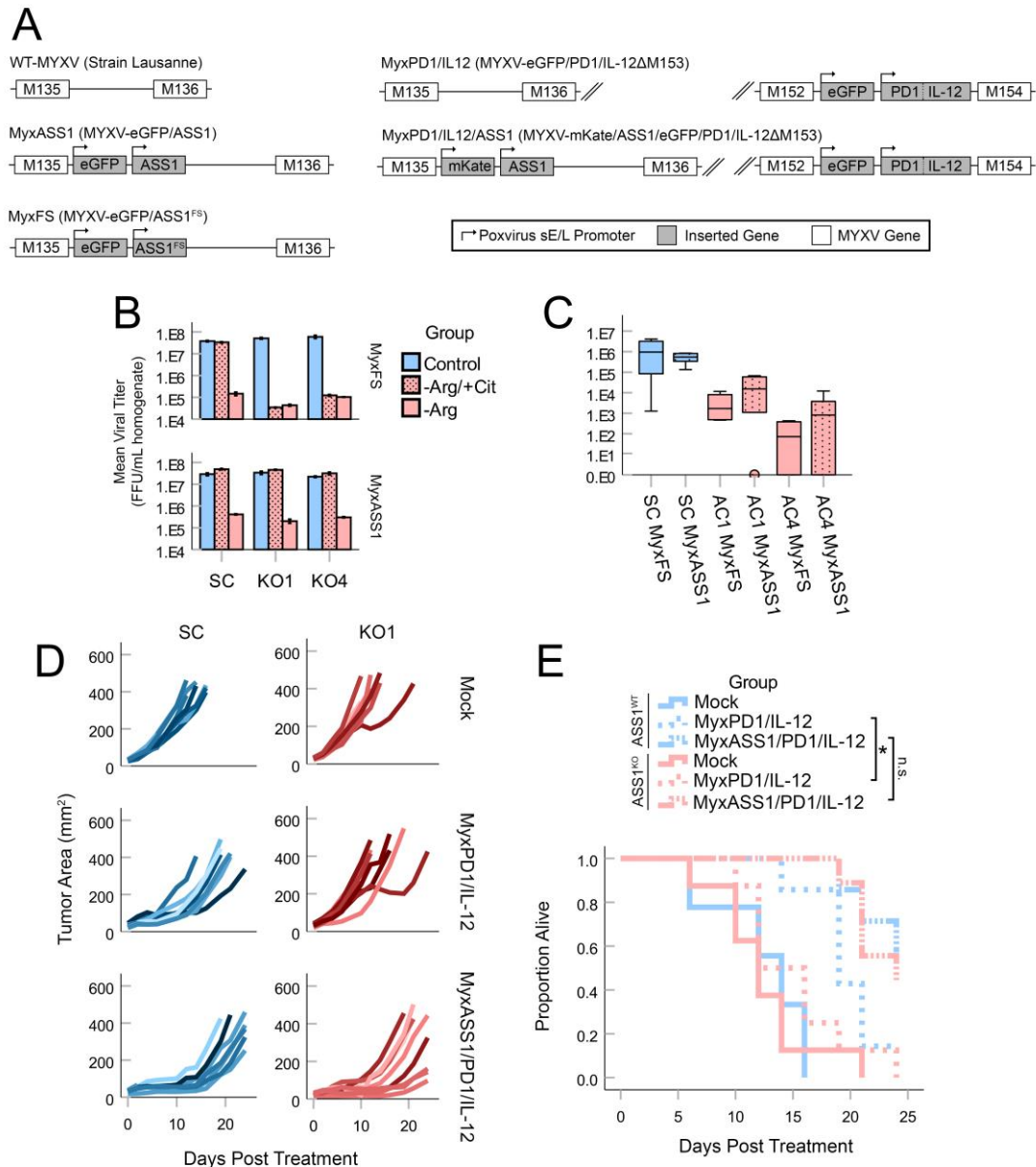


Figure 20: Viral reconstitution of Arg biosynthesis partially restores viral replication and therapeutic efficacy. **(A)** Design of ASS1 bearing MYXV constructs. All constructs generated from the parental Lausanne strain. MyxFS is a frameshifted control bearing a frameshifted version of ASS1 in the same insertion site as MyxASS1. MyxPD1/IL12/ASS1 is a recombination of the MyxPD1/IL12 virus. **(B)** MyxFS and MyxASS1 titer from ASS1^{WT} and ASS1^{KO} cells in Arg variant media. **(C)** Viral burden of ASS1^{WT} and ASS1^{KO} tumors 6 days post infection with either MyxFS or MyxASS1. n = 5-8 per group. **(D-E)** B16F10 SC or B16F10 KO1 tumors were established in C57Bl/6J mice, and mice were sorted and binned upon tumor sizes reaching ~25mm² into Mock and Treated cohorts. Treated cohorts received 1E+5 FFU injections of MyxPD1/IL-12 or MyxASS1/PD1/IL-12 intratumorally every other day for 6 days (3 treatments total), and tumor burden monitored every other day in all cohorts. n = 9-10 mice per treatment group. **(D)** Spaghetti plots of individual tumor size over time. **(E)** Survival curves of mice. Significance determined by Breslow test for survival. * = p < 0.05; ns = no significance.

7.4: Discussion

The efficacy of most OV is influenced by the replication of the viral agent within the TME. However, despite this dependence, the barriers to optimal replication remain incompletely understood. Previous work has clearly established that an intact antiviral host response represents one major obstacle to achieving effective infection within treated tumors [195, 196]. However, even within the context of severe immunodeficiency, such as immune deficient NSG mice, many oncolytic infections – including MYXV – still fail to achieve complete tumor infection [106]. These data suggest that barriers to viral infection exist beyond the context of antiviral immunity. Determining the identity of these barriers therefore represents an opportunity to improve our basic understanding of OV as well as enhance its therapeutic potential. In this context, our results suggest that metabolic deficiencies resulting from dysregulation of the cellular Arg biosynthesis machinery may contribute to OV resistance.

The status of cellular ASS1 competency had a clear, robust effect on viral replication *in vivo*. This suggests both that bioavailable Arg is inherently limiting within the TME of B16F10 tumors and that citrulline is relatively abundant. Unfortunately, due to technical limitations, neither our present work nor previously published studies examining the role of Arg in anti-tumor immunity have been able to directly confirm these hypotheses, though there are some tangential observations such as decreased Arg content in cancer-bearing patients [217]. Interestingly, even in ASS1^{KO} tumors, some evidence of MYXV replication was observed (Fig 6). This replication occurred in significantly fewer distinct viral foci, with the majority being much smaller and dimmer than the ASS1^{WT} counterparts; however, a few foci in ASS1^{KO} tumors were individually comparable in size and GFP signal to the ASS1^{WT} tumors. While not definitive, this observation seems to reinforce the notion that loss of ASS1 decreases the portion of a tumor that is amenable to infection. These results potentially indicate that Arg bioavailability could be heterogeneous

throughout the tumor, and if so, recapitulate our observations *in vitro* that infection can proceed unabated in ASS1^{KO} cell lines so long as Arg is available exogenously.

Interestingly, despite the massive reduction in infectious virus present, the phenotypic immune response to MYXV treatment in both ASS1^{WT} and KO tumors was comparable (Fig 18). This result is similar to previous results suggesting that the induction of anti-tumor immunity following MYXV-based OV is likely a thresholded event [213]. However, unlike our previous work, while the phenotype of the immune response was similar in ASS1^{WT} and ASS1^{KO} tumors, KO tumors displayed significantly reduced levels of IFN- γ . It is currently unclear whether the reduced levels of this cytokine correspond to lower viral burdens or a unique type of intrinsic immune suppression resulting from ASS1 deficiency; however, this provides an attractive explanation as to why tumors lacking ASS1 displayed a reduced therapeutic response to treatment with recombinant MYXV (Fig 19). Future studies will be required to evaluate exactly how ASS1 competency influences both the maximum therapeutic response and the required viral dose to elicit it.

In vitro, rescue of viral replication within tumors was rescued entirely from the inclusion of ASS1 into the viral backbone. This data may partially argue against the previously proposed model in Chapter 5, where the establishment of an antiviral cellular state stemming from an overlap with amino acid starvation responses explains loss of viral replication, and instead may argue for the simplest explanation that MYXV is losing access to a proteinogenic amino acid necessary for its replication. If this was the case, one may expect to see that translation of the virally encoded ASS1 would be partially blocked by virtue of eIF2 α phosphorylation (not completely, as evidenced by virally encoded GFP still being produced in Arg starved conditions). Clearly, this is not the case, as even after starvation of Arg for 24 hours, enough translation of viral ASS1 protein occurs after infection to reverse this cellular state and restore capacity for viral

replication. Putatively, this would form a positive feedback loop, where the minimal ASS1 expression from the virus begins converting cellular citrulline into Arg, thus liberating more Arg for both cell and virus and partially restoring Arg content in cells, thus resorting in more ASS1 expression.

The kinetics of viral replication may be informative in this regard. Evaluation of replication kinetics by determining if a delay in the single-step growth curves exist would allow for rough quantification of how long it takes for MyxASS1 to begin reversing the Arg induced block of viral replication; however, as the single time point titers at 24 hours did not indicate any loss of MyxASS1 replication, this potential delay would have to be small in magnitude. In this same vein of investigation, re-evaluating viral protein expression over time (by GFP intensity) in MyxASS1 infected cells in –Arg/+Cit conditions compared to control media would also be informative. Since viral replication is clearly rescued, one would expect to observe an early restoration of either GFP expression, where it does not deviate from the control curves at all, or catches up some time after the 6 hour mark where significant changes are first noted.

Of note, while viral replication *in vitro* was clearly restored in ASS1⁻ cells grown in –Arg/+Cit conditions by the inclusion of ASS1 into MYXV, this was not sufficient to restore viral titers *in vivo*. Here, MyxASS1 in KO1/KO4 tumors yielded higher titers compared to the MyxFS treated tumors, but the MyxASS1 titers in these tumor types still did not reach the viral burden observed in the ASS1^{WT} tumors treated with either constructs.

This may be a result of citrulline content in the circulation of mice. In order to mimic the concentration of Arg in DMEM, all *in vitro* studies conducted were performed at 400μM citrulline; *in vivo*, the plasma concentration of citrulline in mice is around 40μM [218]. This significantly lower citrulline content may then slow down the rapidity that MyxASS1 can rescue its own viral replication by the expression of ASS1; however, this explanation would only be logically sound if

the expression of ASS1 in virally infected cells was lower than the expression of ASS1 in natively ASS1 competent cells. This explanation is somewhat complicated by the idea that citrulline with the TME of ASS1⁻ tumors should be higher than their ASS1⁺ counterparts, as citrulline is no longer consumed by tumoral cells through Arg biosynthesis.

An alternative explanation may again be attributable to an insult to replication kinetics that is compounded with each iterative round of infection *in vivo*. The *in vitro* experiments within this study only evaluated single-steps of viral replication at a single time point. If the previously postulated delay in replication does exist, it would lead to an increasingly large lag in viral replication of MyxASS1 in ASS1⁻ tumors compared to MYXV replication in natively ASS1⁺ tumors. This may warrant experiments to evaluate viral replication over time within infected mice rather than the single time point approach taken here. Additional studies *in vitro* that more thoroughly explore the rescue of replication by viral incorporation of ASS1 (quantification of viral ASS1, citrulline dose-dependency, and foci forming assays) would also aid in explaining the disparity of our replication rescue *in vitro* and *in vivo*.

Rescue of therapeutic efficacy was rescued fully, however, by arming constructs with ASS1. This data further suggests that viral replication to achieve tumor control is a thresholded event in this model, as a multi-log reduction in titer is present in ASS1^{WT} tumors compared to ASS1^{KO} tumors treated with MyxASS1. Alternatively, this effect could also be explained by MyxASS1/PD1/IL-12 bearing more robust expression of the therapeutic PD1/IL-12 transgenes by reversal of Arg starvation within host cells. Beyond viral replication and transgene expression, the decrease in Arg consumption by viral reconstitution of Arg biosynthesis may also liberate Arg content for use by T cell responses that depend on Arg for proper function [129]. Given the previous results we observed in IFN- γ content of ASS1^{KO} and ASS1^{WT} tumors this explanation is conceptually attractive, however the total amount of infection area within a tumor rarely exceeds

~5%, logically reducing total tumoral Arg consumption of tumors by the same value at best. This marginal shift to a tumor that is functionally 100% ASS1 deficient to one that is 95% ASS1 deficient would not seem to cause a significant enough change in Arg consumption to explain this rescue. Nonetheless, viral reconstitution of ASS1 clearly improved therapeutic outcomes in the ASS1 deficient model, and future research will be required to definitively determine the mechanism at hand.

While modest changes to therapeutic response were noted in response to ASS1 expression status (either cellular or virally encoded), the nature of MYXV's mechanism of efficacy in most tumor models may result in weaker effects compared to other OV platforms. Unlike OVs such as AdV and HSV, response to MYXV is mediated almost entirely by the recruited immune response by virtue of infection, rather than direct oncolysis. This is exemplified in tumor-bearing NSG mice, where inoculation with MYXV results in exceptionally robust infection (50-70% total infection of tumors as measured by GFP positivity in infected tumor sections, and ~1-2 log increases in viral replication (unpublished observations; Appendix C) but does not confer any therapeutic benefit to these mice in either tumor control or survival time. As immunodeficiency leads to total loss of therapeutic response to MYXV with some very specific exceptions [219], replication and spread throughout the tumor is likely less important to MYXV-based OV as more lytic platforms. As such, exploring the role of ASS1 competency within the context of other OV platforms – particularly those that base their efficacy off of virally-mediated cell lysis – is a worthwhile endeavor.

Even within the context of MYXV, however, further modifications to alter Arg accessibility may carry practical merit. The efficacy of MyxASS1 in ASS1⁻ tumors was compared against the performance of MyxASS1/MyxFS in ASS1⁺ tumors; given our results in Chapter 6 that were all performed in the context of the ASS1⁺ B16F10 cell line, the loss of ARG1⁺ MDSCs increasing viral

replication in an Arg dependent manner imply that biosynthesis of Arg is *not* capable of completely sustaining Arg consumption in B16F10 cells by itself. This result was recapitulated *in vitro*, where even 400 μ M citrulline was not sufficient to rescue cell replication entirely, implying failure to meet cellular demand completely.

This observation indicates a certain future line of study may be worth pursuing: does further amplification of Arg availability improve metrics of viral health and therapeutic response *in vivo*. The simple inclusion of other enzymes involved within Arg biosynthesis or its import may further improve MYXV-mediated OV. Inclusion of ornithine transcarbamylase (the enzyme responsible for the conversion of L-ornithine and carbamoyl phosphate into citrulline) would act to provide a way of increasing citrulline content within infected cells to be used by ASS1, which again may be suboptimal. Inclusion of CAT2b, a high-affinity Arg importer utilized by myeloid lineage cells to increase their import of Arg [109, 113], may give MYXV infected cells a competitive edge in sourcing Arg from their uninfected neighbors (though, in the zero-sum game of metabolism, this particular strategy may both end up further depriving T cell responses of Arg, and starving soon-to-be-infected cells neighboring those initially infected may be self-defeating).

The rescue of viral replication by inclusion of metabolic enzymes also provides proof-of-concept that alterations to tumoral metabolism may be achievable through OV, and targets beyond Arg metabolism are evident. While the concept of tumoral metabolism and its pertinence to OV has been explored in a theoretical context as seen in recent reviews [220], no studies have been conducted within this context beyond an interesting report by Rivadeneira et al. of metabolically modulating OV-mediated T cell responses by the inclusion of leptin into the backbone of an oncolytic VACV platform [151]. This work and that of Rivadeneira et al. demonstrate feasibility of using OV to beneficially alter host metabolism (though to different ends), and as such, indicate that this is a strategy worth pursuing further. But beyond the

restoration of broken or dysregulated biosynthetic pathways, or sending molecular messages to infiltrating T cells, OVs may be able to act as metabolic “sinks” or scavengers to improve the metabolic landscape of the TME for either itself or the impending immune response. Many immunosuppressive metabolites are used by cancers to support immune evasion, such as adenosine and kynurenine [221]. Excessive adenosine within the TME occurs as a result of both cancerous cells themselves, and immune cells such as regulatory T cells expressing CD73 that convert pro-inflammatory extracellular ATP into adenosine [222]. Adenosine itself can be irreversibly de-aminated by the function of adenosine deaminase (ADA), converting it to inosine, a nucleoside that does not possess the immunosuppressive activity of its immediate precursor (and may actually be beneficial to CD8⁺ T cells by acting as an alternative carbon source when glucose is limited, as it can become within the TME [223]). Arming OV constructs with the intent of scavenging these metabolites into infected cells and causing their degradation, such as encoding adenosine importers and ADA into an OV’s backbone, could reverse or at least reduce the circulation of these metabolites within the TME.

Ultimately, our results demonstrate that considering changes to tumor metabolism in the context of OV performance is a worthwhile endeavor, particularly for metabolic dysregulations that are as highly penetrant as loss of ASS1. Compared to normal tissues, numerous metabolites have been experimentally shown to be altered within the TME. Though our current studies focus on the role of Arg and ASS1 competency in the replication of MYXV, it is highly likely that changes to other metabolites can influence viral replication within the context of OV. Identifying how these changes affect both the quality of viral infection, as well as the subsequent anti-tumor immune response, may provide additional strategies to improve the therapeutic efficacy of OV and are therefore deserving of further study.

Chapter 8: Summary and Future Work

The power of OV through both oncolysis and oncolytic vaccination is palpable and contains promise as a modern modality of cancer therapeutics, but is marred by poor insight into mechanistic specifics, inconsistencies, and barriers to viral replication. Despite this, many preclinical studies largely prioritize building ‘better’ viruses (i.e., viruses bearing new transgenes or combinations thereof that improve response in animal models), sometimes through trial-and-error. These studies are important, valuable, and prioritize translatability from bench to bedside. However, few studies consider more fundamental and mechanistic aspects of OV. For many OV platforms, even data addressing the variability in efficacy imparted from changes in dosing regimens has not been evaluated, let alone how this may influence replication kinetics and quality of OV response. As another example, how “virally-mediated cell lysis” is occurring remains poorly understood. Is the virus causing cell death through engagement of apoptotic factors within cancer cells? Perhaps by immune-response induced necroptosis? Possibly, cell death not as a result of viral infection, but in defense against it by engagement of semi-intact antiviral response pathways? By no means should these be considered metrics of quality within the respective studies, and to some degree are purely arguments of semantics; however, they do illustrate that often fundamental understanding of OV is a secondary, “bonus” objective.

This is best exemplified by the disclaimer for Imlygic within its product information, present as of writing, that “exactly how Imlygic works is not known.” OV as a therapy is very unique in the sense that three biological entities – the cancer, the virus, and the immune system – are all simultaneously influencing therapeutic outcome; this tripartite composition makes interrogating the underlying biology more difficult (and, at least, necessitates a wider breadth of study) and more critical at the same time. Understanding what variables affect these three components both collectively and separately is of practical merit.

The disparate biology of “normal” tissues and their malignant relatives may make it difficult to immediately translate virology studies within a normal host context to a tumoral context in OV. Indeed, the very basis for cancer tropism – factors that render tumors permissive to infection – are largely based not on viral biology but dysfunctions within the cancer itself [1, 32, 79, 104]. The same pathways that stave off viral infection frequently overlap with tumor suppressor pathways, such as STAT-1 and p53. However, it is reasonable to assume that within the distribution of aberrancies intrinsic to cancer, some changes may exert an opposite effect to coincidentally render tumors resistant to infection. Permissivity and resistance are not mutually exclusive. A cell type that *can* be infected by no means indicates replication in this cell is occurring at optimal levels.

The work herein attempted to make a very modest contribution towards the goal of understanding factors that hinder replication of OV agents specific to a tumoral context. Given the dependency of some inflammatory immune responses on Arg content [109, 129], the several ways cancers increase Arg consumption [115-117, 126, 138, 191], and the historical studies demonstrating some DNA viruses particularly rely on Arg [139-141, 143, 144, 146, 148], we hypothesized that this metabolite was perfectly positioned to be of importance *in vivo*.

As presented, we first established that MYXV exhibits a dependency on Arg pools for replication. However, our data is limited in that it does not reveal if this is due to the cellular state induced by a lack of Arg, or resulting from a block purely within the MYXV life cycle. Conceptually, the metabolism of the host cell is the same ‘metabolism’ used by the virus during infection: they are one and the same. In this regard, loss of viral replication seems likely to stem from both cellular disorder and viral dysfunction. Regardless, more pointed interrogation of the viral life cycle would help identify this/these block(s) in replication, and thus provide opportunity to circumvent them in the rational design of OV platforms. Data that are more definitive in this

regard would include evaluating particle assembly, as discussed, but would also need to determine what cellular pathways may be contributing to a block, such as engagement of GCN2 or lack of Arg-mediated inhibition of CASTOR1 signaling through mTORC1.

After observing an Arg dependence of MYXV, we next wanted to evaluate how (if at all) two different paths of Arg depression within tumors may influence MYXV based OV: the activity of ARG1⁺ myeloid cells causing increased turnover of Arg, and the loss of ASS1 within tumors putatively leading to heightened Arg competition within the TME.

Ultimately, the work here specific to ARG1⁺ myeloid cells is conceptually intriguing but poorly supported by the current data at hand. It is clear that loss of the myeloid compartment via α Gr-1 within the B16F10 model leads to higher viral burden within tumors, and loss of the myeloid compartment within the B16F10 model modestly improves efficacy. It is clear that MYXV needs Arg, and a hallmark of MDSCs and TAMs is expression of ARG1, which are present in this model. As discussed, however, the causal link between ARG1 activity and myeloid-mediated depressions of viral titer are only tenuously supported by the co-culture experiments of this section (Fig 11), as mentioned in the respective discussion section. Ultimately, determining if ARG1 in MDSCs/TAMs is capable of reducing viral replication within tumors will require transgenic mouse models bearing myeloid specific knockout of *ARG1*. Determining if titers are higher in these mice at baseline, and if they are no longer increased in response to α Gr-1, would lend immense credence to this being biologically relevant and real. Without this data, there is not enough compelling evidence to verify this hypothesis, and requires this capstone experiment for this line of inquiry.

The second pathway evaluated, Arg biosynthesis via ASS1, was comparatively cleaner with results more readily interpretable. In this section, we considered the impact of ASS1 competency in determining the capacity of tumors to support viral infection. These results

indicated that the function of cellular ASS1 could support viral infection in the absence of Arg so long as access to Cit was provided. As expected, breaking this Arg biosynthetic pathway rendered cells incapable of supporting viral replication even in the presence of Cit. As loss of ASS1 is a clinically relevant phenotype in several cancers, this poses a real potential barrier to OV performance. The genetic knockout nature of this model compared to the epigenetic silencing within clinically presenting cancers does add some level of questionability in how well these observations can be translated towards the relevant biology, but certainly demonstrates that loss of this enzyme can negatively impact the potential for MYXV to replicate within tumors. Just as important, it is worth determining if rescue of these dysfunctional metabolic pathways can be achieved by viral reconstitution of the respective pathways. Though here we did partially rescue phenotypes associated with loss of ASS1 (fully so in terms of therapeutic response), more aggressively altering Arg content through increasing capacity for Arg import (e.g., encoding high-affinity Arg CATs) could give MYXV infected cells a competitive edge in further sourcing Arg.

Determining if OV is negatively affected by clinically relevant dysfunctions within metabolism simultaneously informs OV design as well as our understanding of what can restrict viral replication within tumors. Beyond a very recent review suggesting OV-mediated remodeling of anaplerosis may be worth investigating [224], no studies to our knowledge have yet investigated the impact of changes within constructive metabolism. The variety of metabolic dysfunctions within cancers extend well beyond the TCA and Arg metabolism, and it is exceedingly unlikely that either of these two pathways are the most important to OV replication, let alone the only ones that matter at all. OV is an inherently clinically-minded field of research; by definition, OV is entirely concerned with the treatment of malignancies. However, this should not exclude mechanistic studies aiming to characterize tumor-specific limitations to replication or to individual

facets of the viral life cycle. The immense diversity of strategies cancer uses to resist treatments of all types warrants an equally diverse attentiveness in identifying these same barriers.

References

1. Kelly, E. and S.J. Russell, *History of Oncolytic Viruses: Genesis to Genetic Engineering*. Molecular Therapy, 2007. **15**(4): p. 651-659.
2. Dock, G., *THE INFLUENCE OF COMPLICATING DISEASES UPON LEUKAEMIA.: CASES OF TUBERCULOSIS AND LEUKOEMIA. MISCELLANEOUS INFECTIONS. CHANGES IN THE RED BLOOD CORPUSCLES. QUALITATIVE CHANGES IN THE BLOOD, ESPECIALLY IN THE LEUKOCYTES. WHEN DOES THE CHANGE OCCUR? THE EFFECTS OF VARIOUS PROCESSES OTHER THAN INFECTION ON LEUKOEMIA. BIBLIOGRAPHY*. The American Journal of the Medical Sciences (1827-1924), 1904. **127**(4): p. 563.
3. Pack, G.T., *Note on the experimental use of rabies vaccine for melanomatosis*. AMA Arch Derm Syphilol, 1950. **62**(5): p. 694-5.
4. Taylor, A.W., *Effects of Glandular Fever Infection in Acute Leukaemia*. British Medical Journal, 1953. **1**(4810): p. 589-593.
5. Pasquinucci, G., *Possible effect of measles on leukaemia*. Lancet, 1971. **1**(7690): p. 136.
6. Zygiert, Z., *Hodgkin's disease: remissions after measles*. Lancet, 1971. **1**(7699): p. 593.
7. Liang, M., *Oncorine, the World First Oncolytic Virus Medicine and its Update in China*. Curr Cancer Drug Targets, 2018. **18**(2): p. 171-176.
8. Aurelian, L., *Oncolytic viruses as immunotherapy: progress and remaining challenges*. Onco Targets Ther, 2016. **9**: p. 2627-37.
9. Mondal, M., et al., *Recent advances of oncolytic virus in cancer therapy*. Human Vaccines & Immunotherapeutics, 2020. **16**(10): p. 2389-2402.
10. Kaufman, H.L., F.J. Kohlhapp, and A. Zloza, *Oncolytic viruses: a new class of immunotherapy drugs*. Nat Rev Drug Discov, 2015. **14**(9): p. 642-62.
11. Wang, W., et al., *Elucidating mechanisms of antitumor immunity mediated by live oncolytic vaccinia and heat-inactivated vaccinia*. Journal for ImmunoTherapy of Cancer, 2021. **9**(9): p. e002569.
12. Russell, S.J. and G.N. Barber, *Oncolytic Viruses as Antigen-Agnostic Cancer Vaccines*. Cancer Cell, 2018. **33**(4): p. 599-605.
13. Georgi, F. and U.F. Greber, *The Adenovirus Death Protein – a small membrane protein controls cell lysis and disease*. FEBS Letters, 2020. **594**(12): p. 1861-1878.
14. Kaminsky, V. and B. Zhivotovsky, *To kill or be killed: how viruses interact with the cell death machinery*. Journal of Internal Medicine, 2010. **267**(5): p. 473-482.
15. Finlay, B.B. and G. McFadden, *Anti-immunology: evasion of the host immune system by bacterial and viral pathogens*. Cell, 2006. **124**(4): p. 767-82.
16. Imre, G., *Cell death signalling in virus infection*. Cell Signal, 2020. **76**: p. 109772.
17. Bowie, A.G. and L. Unterholzner, *Viral evasion and subversion of pattern-recognition receptor signalling*. Nature Reviews Immunology, 2008. **8**(12): p. 911-922.
18. Cesaro, T. and T. Michiels, *Inhibition of PKR by Viruses*. Frontiers in Microbiology, 2021. **12**.
19. Schneider, W.M., M.D. Chevillotte, and C.M. Rice, *Interferon-stimulated genes: a complex web of host defenses*. Annu Rev Immunol, 2014. **32**: p. 513-45.
20. Malireddi, R.K.S. and T.-D. Kanneganti, *Role of type I interferons in inflammasome activation, cell death, and disease during microbial infection*. Frontiers in Cellular and Infection Microbiology, 2013. **3**.
21. Stewart, G., A. Chantry, and M. Lawson, *The Use of Oncolytic Viruses in the Treatment of Multiple Myeloma*. Cancers (Basel), 2021. **13**(22).

22. Zhang, L., et al., *Robust Oncolytic Virotherapy Induces Tumor Lysis Syndrome and Associated Toxicities in the MPC-11 Plasmacytoma Model*. *Mol Ther*, 2016. **24**(12): p. 2109-2117.
23. Hoster, H.A., R.P. Zanes, Jr., and E. Von Haam, *Studies in Hodgkin's syndrome; the association of viral hepatitis and Hodgkin's disease; a preliminary report*. *Cancer Res*, 1949. **9**(8): p. 473-80.
24. Southam, C.M. and A.E. Moore, *Clinical studies of viruses as antineoplastic agents with particular reference to Egypt 101 virus*. *Cancer*, 1952. **5**(5): p. 1025-34.
25. Flint, J. and T. Shenk, *Viral transactivating proteins*. *Annu Rev Genet*, 1997. **31**: p. 177-212.
26. de Stanchina, E., et al., *E1A signaling to p53 involves the p19(ARF) tumor suppressor*. *Genes Dev*, 1998. **12**(15): p. 2434-42.
27. Kao, C.C., P.R. Yew, and A.J. Berk, *Domains required for in vitro association between the cellular p53 and the adenovirus 2 E1B 55K proteins*. *Virology*, 1990. **179**(2): p. 806-14.
28. Ries, S. and W.M. Korn, *ONYX-015: mechanisms of action and clinical potential of a replication-selective adenovirus*. *Br J Cancer*, 2002. **86**(1): p. 5-11.
29. Ozaki, T. and A. Nakagawara, *Role of p53 in Cell Death and Human Cancers*. *Cancers (Basel)*, 2011. **3**(1): p. 994-1013.
30. McCart, J.A., et al., *Systemic cancer therapy with a tumor-selective vaccinia virus mutant lacking thymidine kinase and vaccinia growth factor genes*. *Cancer Res*, 2001. **61**(24): p. 8751-7.
31. Liu, N., et al., *Oncogenic viral infection and amino acid metabolism in cancer progression: Molecular insights and clinical implications*. *Biochim Biophys Acta Rev Cancer*, 2022. **1877**(3): p. 188724.
32. Sokolowski, N.A., H. Rizos, and R.J. Diefenbach, *Oncolytic virotherapy using herpes simplex virus: how far have we come?* *Oncolytic Virother*, 2015. **4**: p. 207-19.
33. Springfield, C., et al., *Oncolytic Efficacy and Enhanced Safety of Measles Virus Activated by Tumor-Secreted Matrix Metalloproteinases*. *Cancer Research*, 2006. **66**(15): p. 7694-7700.
34. Edge, R.E., et al., *A let-7 MicroRNA-sensitive Vesicular Stomatitis Virus Demonstrates Tumor-specific Replication*. *Molecular Therapy*, 2008. **16**(8): p. 1437-1443.
35. Harrington, K., et al., *Optimizing oncolytic virotherapy in cancer treatment*. *Nature Reviews Drug Discovery*, 2019. **18**(9): p. 689-706.
36. Chalikonda, S., et al., *Oncolytic virotherapy for ovarian carcinomatosis using a replication-selective vaccinia virus armed with a yeast cytosine deaminase gene*. *Cancer Gene Therapy*, 2008. **15**(2): p. 115-125.
37. Ostertag, D., et al., *Brain tumor eradication and prolonged survival from intratumoral conversion of 5-fluorocytosine to 5-fluorouracil using a nonlytic retroviral replicating vector*. *Neuro Oncol*, 2012. **14**(2): p. 145-59.
38. Yamada, S., et al., *Oncolytic Herpes simplex virus expressing yeast cytosine deaminase: relationship between viral replication, transgene expression, prodrug bioactivation*. *Cancer Gene Therapy*, 2012. **19**(3): p. 160-170.
39. Conticello, S.G., *The AID/APOBEC family of nucleic acid mutators*. *Genome Biology*, 2008. **9**(6): p. 229.
40. Vermes, A., H.J. Guchelaar, and J. Dankert, *Flucytosine: a review of its pharmacology, clinical indications, pharmacokinetics, toxicity and drug interactions*. *Journal of Antimicrobial Chemotherapy*, 2000. **46**(2): p. 171-179.

41. Sethy, C. and C.N. Kundu, *5-Fluorouracil (5-FU) resistance and the new strategy to enhance the sensitivity against cancer: Implication of DNA repair inhibition*. Biomedicine & Pharmacotherapy, 2021. **137**: p. 111285.
42. Ferguson, M.S., N.R. Lemoine, and Y. Wang, *Systemic delivery of oncolytic viruses: hopes and hurdles*. Adv Virol, 2012. **2012**: p. 805629.
43. Blitz, S.E., et al., *Tumor-Associated Macrophages/Microglia in Glioblastoma Oncolytic Virotherapy: A Double-Edged Sword*. Int J Mol Sci, 2022. **23**(3).
44. Gujar, S., et al., *Antitumor Benefits of Antiviral Immunity: An Underappreciated Aspect of Oncolytic Virotherapies*. Trends Immunol, 2018. **39**(3): p. 209-221.
45. Mealiea, D. and J.A. McCart, *Cutting both ways: the innate immune response to oncolytic virotherapy*. Cancer Gene Therapy, 2022. **29**(6): p. 629-646.
46. Dunn, G.P., L.J. Old, and R.D. Schreiber, *The Three Es of Cancer Immunoediting*. Annual Review of Immunology, 2004. **22**(1): p. 329-360.
47. Hanahan, D. and Robert A. Weinberg, *Hallmarks of Cancer: The Next Generation*. Cell, 2011. **144**(5): p. 646-674.
48. Akbay, E.A., et al., *Activation of the PD-1 pathway contributes to immune escape in EGFR-driven lung tumors*. Cancer Discov, 2013. **3**(12): p. 1355-63.
49. Inoue, M., et al., *Expression of MHC Class I on breast cancer cells correlates inversely with HER2 expression*. Oncoimmunology, 2012. **1**(7): p. 1104-1110.
50. Roetman, J.J., M.K.I. Apostolova, and M. Philip, *Viral and cellular oncogenes promote immune evasion*. Oncogene, 2022. **41**(7): p. 921-929.
51. Wu, S., et al., *HER2 recruits AKT1 to disrupt STING signalling and suppress antiviral defence and antitumour immunity*. Nature Cell Biology, 2019. **21**(8): p. 1027-1040.
52. Velcheti, V. and K. Schalper, *Basic Overview of Current Immunotherapy Approaches in Cancer*. American Society of Clinical Oncology Educational Book, 2016(36): p. 298-308.
53. Kahlon, N., et al., *Melanoma Treatments and Mortality Rate Trends in the US, 1975 to 2019*. JAMA Network Open, 2022. **5**(12): p. e2245269-e2245269.
54. Hemminki, O., J.M. dos Santos, and A. Hemminki, *Oncolytic viruses for cancer immunotherapy*. Journal of Hematology & Oncology, 2020. **13**(1): p. 84.
55. Duan, Q., et al., *Turning Cold into Hot: Firing up the Tumor Microenvironment*. Trends in Cancer, 2020. **6**(7): p. 605-618.
56. van Vloten, J.P., et al., *Critical Interactions between Immunogenic Cancer Cell Death, Oncolytic Viruses, and the Immune System Define the Rational Design of Combination Immunotherapies*. The Journal of Immunology, 2018. **200**(2): p. 450-458.
57. Morse, M.A., W.R. Gwin, and D.A. Mitchell, *Vaccine Therapies for Cancer: Then and Now*. Targeted Oncology, 2021. **16**(2): p. 121-152.
58. Nguyen, K.G., et al., *Localized Interleukin-12 for Cancer Immunotherapy*. Frontiers in Immunology, 2020. **11**.
59. Stritzker, J., et al., *Inducible gene expression in tumors colonized by modified oncolytic vaccinia virus strains*. J Virol, 2014. **88**(19): p. 11556-67.
60. Blank, C. and A. Mackensen, *Contribution of the PD-L1/PD-1 pathway to T-cell exhaustion: an update on implications for chronic infections and tumor evasion*. Cancer Immunology, Immunotherapy, 2007. **56**(5): p. 739-745.
61. Patel, S.P. and R. Kurzrock, *PD-L1 Expression as a Predictive Biomarker in Cancer Immunotherapy*. Molecular Cancer Therapeutics, 2015. **14**(4): p. 847-856.
62. Patel, S.A. and A.J. Minn, *Combination Cancer Therapy with Immune Checkpoint Blockade: Mechanisms and Strategies*. Immunity, 2018. **48**(3): p. 417-433.

63. Chesney, J., et al., *Randomized, Open-Label Phase II Study Evaluating the Efficacy and Safety of Talimogene Laherparepvec in Combination With Ipilimumab Versus Ipilimumab Alone in Patients With Advanced, Unresectable Melanoma*. *Journal of Clinical Oncology*, 2018. **36**(17): p. 1658-1667.
64. Engeland, C.E., et al., *CTLA-4 and PD-L1 Checkpoint Blockade Enhances Oncolytic Measles Virus Therapy*. *Molecular Therapy*, 2014. **22**(11): p. 1949-1959.
65. Marchini, A., E.M. Scott, and J. Rommelaere, *Overcoming Barriers in Oncolytic Virotherapy with HDAC Inhibitors and Immune Checkpoint Blockade*. *Viruses*, 2016. **8**(1).
66. Yoon, C., et al., *Charged residues dominate a unique interlocking topography in the heterodimeric cytokine interleukin-12*. *Embo j*, 2000. **19**(14): p. 3530-41.
67. Zhang, S. and Q. Wang, *Factors determining the formation and release of bioactive IL-12: Regulatory mechanisms for IL-12p70 synthesis and inhibition*. *Biochemical and Biophysical Research Communications*, 2008. **372**(4): p. 509-512.
68. Dai, M., et al., *Tumor Regression and Cure Depends on Sustained Th1 Responses*. *Journal of Immunotherapy*, 2018. **41**(8).
69. Lee, J., et al., *The Multifaceted Role of Th1, Th9, and Th17 Cells in Immune Checkpoint Inhibition Therapy*. *Frontiers in Immunology*, 2021. **12**.
70. Nishimura, T., et al., *The critical role of Th1-dominant immunity in tumor immunology*. *Cancer Chemother Pharmacol*, 2000. **46 Suppl**: p. S52-61.
71. Jenks, S., *After Initial Setback, IL-12 Regaining Popularity*. *JNCI: Journal of the National Cancer Institute*, 1996. **88**(9): p. 576-577.
72. Bramson, J.L., et al., *Direct Intratumoral Injection of an Adenovirus Expressing Interleukin-12 Induces Regression and Long-Lasting Immunity That Is Associated with Highly Localized Expression of Interleukin-12*. *Human Gene Therapy*, 1996. **7**(16): p. 1995-2002.
73. Nguyen, H.-M., K. Guz-Montgomery, and D. Saha, *Oncolytic Virus Encoding a Master Pro-Inflammatory Cytokine Interleukin 12 in Cancer Immunotherapy*. *Cells*, 2020. **9**(2): p. 400.
74. Liu, B.L., et al., *ICP34.5 deleted herpes simplex virus with enhanced oncolytic, immune stimulating, and anti-tumour properties*. *Gene Ther*, 2003. **10**(4): p. 292-303.
75. Kumar, A., et al., *GM-CSF: A Double-Edged Sword in Cancer Immunotherapy*. *Front Immunol*, 2022. **13**: p. 901277.
76. Berkey, S.E., S.H. Thorne, and D.L. Bartlett, *Oncolytic Virotherapy and the Tumor Microenvironment*. *Adv Exp Med Biol*, 2017. **1036**: p. 157-172.
77. Macedo, N., et al., *Clinical landscape of oncolytic virus research in 2020*. *J Immunother Cancer*, 2020. **8**(2).
78. Pol, J.G., et al., *Cytokines in oncolytic virotherapy*. *Cytokine Growth Factor Rev*, 2020. **56**: p. 4-27.
79. Ylösmäki, E. and V. Cerullo, *Design and application of oncolytic viruses for cancer immunotherapy*. *Curr Opin Biotechnol*, 2020. **65**: p. 25-36.
80. Kottke, T., et al., *Treg Depletion-enhanced IL-2 Treatment Facilitates Therapy of Established Tumors Using Systemically Delivered Oncolytic Virus*. *Molecular Therapy*, 2008. **16**(7): p. 1217-1226.
81. Hastie, E. and V.Z. Grzelishvili, *Vesicular stomatitis virus as a flexible platform for oncolytic virotherapy against cancer*. *J Gen Virol*, 2012. **93**(Pt 12): p. 2529-2545.
82. Wertz, G.W., R. Moudy, and L.A. Ball, *Adding genes to the RNA genome of vesicular stomatitis virus: positional effects on stability of expression*. *J Virol*, 2002. **76**(15): p. 7642-50.
83. Zhao, Y., et al., *Oncolytic Adenovirus: Prospects for Cancer Immunotherapy*. *Frontiers in Microbiology*, 2021. **12**.

84. Cameron, C., et al., *The complete DNA sequence of myxoma virus*. *Virology*, 1999. **264**(2): p. 298-318.
85. Lun, X., et al., *Myxoma virus is a novel oncolytic virus with significant antitumor activity against experimental human gliomas*. *Cancer Res*, 2005. **65**(21): p. 9982-9990.
86. Lalani, A.S., et al., *The purified myxoma virus gamma interferon receptor homolog M-T7 interacts with the heparin-binding domains of chemokines*. *J Virol*, 1997. **71**(6): p. 4356-63.
87. McFadden, G., *Poxvirus tropism*. *Nat Rev Microbiol*, 2005. **3**(3): p. 201-13.
88. Spiesschaert, B., et al., *The current status and future directions of myxoma virus, a master in immune evasion*. *Vet Res*, 2011. **42**(1): p. 76.
89. Wang, F., et al., *Disruption of Erk-dependent type I interferon induction breaks the myxoma virus species barrier*. *Nature Immunology*, 2004. **5**(12): p. 1266-1274.
90. Wang, G., et al., *Infection of human cancer cells with myxoma virus requires Akt activation via interaction with a viral ankyrin-repeat host range factor*. *Proceedings of the National Academy of Sciences*, 2006. **103**(12): p. 4640-4645.
91. Werden, S.J. and G. McFadden, *The role of cell signaling in poxvirus tropism: The case of the M-T5 host range protein of myxoma virus*. *Biochimica et Biophysica Acta (BBA) - Proteins and Proteomics*, 2008. **1784**(1): p. 228-237.
92. Kerr, P.J., et al., *Punctuated Evolution of Myxoma Virus: Rapid and Disjunct Evolution of a Recent Viral Lineage in Australia*. *J Virol*, 2019. **93**(8).
93. Bertagnoli, S. and S. Marchandeu, *Myxomatosis*. *Rev Sci Tech*, 2015. **34**(2): p. 549-56, 539-47.
94. Fenner, F., *Deliberate introduction of the European rabbit, *Oryctolagus cuniculus*, into Australia*. *Rev Sci Tech*, 2010. **29**(1): p. 103-11.
95. Seamark, R.F., *Biotech prospects for the control of introduced mammals in Australia*. *Reprod Fertil Dev*, 2001. **13**(7-8): p. 705-11.
96. Burnet, F.M., *Myxomatosis as a method of biological control against the Australian rabbit*. *Am J Public Health Nations Health*, 1952. **42**(12): p. 1522-6.
97. Kerr, P.J., *Myxomatosis in Australia and Europe: a model for emerging infectious diseases*. *Antiviral Res*, 2012. **93**(3): p. 387-415.
98. Flores, E.B., M.Y. Bartee, and E. Bartee, *Reduced cellular binding affinity has profoundly different impacts on the spread of distinct poxviruses*. *PLoS One*, 2020. **15**(4): p. e0231977.
99. Khodarev, N.N., B. Roizman, and R.R. Weichselbaum, *Molecular Pathways: Interferon/Stat1 Pathway: Role in the Tumor Resistance to Genotoxic Stress and Aggressive Growth*. *Clinical Cancer Research*, 2012. **18**(11): p. 3015-3021.
100. Rascio, F., et al., *The Pathogenic Role of PI3K/AKT Pathway in Cancer Onset and Drug Resistance: An Updated Review*. *Cancers (Basel)*, 2021. **13**(16).
101. Ogbomo, H., et al., *Myxoma Virus Infection Promotes NK Lysis of Malignant Gliomas In Vitro and In Vivo*. *PLOS ONE*, 2013. **8**(6): p. e66825.
102. Wu, Y., et al., *Oncolytic Efficacy of Recombinant Vesicular Stomatitis Virus and Myxoma Virus in Experimental Models of Rhabdoid Tumors*. *Clinical Cancer Research*, 2008. **14**(4): p. 1218-1227.
103. Pisklakova, A., et al., *M011L-deficient oncolytic myxoma virus induces apoptosis in brain tumor-initiating cells and enhances survival in a novel immunocompetent mouse model of glioblastoma*. *Neuro Oncol*, 2016. **18**(8): p. 1088-1098.
104. Rahman, M.M. and G. McFadden, *Oncolytic Virotherapy with Myxoma Virus*. *Journal of Clinical Medicine*, 2020. **9**(1): p. 171.

105. Valenzuela-Cardenas, M., et al., *TNF blockade enhances the efficacy of myxoma virus-based oncolytic virotherapy*. Journal for ImmunoTherapy of Cancer, 2022. **10**(5): p. e004770.
106. Kellish, P., et al., *Oncolytic virotherapy for small-cell lung cancer induces immune infiltration and prolongs survival*. The Journal of Clinical Investigation, 2019. **129**(6): p. 2279-2292.
107. Stechmiller, J.K., B. Childress, and L. Cowan, *Arginine Supplementation and Wound Healing*. Nutrition in Clinical Practice, 2005. **20**(1): p. 52-61.
108. Tapiero, H., et al., *I. Arginine*. Biomedicine & Pharmacotherapy, 2002. **56**(9): p. 439-445.
109. Jungnickel, K.E.J., J.L. Parker, and S. Newstead, *Structural basis for amino acid transport by the CAT family of SLC7 transporters*. Nature Communications, 2018. **9**(1): p. 550.
110. Nałęcz, K.A., *Amino Acid Transporter SLC6A14 (ATB(0,+)) - A Target in Combined Anti-cancer Therapy*. Front Cell Dev Biol, 2020. **8**: p. 594464.
111. Sloan, J.L., B.R. Grubb, and S. Mager, *Expression of the amino acid transporter ATB0+ in lung: possible role in luminal protein removal*. American Journal of Physiology-Lung Cellular and Molecular Physiology, 2003. **284**(1): p. L39-L49.
112. Closs, E.I., et al., *Structure and Function of Cationic Amino Acid Transporters (CATs)*. The Journal of Membrane Biology, 2006. **213**(2): p. 67-77.
113. Closs, E.I., *Expression, regulation and function of carrier proteins for cationic amino acids*. Current Opinion in Nephrology and Hypertension, 2002. **11**(1).
114. Christensen, H.H., *A retrovirus uses a cationic amino acid transporter as a cell surface receptor*. Nutr Rev, 1992. **50**(2): p. 47-8.
115. Dillon, B.J., et al., *Incidence and distribution of argininosuccinate synthetase deficiency in human cancers*. Cancer, 2004. **100**(4): p. 826-833.
116. Feun, L., et al., *Arginine deprivation as a targeted therapy for cancer*. Curr Pharm Des, 2008. **14**(11): p. 1049-57.
117. Ensor, C.M., et al., *Pegylated Arginine Deiminase (ADI-SS PEG20,000 mw) Inhibits Human Melanomas and Hepatocellular Carcinomas in Vitro and in Vivo*. Cancer Research, 2002. **62**(19): p. 5443-5450.
118. Sugimura, K., et al., *High sensitivity of human melanoma cell lines to the growth inhibitory activity of mycoplasmal arginine deiminase in vitro*. Melanoma Res, 1992. **2**(3): p. 191-6.
119. Bean, G.R., et al., *A metabolic synthetic lethal strategy with arginine deprivation and chloroquine leads to cell death in ASS1-deficient sarcomas*. Cell Death & Disease, 2016. **7**(10): p. e2406-e2406.
120. Kim, Y., et al., *Reduced argininosuccinate synthetase expression in refractory sarcomas: Impacts on therapeutic potential and drug resistance*. Oncotarget; Vol 7, No 43, 2016.
121. Rogers, L.C. and B.A. Van Tine, *Innate and adaptive resistance mechanisms to arginine deprivation therapies in sarcoma and other cancers*. Cancer Drug Resist, 2019. **2**(3): p. 516-526.
122. Du, D., et al., *Metabolic dysregulation and emerging therapeutical targets for hepatocellular carcinoma*. Acta Pharm Sin B, 2022. **12**(2): p. 558-580.
123. Wu, L., et al., *Expression of argininosuccinate synthetase in patients with hepatocellular carcinoma*. Journal of Gastroenterology and Hepatology, 2013. **28**(2): p. 365-368.
124. Kim, R.H., et al., *Arginine Deiminase as a Novel Therapy for Prostate Cancer Induces Autophagy and Caspase-Independent Apoptosis*. Cancer Research, 2009. **69**(2): p. 700-708.
125. Rabinovich, S., et al., *Diversion of aspartate in ASS1-deficient tumours fosters de novo pyrimidine synthesis*. Nature, 2015. **527**(7578): p. 379-383.

126. Giatromanolaki, A., A.L. Harris, and M.I. Koukourakis, *The prognostic and therapeutic implications of distinct patterns of argininosuccinate synthase 1 (ASS1) and arginase-2 (ARG2) expression by cancer cells and tumor stroma in non-small-cell lung cancer*. *Cancer Metab*, 2021. **9**(1): p. 28.
127. Silberman, A., et al., *Acid-Induced Downregulation of ASS1 Contributes to the Maintenance of Intracellular pH in Cancer*. *Cancer Res*, 2019. **79**(3): p. 518-533.
128. Szeffel, J., A. Danielak, and W.J. Kruszewski, *Metabolic pathways of L-arginine and therapeutic consequences in tumors*. *Advances in Medical Sciences*, 2019. **64**(1): p. 104-110.
129. Geiger, R., et al., *L-Arginine Modulates T Cell Metabolism and Enhances Survival and Anti-tumor Activity*. *Cell*, 2016. **167**(3): p. 829-842.e13.
130. Fultang, L., et al., *Molecular basis and current strategies of therapeutic arginine depletion for cancer*. *International Journal of Cancer*, 2016. **139**(3): p. 501-509.
131. Gabrilovich, D.I., *Myeloid-Derived Suppressor Cells*. *Cancer Immunology Research*, 2017. **5**(1): p. 3-8.
132. Li, B.H., M.A. Garstka, and Z.F. Li, *Chemokines and their receptors promoting the recruitment of myeloid-derived suppressor cells into the tumor*. *Mol Immunol*, 2020. **117**: p. 201-215.
133. Lim, H.X., T.S. Kim, and C.L. Poh, *Understanding the Differentiation, Expansion, Recruitment and Suppressive Activities of Myeloid-Derived Suppressor Cells in Cancers*. *Int J Mol Sci*, 2020. **21**(10).
134. Law, A.M.K., F. Valdes-Mora, and D. Gallego-Ortega, *Myeloid-Derived Suppressor Cells as a Therapeutic Target for Cancer*. *Cells*, 2020. **9**(3): p. 561.
135. Li, K., et al., *Myeloid-derived suppressor cells as immunosuppressive regulators and therapeutic targets in cancer*. *Signal Transduction and Targeted Therapy*, 2021. **6**(1): p. 362.
136. Rahma, O.E. and F.S. Hodi, *The Intersection between Tumor Angiogenesis and Immune Suppression*. *Clinical Cancer Research*, 2019. **25**(18): p. 5449-5457.
137. Dysthe, M. and R. Parihar, *Myeloid-Derived Suppressor Cells in the Tumor Microenvironment*, in *Tumor Microenvironment: Hematopoietic Cells – Part A*, A. Birbrair, Editor. 2020, Springer International Publishing: Cham. p. 117-140.
138. Grzywa, T.M., et al., *Myeloid Cell-Derived Arginase in Cancer Immune Response*. *Front Immunol*, 2020. **11**: p. 938.
139. Archard, L.C. and J.D. Williamson, *The Effect of Arginine Deprivation on the Replication of Vaccinia Virus*. *Journal of General Virology*, 1971. **12**(3): p. 249-258.
140. Becker, Y., U. Olshevsky, and J. Levitt, *The Role of Arginine in the Replication of Herpes Simplex Virus*. *Journal of General Virology*, 1967. **1**(4): p. 471-478.
141. Tankersley, R.W., Jr., *AMINO ACID REQUIREMENTS OF HERPES SIMPLEX VIRUS IN HUMAN CELLS*. *J Bacteriol*, 1964. **87**(3): p. 609-13.
142. Singer, S.H., et al., *Effect of mycoplasmas on vaccinia virus growth: requirement for arginine*. *Proc Soc Exp Biol Med*, 1970. **133**(4): p. 1439-42.
143. Williamson, J.D. and B.C. Cooke, *Argininosuccinate Synthetase-lyase Activity in Vaccinia Virus-infected HeLa and Mouse L Cells*. *Journal of General Virology*, 1973. **21**(2): p. 349-357.
144. Everitt, E., B. Sundquist, and L. Philipson, *Mechanism of the arginine requirement for adenovirus synthesis. I. Synthesis of structural proteins*. *J Virol*, 1971. **8**(5): p. 742-53.
145. Laver, W.G., *Isolation of an arginine-rich protein from particles of adenovirus type 2*. *Virology*, 1970. **41**(3): p. 488-500.

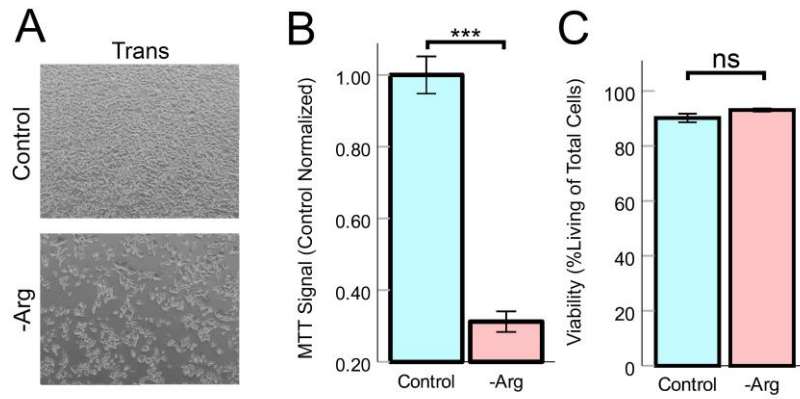
146. Prage, L. and U. Pettersson, *Structural proteins of adenoviruses: VII. Purification and properties of an arginine-rich core protein from adenovirus type 2 and type 3*. *Virology*, 1971. **45**(2): p. 364-373.
147. Kulanayake, S. and S.K. Tikoo, *Adenovirus Core Proteins: Structure and Function*. *Viruses*, 2021. **13**(3).
148. Wildy, P., et al., *Inhibition of herpes simplex virus multiplication by activated macrophages: a role for arginase?* *Infect Immun*, 1982. **37**(1): p. 40-5.
149. Inglis, V.B.M., *Requirement of Arginine for the Replication of Herpes Virus*. *Journal of General Virology*, 1968. **3**(1): p. 9-17.
150. Wang, Y., et al., *Metabolic Regulation of Myeloid-Derived Suppressor Cell Function in Cancer*. *Cells*, 2020. **9**(4): p. 1011.
151. Rivadeneira, D.B., et al., *Oncolytic Viruses Engineered to Enforce Leptin Expression Reprogram Tumor-Infiltrating T Cell Metabolism and Promote Tumor Clearance*. *Immunity*, 2019. **51**(3): p. 548-560.e4.
152. Kaufman, H.L., F.J. Kohlhapp, and A. Zloza, *Oncolytic viruses: a new class of immunotherapy drugs*. *Nature Reviews Drug Discovery*, 2015. **14**(9): p. 642-662.
153. Barteel, M.Y., P.C. Dryja, and E. Barteel, *Chimeric tumor modeling reveals role of partial PDL1 expression in resistance to virally induced immunotherapy*. *J Immunother Cancer*, 2019. **7**(1): p. 11.
154. Barteel, M.Y., K.M. Dunlap, and E. Barteel, *Tumor-Localized Secretion of Soluble PD1 Enhances Oncolytic Virotherapy*. *Cancer Research*, 2017. **77**(11): p. 2952.
155. Stanford, M.M., et al., *Myxoma virus oncolysis of primary and metastatic B16F10 mouse tumors in vivo*. *Molecular Therapy*, 2008. **16**(1): p. 52-59.
156. Rahman, M.M. and G. McFadden, *Oncolytic Virotherapy with Myxoma Virus*. *J Clin Med*, 2020. **9**(1).
157. Valenzuela -Cardenas, M., et al., *TNF-Blockade Enhances the Efficacy of Oncolytic Virotherapy*. *Journal for ImmunoTherapy of Cancer*, under review.
158. Smallwood, S.E., et al., *Myxoma virus: propagation, purification, quantification, and storage*. *Curr Protoc Microbiol*, 2010. **Chapter 14**: p. Unit 14A 1.
159. Weinberg, S.E., et al., *Mitochondrial complex III is essential for suppressive function of regulatory T cells*. *Nature*, 2019. **565**(7740): p. 495-499.
160. Xia, J., et al., *MetaboAnalyst: a web server for metabolomic data analysis and interpretation*. *Nucleic Acids Research*, 2009. **37**(suppl_2): p. W652-W660.
161. Archard, L.C. and J.D. Williamson, *The effect of arginine deprivation on the replication of vaccinia virus*. *J Gen Virol*, 1971. **12**(3): p. 249-58.
162. Joanna, G.E.O., P.M. Chesters, and J.D. Williamson, *Arginine Metabolism in Infected Cell Cultures as a Marker Character for the Differentiation of Orthopoxviruses*. *The Journal of Hygiene*, 1984. **93**(2): p. 213-223.
163. Luiking, Y.C., et al., *In Vivo Whole Body and Organ Arginine Metabolism During Endotoxemia (Sepsis) Is Dependent on Mouse Strain and Gender*. *The Journal of Nutrition*, 2004. **134**(10): p. 2768S-2774S.
164. Lüneburg, N., et al., *Reference intervals for plasma L-arginine and the L-arginine:asymmetric dimethylarginine ratio in the Framingham Offspring Cohort*. *J Nutr*, 2011. **141**(12): p. 2186-90.
165. Nieves Jr, C., et al., *Pharmacologic Levels of Dietary Arginine in CB6F1 Mice Increase Serum Ammonia in the Healthy State and Serum Nitrite in Endotoxemia*. *Journal of Parenteral and Enteral Nutrition*, 2007. **31**(2): p. 101-108.

166. Marini, J.C., et al., *Plasma arginine and ornithine are the main citrulline precursors in mice infused with arginine-free diets*. The Journal of nutrition, 2010. **140**(8): p. 1432-1437.
167. Chan, W.M., et al., *Myxoma and vaccinia viruses bind differentially to human leukocytes*. J Virol, 2013. **87**(8): p. 4445-60.
168. Wolfe, A.M., et al., *Myxoma Virus M083 Is a Virulence Factor Which Mediates Systemic Dissemination*. J Virol, 2018. **92**(7).
169. Howley, P.M. and D.M. Knipe, *Fields virology: Emerging viruses*. 2020: Lippincott Williams & Wilkins.
170. M. Beals, L.G., S. Harrell. *AMINO ACID FREQUENCY*. 1999 [cited 2023 03/10/2023].
171. Jones, S., A. Marin, and J.M. Thornton, *Protein domain interfaces: characterization and comparison with oligomeric protein interfaces*. Protein Eng, 2000. **13**(2): p. 77-82.
172. Johnston, J.B., et al., *Myxoma virus M-T5 protects infected cells from the stress of cell cycle arrest through its interaction with host cell cullin-1*. J Virol, 2005. **79**(16): p. 10750-63.
173. Gao, L. and J. Qi, *Whole genome molecular phylogeny of large dsDNA viruses using composition vector method*. BMC Evolutionary Biology, 2007. **7**(1): p. 41.
174. Pakos-Zebrucka, K., et al., *The integrated stress response*. EMBO reports, 2016. **17**(10): p. 1374-1395.
175. Harding, H.P., et al., *The ribosomal P-stalk couples amino acid starvation to GCN2 activation in mammalian cells*. eLife, 2019. **8**: p. e50149.
176. Ye, J., et al., *GCN2 sustains mTORC1 suppression upon amino acid deprivation by inducing Sestrin2*. Genes & development, 2015. **29**(22): p. 2331-2336.
177. Liu, Y., et al., *The role of host eIF2 α in viral infection*. Virol J, 2020. **17**(1): p. 112.
178. Chantranupong, L., et al., *The CASTOR Proteins Are Arginine Sensors for the mTORC1 Pathway*. Cell, 2016. **165**(1): p. 153-164.
179. Li, T., et al., *RNF167 activates mTORC1 and promotes tumorigenesis by targeting CASTOR1 for ubiquitination and degradation*. Nature Communications, 2021. **12**(1): p. 1055.
180. Dunlap, K.M., M.Y. Bartee, and E. Bartee, *Myxoma virus attenuates expression of activating transcription factor 4 (ATF4) which has implications for the treatment of proteasome inhibitor-resistant multiple myeloma*. Oncolytic virotherapy, 2015. **4**: p. 1-11.
181. Berlanga, J.J., et al., *Antiviral effect of the mammalian translation initiation factor 2alpha kinase GCN2 against RNA viruses*. Embo j, 2006. **25**(8): p. 1730-40.
182. del Pino, J., et al., *GCN2 has inhibitory effect on human immunodeficiency virus-1 protein synthesis and is cleaved upon viral infection*. PLoS One, 2012. **7**(10): p. e47272.
183. Krishnamoorthy, J., et al., *The eIF2alpha kinases inhibit vesicular stomatitis virus replication independently of eIF2alpha phosphorylation*. Cell Cycle, 2008. **7**(15): p. 2346-51.
184. Liu, Y., et al., *The role of host eIF2 α in viral infection*. Virology Journal, 2020. **17**(1): p. 112.
185. Sanchez, E.L. and M. Lagunoff, *Viral activation of cellular metabolism*. Virology, 2015. **479-480**: p. 609-618.
186. Sumbria, D., et al., *Virus Infections and Host Metabolism—Can We Manage the Interactions?* Frontiers in Immunology, 2021. **11**.
187. Thaker, S.K., J. Ch'ng, and H.R. Christofk, *Viral hijacking of cellular metabolism*. BMC Biology, 2019. **17**(1): p. 59.
188. Martínez-Reyes, I. and N.S. Chandel, *Cancer metabolism: looking forward*. Nature Reviews Cancer, 2021. **21**(10): p. 669-680.
189. Pavlova, N.N. and C.B. Thompson, *The Emerging Hallmarks of Cancer Metabolism*. Cell metabolism, 2016. **23**(1): p. 27-47.

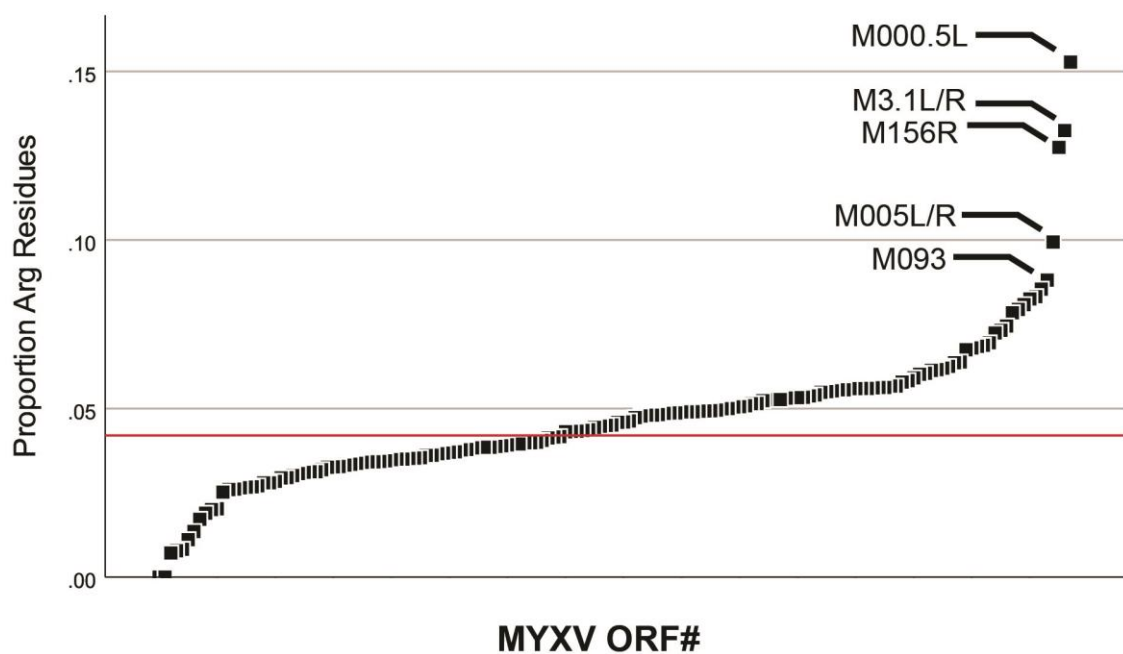
190. DeBerardinis, R.J. and N.S. Chandel, *Fundamentals of cancer metabolism*. Science Advances, 2016. **2**(5): p. e1600200.
191. G, S.C., et al., *Arginase as a Potential Biomarker of Disease Progression: A Molecular Imaging Perspective*. Int J Mol Sci, 2020. **21**(15).
192. Schindelin, J., et al., *Fiji: an open-source platform for biological-image analysis*. Nature Methods, 2012. **9**(7): p. 676-682.
193. Rodríguez, P.C. and A.C. Ochoa, *Arginine regulation by myeloid derived suppressor cells and tolerance in cancer: mechanisms and therapeutic perspectives*. Immunological reviews, 2008. **222**: p. 180-191.
194. Grzywa, T.M., et al., *Myeloid Cell-Derived Arginase in Cancer Immune Response*. Frontiers in Immunology, 2020. **11**.
195. Zheng, M., et al., *Oncolytic Viruses for Cancer Therapy: Barriers and Recent Advances*. Molecular Therapy - Oncolytics, 2019. **15**: p. 234-247.
196. Shin, D.H., et al., *Current strategies to circumvent the antiviral immunity to optimize cancer virotherapy*. Journal for ImmunoTherapy of Cancer, 2021. **9**(4): p. e002086.
197. Cai, W., et al., *Clinical significance and functional studies of myeloid-derived suppressor cells in chronic hepatitis C patients*. J Clin Immunol, 2013. **33**(4): p. 798-808.
198. Yaseen, M.M., N.M. Abuharfeil, and H. Darmani, *Myeloid-derived suppressor cells and the pathogenesis of human immunodeficiency virus infection*. Open biology, 2021. **11**(11): p. 210216-210216.
199. Hao, Z., et al., *Landscape of Myeloid-derived Suppressor Cell in Tumor Immunotherapy*. Biomarker Research, 2021. **9**(1): p. 77.
200. Srivastava, M.K., et al., *Myeloid-derived suppressor cells inhibit T-cell activation by depleting cystine and cysteine*. Cancer Res, 2010. **70**(1): p. 68-77.
201. Xing, Y.-F., et al., *Issues with anti-Gr1 antibody-mediated myeloid-derived suppressor cell depletion*. Annals of the Rheumatic Diseases, 2016. **75**(8): p. e49.
202. Bronte, V., et al., *Recommendations for myeloid-derived suppressor cell nomenclature and characterization standards*. Nature Communications, 2016. **7**(1): p. 12150.
203. Flores, E.B., B.A. Aksoy, and E. Barteel, *Initial dose of oncolytic myxoma virus programs durable antitumor immunity independent of in vivo viral replication*. J Immunother Cancer, 2020. **8**(1).
204. Rodríguez, P.C., et al., *Arginase I-producing myeloid-derived suppressor cells in renal cell carcinoma are a subpopulation of activated granulocytes*. Cancer Res, 2009. **69**(4): p. 1553-60.
205. Palte, R.L., et al., *Cryo-EM structures of inhibitory antibodies complexed with arginase 1 provide insight into mechanism of action*. Commun Biol, 2021. **4**(1): p. 927.
206. Sumbria, D., et al., *Virus Infections and Host Metabolism-Can We Manage the Interactions?* Front Immunol, 2020. **11**: p. 594963.
207. Thaker, S.K., J. Ch'ng, and H.R. Christofk, *Viral hijacking of cellular metabolism*. BMC Biol, 2019. **17**(1): p. 59.
208. Chang, C.H., et al., *Metabolic Competition in the Tumor Microenvironment Is a Driver of Cancer Progression*. Cell, 2015. **162**(6): p. 1229-41.
209. Gupta, S., A. Roy, and B.S. Dwarakanath, *Metabolic Cooperation and Competition in the Tumor Microenvironment: Implications for Therapy*. Frontiers in Oncology, 2017. **7**.
210. Siemann, D.W., *The unique characteristics of tumor vasculature and preclinical evidence for its selective disruption by Tumor-Vascular Disrupting Agents*. Cancer Treat Rev, 2011. **37**(1): p. 63-74.

211. Xia, L., et al., *The cancer metabolic reprogramming and immune response*. Molecular Cancer, 2021. **20**(1): p. 28.
212. Doty, R.A., et al., *Histological evaluation of intratumoral myxoma virus treatment in an immunocompetent mouse model of melanoma*. Oncolytic Virother, 2013. **2**: p. 1-17.
213. Flores, E.B., B.A. Aksoy, and E. Barteel, *Initial dose of oncolytic myxoma virus programs durable antitumor immunity independent of in vivo viral replication*. Journal for ImmunoTherapy of Cancer, 2020. **8**(1): p. e000804.
214. Awasthi, V., R. Chauhan, and J. Das, *Administration of L-citrulline prevents Plasmodium growth by inhibiting/modulating T-regulatory cells during malaria pathogenesis*. J Vector Borne Dis, 2022. **59**(1): p. 45-51.
215. Mao, Y., et al., *Citrulline depletion by ASS1 is required for proinflammatory macrophage activation and immune responses*. Mol Cell, 2022. **82**(3): p. 527-541 e7.
216. Lee, Y.C., et al., *L-Arginine and L-Citrulline Supplementation Have Different Programming Effect on Regulatory T-Cells Function of Infantile Rats*. Front Immunol, 2018. **9**: p. 2911.
217. Vissers, Y.L., et al., *Plasma arginine concentrations are reduced in cancer patients: evidence for arginine deficiency?* Am J Clin Nutr, 2005. **81**(5): p. 1142-6.
218. Sailer, M., et al., *Increased plasma citrulline in mice marks diet-induced obesity and may predict the development of the metabolic syndrome*. PLoS One, 2013. **8**(5): p. e63950.
219. Barteel, E., et al., *Systemic therapy with oncolytic myxoma virus cures established residual multiple myeloma in mice*. Mol Ther Oncolytics, 2016. **3**: p. 16032.
220. Wang, S. and J. Wei, *Distinguishing the pros and cons of metabolic reprogramming in oncolytic virus immunotherapy*. Int J Cancer, 2022. **151**(10): p. 1654-1662.
221. Jennings, M.R., D. Munn, and J. Blazek, *Immunosuppressive metabolites in tumoral immune evasion: redundancies, clinical efforts, and pathways forward*. J Immunother Cancer, 2021. **9**(10).
222. Ohta, A., *A Metabolic Immune Checkpoint: Adenosine in Tumor Microenvironment*. Frontiers in Immunology, 2016. **7**.
223. Wang, T., et al., *Inosine is an alternative carbon source for CD8⁺-T-cell function under glucose restriction*. Nature Metabolism, 2020. **2**(7): p. 635-647.
224. Kennedy, B.E., M. Sadek, and S.A. Gujar, *Targeted Metabolic Reprogramming to Improve the Efficacy of Oncolytic Virus Therapy*. Mol Ther, 2020. **28**(6): p. 1417-1421.

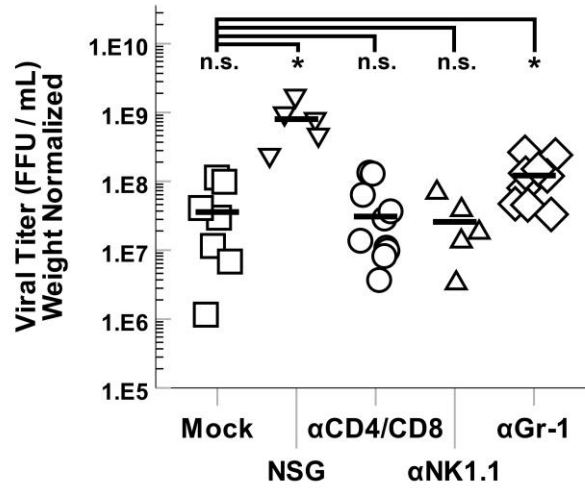
Appendices



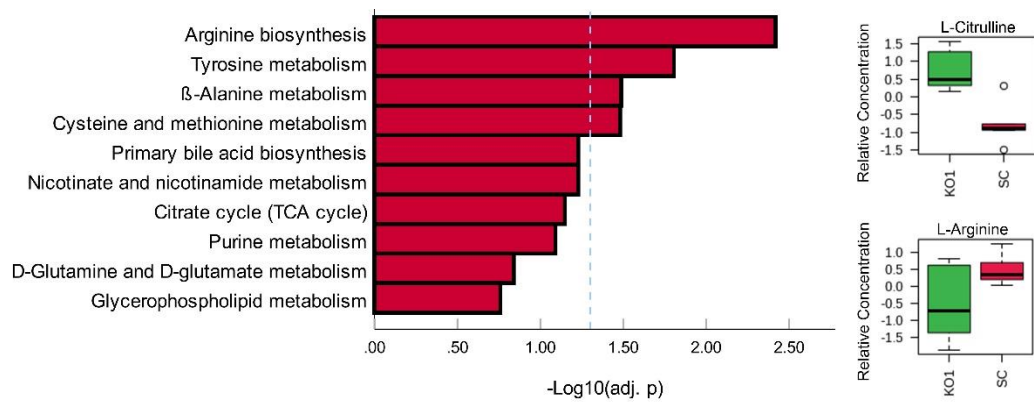
Appendix A: 48 hour Arg starvation of B16F10 cells results in cytotostasis, not death: B16F10 cells cultured in Control DMEM or -Arg DMEM for 48 hours originally plated at equal cell densities. **(A)** Images of Control and -Arg groups. **(B)** MTT assay of cultures. Significance determined by unpaired Student's t-test (***) = $p < 0.0005$). $n = 4$ per group. **(C)** Viability of cells determined via flow cytometry after vital staining. Significance determined by unpaired Student's t-test (ns = $p > 0.05$). $n = 3$ per group.



Appendix B: Frequency of Arg coded in MYXV ORFs. FASTA sequences of MYXV proteins were used to generate frequency of Arg residues within each protein using Biostrings R package, visualized here in increasing order. Red bar denotes frequency of Arg within vertebrate proteome (4.2%).



Appendix C: Depletion of MDSCs uniquely increases viral titer *in vivo*. Viral titers yielded from MyxGFP treated B16F10 tumors of C57Bl/6J or NSG mice pre-depleted of various immune compartments. Tumors harvested 8 days post-infection. Statistical significance determined by an unpaired Student's t-test (* = $p < 0.05$).



Appendix D: MSEA of $ASS1^{WT}$ and $ASS1^{KO}$ tumors. KO1 or SC tumors established in C57Bl/6J mice were grown for 18 days. Tumors were harvested and immediately snap frozen in liquid nitrogen. Whole tumor homogenates were then used to quantify a set of 189-metabolite species via LC-MS. Bar graph indicates top 10 most significantly changed pathways after TIC normalization and mean centering data. Blue dotted bar denotes cutoff for statistical significance by the Holm adjusted p value ($-\text{Log}_{10}(0.05) = 1.301$). Top right panel indicates relative L-citrulline concentration of KO1 compared to SCs. Bottom right panel indicates relative L-arginine concentration of KO1 compared to SCs. n = 5 mice per group.